S
697.78
N7shp
1983

RENEWABLE ENERGY REPORT LIBRARY

PLEASE RETURN

STATE DOCUMENTS COLLECTION

APR 3 1984

MONTANA STATE LIBRARY
1515 E. 6th AVE.
HELENA, MONTANA 59620

SOLAR HEATING SYSTEM PERFORMANCE MONITORING

Prepared for

MONTANA DEPARTMENT of NATURAL RESOURCES and CONSERVATION

Digitized by the Internet Archive
in 2017 with funding from
Montana State Library

https://archive.org/details/solarheatingsyst1983fowl

MONTANA STATE LIBRARY
S 697.78 N7shp 1983 c.1 Fowlkes
Solar heating system performance monitor
3 0864 00047976 9

SOLAR HEATING SYSTEM PERFORMANCE MONITORING

Prepared by

Charless Fowlkes
30 Gardner Park Drive
Bozeman, MT 59715

April, 1983

Prepared for

Montana Department of Natural Resources and Conservation
32 South Ewing, Helena, Montana 59620
Renewable Energy and Conservation Program
Grant Agreement Number 147-811

Available on loan from

Montana State Library, 1515 East Sixth Avenue
Justice and State Library Building, Helena, Montana 59620

This report was prepared under an agreement funded by the Montana Department of Natural Resources and Conservation. Neither the Department, nor any of its employees makes any warranty, express or implied, or assumes any legal liability or responsibility for the accuracy, completeness, or usefulness of any information apparatus, product, or process disclosed, or represents that its use would not infringe on privately owned rights. Reference herein to any specific commercial product, process, or service by trade name, trademark, manufacturer, or otherwise, does not necessarily constitute or imply its endorsement, recommendation, or favoring by the Department of Natural Resources and Conservation or any employee thereof. The reviews and opinion of authors expressed herein do not necessarily state or reflect those of the Department or any employee thereof.

INTRODUCTION

This is the final report for Grant #147-811 SOLAR HEATING SYSTEM PERFORMANCE MONITORING. Three solar systems were instrumented to produce hourly performance data:

(a) The Life of Montana Building: an active liquid system having 3880ft^2 of collector aperature.

(b) The Belgrade Junior High School building: an active liquid system having 782ft^2 of collector aperature.

(c) The Darcy Residence: a passive solar system using the double envelope design with a direct gain sunspace in the outer envelope.

Six other solar systems were studied using fuel bill analysis, computer analysis and site visitation. The thermal performance of these systems was estimated by combining these data.

This report is arranged into four separate sections. Each instrumented project is presented in a separate, self contained, section. The six surveyed systems are grouped together and discussed in the final Section. A brief overview of these results are given on the following pages. The contents are shown below.

SECTION 1: Life of Montana Building 1

SECTION 2: Belgrade Junior High School 17

SECTION 3: Darcy Passive Envelope House 45

SECTION 4: Class C Survey Results 61

Horizon Lodge 65

John Allenmeier 69

James Coons 73

Clark MacDonald 77

John MacDonald 81

James Taylor 85

OVERVIEW OF PERFORMANCE OF INSTRUMENTED SOLAR SYSTEMS

COST

Industrial demonstration systems installed around 1980 with Department of Energy funding were costing \$45 to \$50/ft^2 of aperature. Earlier demonstration systems (1976) typically cost \$60 to \$80/ft^2 of aperature.

(a) The large Life of Montana system in Bozeman cost about \$77/ft^2 of aperature.

(b) The Belgrade Junior High School solar system cost \$132/ft^2.

(c) The incremental cost of the passive solar features for the Darcy envelope house are estimated at \$25/ft^2 of solar aperature.

OPERATION

(a) The Life of Montana solar system operated normally with the exception of periodic air locks causing a portion of the collector array to stagnate. The remote location of the collectors, a design feature, produced a 25% reduction in solar energy due to line losses and thermal copacitance. The system was well maintained.

(b) The Belgrade Junior High School solar system exhibited a variety of serious operational anomalies primarily related to the controls. Some of these problems caused the system to pump heat out of the building. Parasitic electrical energy to operate pumps was about 3x that of a normal solar system.

(c) The Darcy envelope house is entirely passive so there were no "operational" feature. The house was carefully built and the construction, insulation and finish details are excellent.

SYSTEM THERMAL PERFORMANCE

(a) The Life of Montana solar system provided 7% of the building energy requirements during cold weather. The annual solar contribution is projected as 12% of the building energy requirements. Incidental passive solar energy contributions were 6% during cold weather.

(b) The Belgrade Junior High School System solar system produced a negligible net energy contribution to the building during the monitoring period. The passive solar energy contribution

SYSTEM THERMAL PERFORMANCE

was 1% of the building energy requirements.

(c) The envelope house collected negligible net solar heat during very cold weather due to the absence of a movable insulation system. The annual contribution is projected as 30% of the heating requirements. The inner envelope has low heat loss and the fossil fuel requirements are much better than average homes built in the mid 1970's.

BUILDING ENVELOPE PERFORMANCE

The instrumented buildings were rated on the basis of annual Btu's of auxiliary (non solar) energy per square foot per degree day. The auxiliary energy includes electrical, dissipation as well as natural gas (where used). The individual buildings rating is shown by an arrow on a scale indicating the range of values for that building type in the United States.

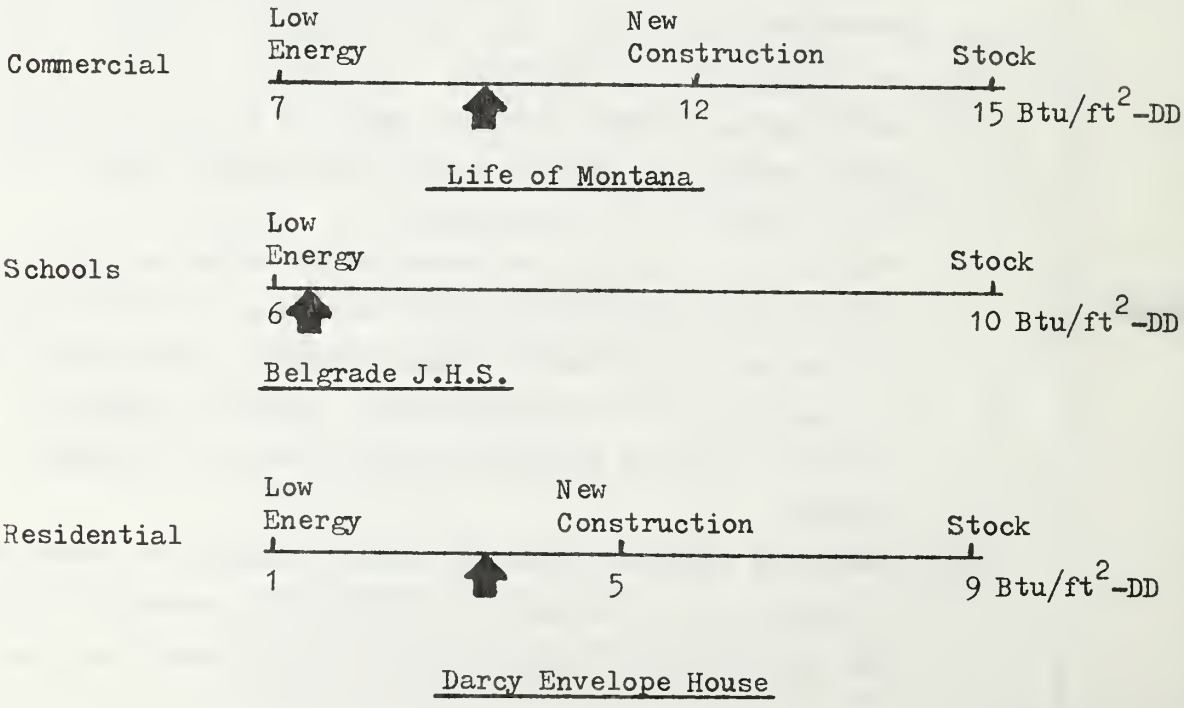

THERMAL PERFORMANCE OF THE LIFE OF MONTANA SOLAR SYSTEM AND BUILDING

ABSTRACT

This paper reports thermal performance data gathered on a 5,300 m^2 office building incorporating an active solar collector heating system. The data resulted from the application of low cost instrumentation applied to selected measurement sites. Data on the thermal performance of the building system is presented. Thermal capacity effects and line losses due to the remote location of the collector array significantly reduced the performance of this solar system.

1.0 INTRODUCTION

The project covered in this report is located in Bozeman, Montana, at an altitude of 1,520 m. There are typically 4,500 heating degree days per year. The temperatures in January average -8°C and will often drop to -20°C for periods of several days. Solar radiation on a 60° tilted collector surface will average 3.8 $kWh{\cdot}m^{-2}$ per day during the winter season. This building was completed in September, 1979, and is the home office of the Life of Montana Insurance Company. The company president, Herb Richards, received a demonstration grant from the Montana Department of Natural Resources Renewable Energy Program for $59,000. According to the operating engineer, Ivan Newnham, the total system cost is estimated as $303,000 or 840\cdot m^{-2}$ of collector area.

2.0 DESCRIPTION OF BUILDING

A photograph of the building is shown in Figure 1. The three story building has a total floor area of 5,300 m^2. The walls contain large areas of glass comprising 47% of the total wall area. Auxiliary heat is provided by a natural gas fired hot water boiler. Heat is distributed to the building through five air handlers, each located in a

separate zone. The space between the drop ceiling and the structural ceiling is used as a return plenum for the air handlers for the purpose of circulating heat dissipated by the lighting fixtures.

The active collector array is located at ground level at about 120 m from the building, Figure 2. Two hundred ten collector panels are tilted at 60^{o} and face about 22^{o} west of true south. The collectors are double glazed with low-iron glass and use selective surface absorber plates.

The collector fluid, a 50/50 ethylene glycol-water mixture, is circulated through buried insulated pipes to a heat exchanger in the basement of the building. Water circulates through the other side of the heat exchanger to two 11,300 l heat storage tanks. The collector loop contains about 2,600 l of fluid. The collectors are controlled by a differential thermostat. A second, adjustable thermostat in the building connects the solar storage tanks to the building circulation system, if the storage temperature is above the set point (normally 49^{o} C). All of the solar system piping is well insulated and the mechanical equipment and controls are in excellent condition.

3.0 DATA ACQUISITION SYSTEM

The data acquisition system used to monitor this building is shown in the photo in Figure 3. This is one of three home-made data systems constructed three years ago and subsequently used to monitor 15 solar heating projects. A Radio Shack TRS-80 microcomputer controls the data acquisition. The instrumentation interface contains a 12 bit A/D converter, and a real time clock. There are 40 input channels with integrated signal conditioning for temperature probes, flow meters, clamp-on ammeters, pyranometers and status switches. Up to 40 channels are sampled and processed each five seconds and hourly averages are stored on cassette tape.

4.0 INSTRUMENTATION LAYOUT

The instrumentation layout is shown on the schematic diagram in Figure 4. Solar radiation was sensed by a Li-Cor 200S radiometer mounted in the plane of the collector array at mid-height. An ambient air temperature probe was mounted in the shade of the collectors and another probe was mounted in the thermal well containing the differential con-

trol transducer at the collector array. Extension leads from these remote transducers ran 130 m through an underground conduit to the data acquisition system located in the mechanical room. Fluid temperatures in the solar system were measured by Analog Devices AD-590F probes inserted in the wells in the fluid. Two special probes having stems approximately 1 m long measured the temperature near the center of the heat storage tanks.

Flow in the collector loop was measured by interfacing a differential pressure transducer to an existing orifice plate. The pressure transducer was calibrated on site. The calibration of the orifice plate was provided by the manufacturer, as well as the correction curve to account for the glycol-water mixture. A status switch was connected to the gas valve of the auxiliary boiler allowing the data system to accumulate boiler on-time. Another status switch was attached to the valve which selects either boiler heat or solar heat for the building. The air temperature within the building was measured at five different locations. A pulse-initiating, watt-hour meter was also interfaced to the data system at a later date.

The temperature transducers were individually calibrated using a precision thermometer and an ice-point reference. The relative accuracy of the temperature transducers was 0.1° C (the resolution of the data system). The absolute accuracy is better than 0.5° C. This relative accuracy is needed because the temperature differentials through the heat exchanger are typically only a few degrees Celsius.

Being uncertain of the effect of 130 m of lead wire, the Li-Cor radiometer was calibrated on-site after the entire system was connected. A recently calibrated Eppley PSP was used for the reference. The data system has performed quite well in the electrically noisy environment of the mechanical equipment room. The system has run continuously for three months with only a few hours of lost data.

5.0 STEADY-STATE COLLECTOR PERFORMANCE

The collectors are partially shaded in the early morning and late afternoon in the middle of the winter. This shading should have little effect on the overall collector performance. The average flow through the collector array is 0.0148 $l\text{-}sec^{-1}\text{-}m^{-2}$ and storage volume is 62.8 $l\text{-}m^{-2}$.

These values are well within the range of recommended design parameters.

The data base from mid-January through the end of February was scanned to identify periods when the circulation pump was on for a full hour. A total of 39 hours on 13 different days satisfied this requirement. The hourly collector array efficiency was calculated by dividing the total solar heat output by the aperture area and the radiant flux. The corresponding value of collector inlet temperature minus ambient temperature divided by the solar flux was also calculated. The inlet temperature and heat output were measured at the heat exchanger. This procedure debits the collector performance for the line losses between the heat exchanger and the collectors.

These results are plotted in Figure 5. A dashed curve having a y-intercept of 0.73 and an x-intercept of 0.196 $^{o}C-m^{-2}-W^{-1}$ represents the expected performance of a single collector of the type in this array. On the average, experimental points fall below the single collector efficiency curve. This reduced efficiency is typical of collector arrays and is primarily due to heat losses in the manifold lines. A second curve has been drawn which passes approximately through the center of the experimental points. This data indicates that the average, steady-state performance of the array is about 7% below the expected performance of a single collector.

6.0 DAILY AVERAGE COLLECTOR PERFORMANCE

Although steady-state performance departed only slightly from ideal collector performance, the daily and monthly collector performance was clearly below expectations. Hourly data for the month of February was inspected to identify the cause of the reduced solar output. The collector performance curve shown in Figure 5 was used as a basis of comparison. The abscissa of the lower curve in Figure 5 was calculated each hour using measured insolation, ambient temperature and an inlet temperature. The calculated array efficiency was multiplied by the measured solar radiation to arrive at an "ideal" collector heat output. The calculated output of the ideal collector was compared to the measured solar heat output for each hour in February.

Table 1 shows typical measured hourly performance data for February 24

and calculated "ideal" collector performance. The first line in the Table shows that the "ideal" collector would have collected a small amount of heat (104 MJ) while the real collector did not turn on. During the period between 10:00 and 11:00 a.m., the real collector was on an average of 0.2 hour. Its negative heat output indicates that heat was removed from the solar storage tanks. During the same time, the ideal collector delivered 337 MJ. This difference reflects the solar heat being used to warm the fluid and piping in the collector loop. During the next hour, the actual solar system delivered 456 MJ while the "ideal" system delivered 509 MJ.

This comparison indicates the collector loop was warmed up and most of the solar heat was being delivered to the heat exchanger. During the rest of the day, the hourly performance of the real and "ideal" collector agree quite closely.

An overall performance summary for this day shows that the real collector delivered 2,667 MJ while the "ideal" collector delivered 3,149 MJ. On this day, the output of the "ideal" collector was 480 MJ greater than the output of the actual collector. The daily total heat output of the real collector array for the month of February are plotted in Figure 6. A straight line drawn through the data points intersects the actual output axis at about -480 MJ. This data shows that the actual solar heat output is offset about 480 MJ below the ideal output.

TABLE 1
HOURLY COLLECTOR DATA COMPARISON FOR FEBRUARY 24, 1982

	Actual Collector Array									Ideal Collector			Diff
HR	Insol $kW-m^{-2}$	Tamb °C	Tin °C	Tout °C	Xin °C	Xout °C	Con Hrs	Eff %	Qout MJ	Tin °C	Eff %	Qout MJ	Δ Qout MJ
10	0.48	-7.4	29.8	41.1	39.9	39.8	0	0	0	56.3	17	104	-104
11	0.71	-1.3	45.6	44.4	53.7	48.9	0.2	-2	-7	55.0	36	337	-344
12	0.90	0.6	61.0	69.2	54.8	58.1	1.0	38	456	55.1	43	509	-53
13	0.99	-1.2	64.4	73.7	57.0	60.9	1.0	42	559	57.4	44	566	-7
14	1.02	0.8	68.0	77.1	60.2	64.4	1.0	43	595	60.6	44	586	10
15	0.93	1.9	70.3	78.4	63.5	67.3	1.0	42	524	63.9	41	498	26
16	0.80	1.7	70.7	76.7	65.6	68.5	1.0	36	388	65.8	36	376	11
17	0.58	-1.0	69.9	74.0	66.5	68.4	0.5	17	153	65.9	23	174	-21
TOTAL									2667			3149	-480

7.0 HEAT CAPACITY OF THE COLLECTOR LOOP

We looked next at the pipes and manifold which connect the collectors to the heat exchanger. This loop contains about 2,650 l of fluid. We divided this piping into an underground portion and an above ground portion. The underground portion of the piping was estimated to contain 1,300 l of fluid in copper pipes having a mass of approximately 900 kg. Thermal mass of the underground piping is 4.5 MJ-$^{o}C^{-1}$. The above ground portion of the loop, which includes the manifold and the absorber plates, contains about 1,000 l of fluid, while the pipes and absorber plates have a mass of about 2,400 kg. The overall thermal capacity of the above ground portion of the loop is, therefore, about 4.5 MJ-$^{o}C^{-1}$.

Each day when the collectors operate, the fluid temperature reaches 60 - 70^{o} C. Each night, the above ground fluid and pipe comes to equilibrium with the ambient temperature while the undergound pipe and fluid comes to an equilibrium temperature of approximately 20^{o} C. On the average day in February, the above-ground fluid, manifold and collector plate assemblies were raised from -4.8^{o} C to 65^{o} C, requiring 280 MJ of energy each day that the collector operated. The underground portions of the line similarly required about 203 MJ per operating day. The total heat required each collector operating day is estimated at 483 MJ. This value agrees very closely with the intercept of the actual vs. ideal performance shown in Figure 6.

8.0 COLLECTOR PERFORMANCE SUMMARY

The parasitic power for the solar collector system for the month of February was 1,541 MJ or about 5% of the delivered solar heat. This power is the sum of electricity used by the solar circulating pump and the storage tank circulating pump. During the month of February, the solar collectors delivered 20.3% of the incident solar radiation to the building; a total of 29,895 MJ. During the same period, the "ideal" collector would have delivered 41,600 MJ to the building. The collectors were on during 24 days in February. If the heat capacity of the piping and collector system is 480 MJ per day, the resulting heat lost would be 11,500 MJ. This is very close to the difference between the "ideal" collector and the measured collector performance.

9.0 BUILDING PERFORMANCE

This building receives heat from the auxiliary gas boiler, electrical dissipation or internal gains, and active solar gains. The monitoring data for the period from mid-January to early March was formulated into an hourly building heat balance. To estimate the amount of heat delivered by the natural gas furnace, we compared the amount of natural gas entering the building between January 18 and February 16 (251.7 Mcf) to the total hours of on-time for the gas furnace (162.4 hrs). Using a heating value supplied by the utility company and a conversion efficiency of 75%, we estimated the boiler output as 1,061 $MJ\text{-}hr^{-1}$.

This building uses between 36,000 and 55,000 kWh of electricity per month. During the period covered in this report, the building was using 38,000 kWh per month. About 2,800 kWh of this electricity is used for architectural lighting outside the building during the night. This means 35,200 kWh were being dissipated in the building each month. An hourly load schedule was devised which assigned 300 $MJ\text{-}hr^{-1}$ internal gains during the daytime and 52 $MJ\text{-}hr^{-1}$ dissipation during the night. (A pulse-initiating kWh meter was interfaced to the data system in March. Initial results showed that the daytime hourly consumption was slightly higher than 300 $MJ\text{-}hr^{-1}$.) The heat loss of the envelope was calculated using normal ASHRAE procedures assuming an infiltration rate of 0.76 air changes per hour during the day and 0.2 air changes per hour during the night. The daily average load coefficient used for the building was 18 $MJ\text{-}hr^{-1}\text{-}{}^{o}C^{-1}$.

The building contains large areas of south facing glass (195 m^2). This heat absorbing glass has a transmission of 0.35 at normal incidence. To calculate the passive solar gain, the insolation measured on the tilted collectors was multiplied by a shading factor of 0.8, a transmission factor of 0.35, and an angle correction factor of 0.9. This value multiplied by the total area of windows was assumed to represent passive solar gain. The shading coefficient in this calculation is judged conservative and no allowance is made for reflected radiation onto the vertical glazing, which is significant at these latitudes. The estimated passive solar gain may, therefore, be conservative by 10 - 20%.

The active solar heat entering the building was measured at the interface between the collector loop and the heat exchanger. Since practically all of this solar heat is dissipated into the building, only the timing is unknown. To determine when the solar heat enters the building, we constructed a heat balance based on temperature changes of the fluid in the storage tanks. The temperature of the storage tanks at the beginning and end of the hour of interest were interpolated by fitting a second-order polynominal through the three temperature data points centered around the hour of interest. This curve was differentiated to determine the average rate of temperature change of the storage tanks during that hour. This value multiplied by the thermal mass produced an hourly stored energy change.

The hourly solar energy delivered to the building was calculated by subtracting the solar heat delivered by the solar collectors from the stored energy change. This procedure credits the building with heat losses from the storage tanks, which is justified, since the tanks are located within the heated envelope. This procedure for calculating solar heat added to the building is a little crude on an hour-by-hour basis, but the errors tend to average out. For a time period spanning six weeks, the total measured solar heat delivered by the collectors was 32,606 MJ while the solar heat calculated from storage tank temperature changes was 32,993 MJ. This comparison indicates that no large errors are incurred by using this calculation method.

The entire hourly data base was processed using the heat balance procedure on which the summation of all the inputs were compared to the calculated heat loss (based upon an assumed infiltration factor, a conductive factor and a measured ΔT). The thermostat in this building is set back during the night. In the evening when the thermostat is set back, the building "coasts" for several hours and then in the morning when the thermostat is advanced, the furnace runs for almost the entire hour to catchup. The initial hourly heat balances showed the need of a building heat storage term in the heat balance. We devised a heat storage term for the building based upon the air temperature in the building.

The building has an estimated thermal mass of 700 $MJ-^{o}C^{-1}$, but this thermal mass is weakly coupled to the air. To account for this weak coupling, we devised a thermal storage model which had a memory of five hours. The air temperature difference occurring during any given hour is placed in a bin. During each of five succeeding hours, the temperature difference in this bin is sequentially reduced by one-half. For any given hour, the heat stored in the building mass is calculated by multiplying a thermal mass constant by the sum of the ΔT contributions of these five bins. This is a fairly simple algorithm to program and it seems to smooth out the effects of large temperature transients on the building heat balance.

The hourly base from January 19 to March 3 was evaluated using an hourly energy balance which included electrical inputs, gas boiler inputs, passive solar inputs, active solar inputs and building storage exchanges balanced against building losses. Acceptable hourly, daily and monthly heat balances define the overall accuracy of the data and the suitability of the assumptions. The final results of these calculations are shown in Figure 7. The active solar collectors contribute a total of 33 GJ, the passive solar gains total 26 GJ, the electrical dissipation is 181 GJ and the heat supplied by the natural gas boiler is 220 GJ. The total heat losses during this period are 225 GJ from conduction through the skin of the building and 235 GJ due to infiltration (natural and forced). Data in Reference (1) shows that the environmental solar radiation and temperatures were typical during the monitoring period.

10.0 CONCLUSIONS

(1) At thermal equilibrium, the collectors performed to within about 7% of the expected, single collector performance. This reduction in performance is characteristic of practical active solar heating systems.
(2) The remote location of the collectors significantly reduce the system's thermal performance (over 25% in February). Each day, the pipes and fluid in the remote collectors must be heated before the system can deliver useful heat to the building. At night, this solar heat is dissipated to the atmosphere.

(3) During the monitoring period, the passive solar gains (through heat absorbing glass) were nearly as large as the active solar gains.
(4) The controls of the solar system are behaving as expected and there are no large steady-state heat losses since the pipes and heat exchangers are well insulated.
(5) The performance of this system is enhanced due to the maintenance, care and attention of the operating engineer, Ivan Newnham. Solar heating systems, due to their complexity and novelty, require some measure of dedication on the part of the building owner and operator. The owner and operator of the solar system on the Life of Montana Building are dedicated to making it work. Mr. Newnham monitors operation of the system and will often clean the snow from the 316 m^2 of collectors!
(6) During the monitoring period, the resource energy consumed to light the exterior of the building at night was equal to the solar heat collected.
(7) Large amounts of electrical energy are dissipated within this commercial building. Measuring hourly electrical energy facilitates accurate hourly heat balances.

Figure 1. South side of building.

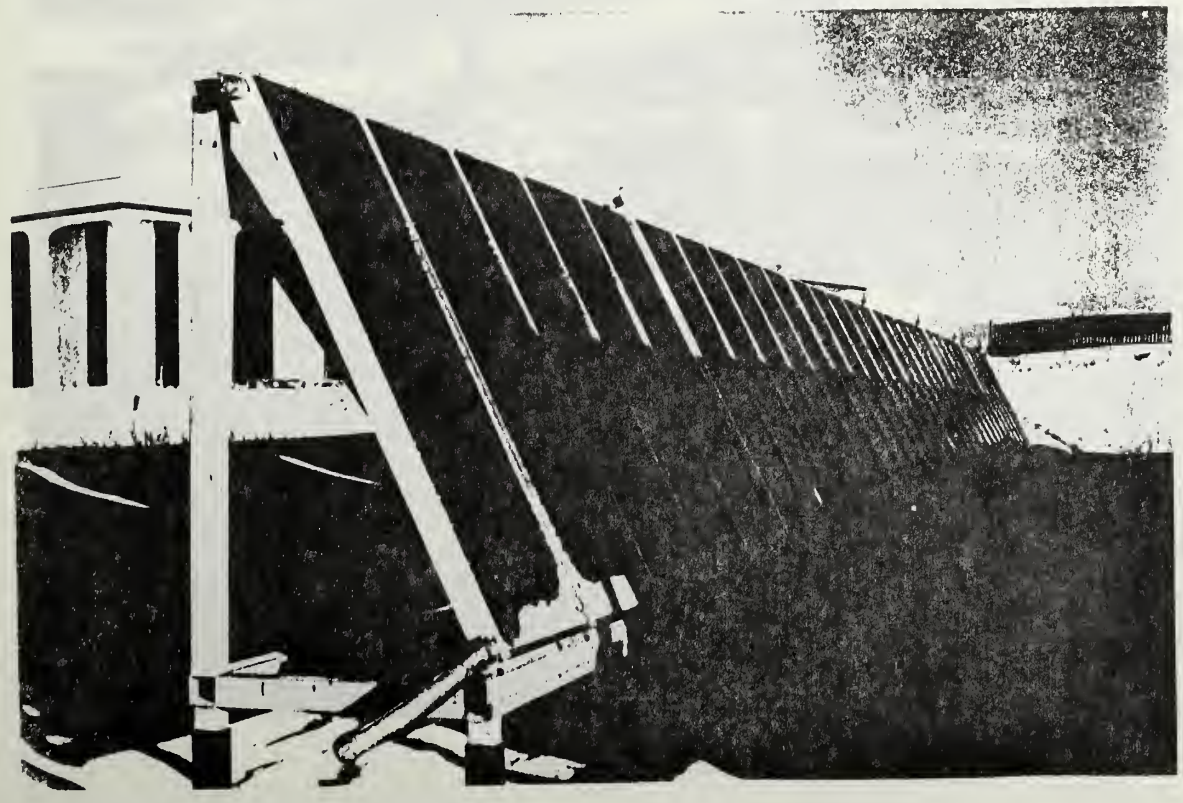

Figure 2. One bank of collectors.

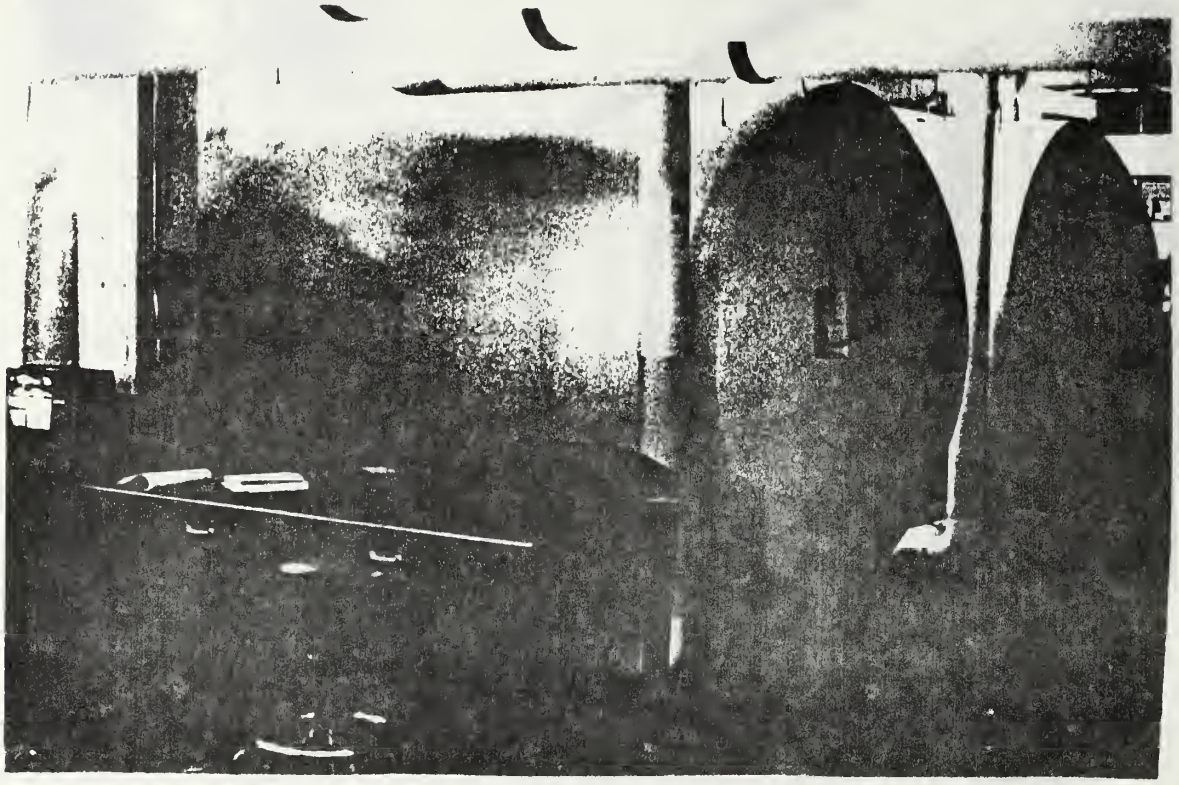

Figure 3. Heat storage tanks and data acquisition system.

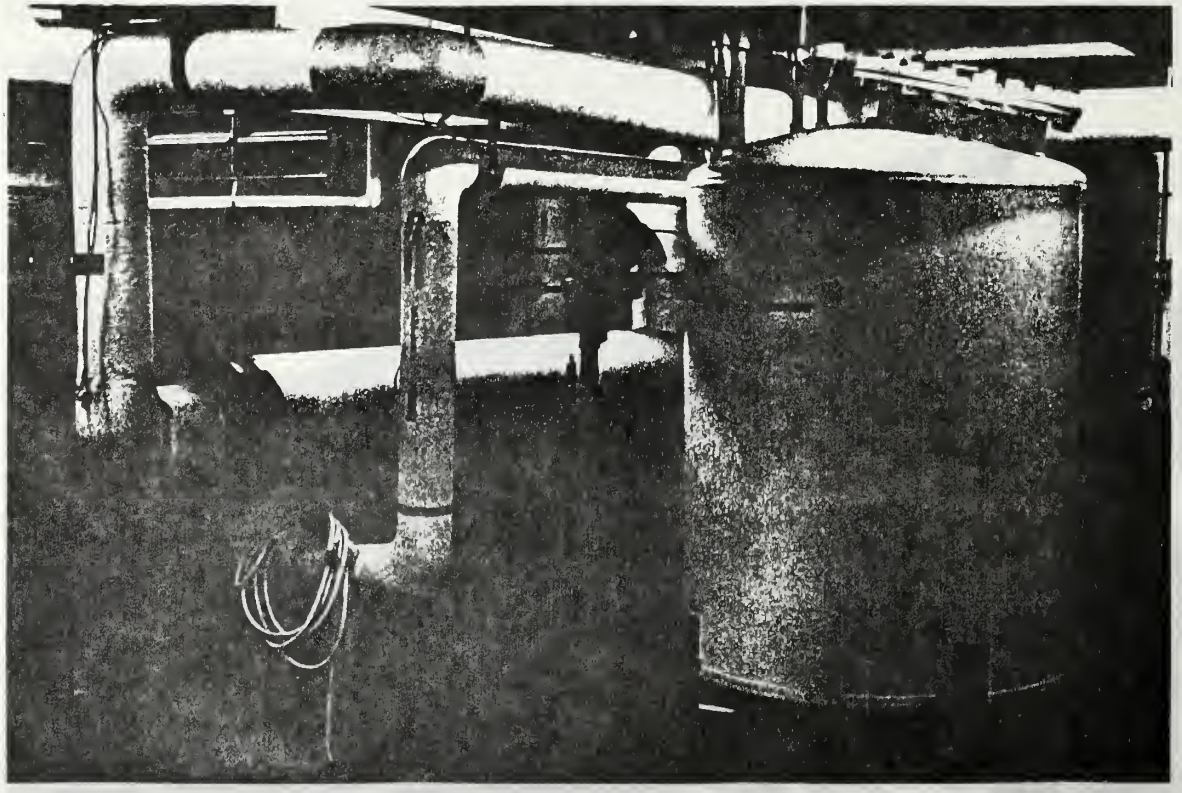

Heat exchanger

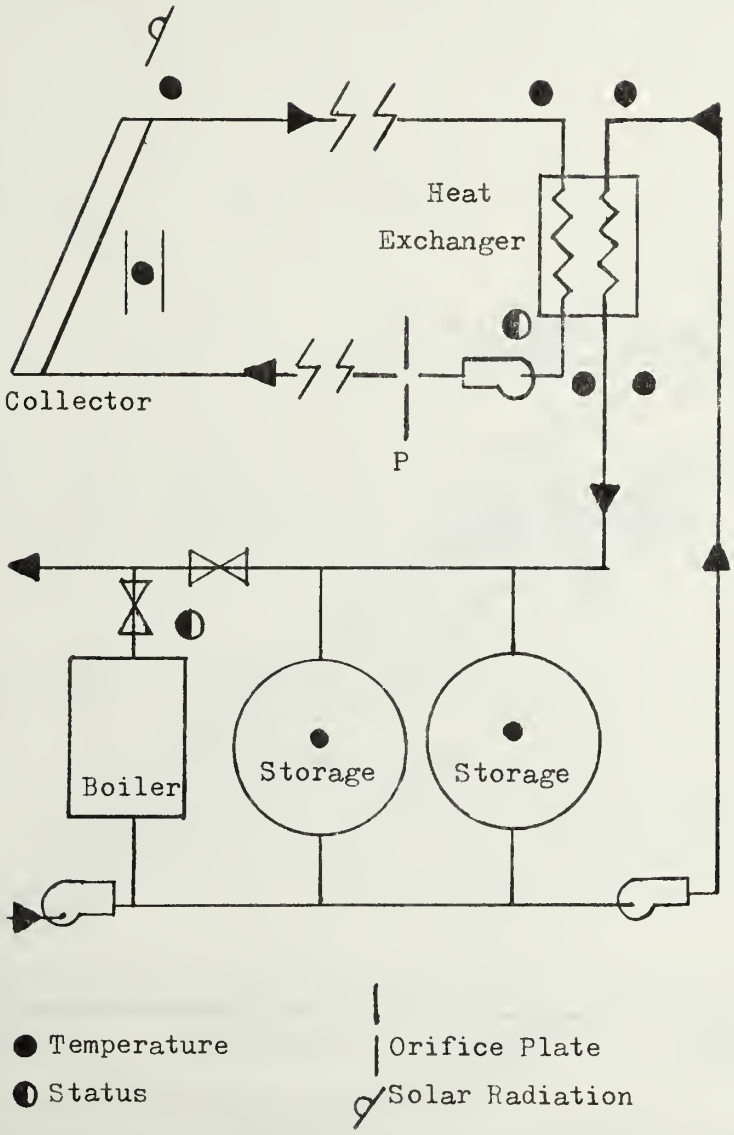

Figure 4. Instrumentation layout

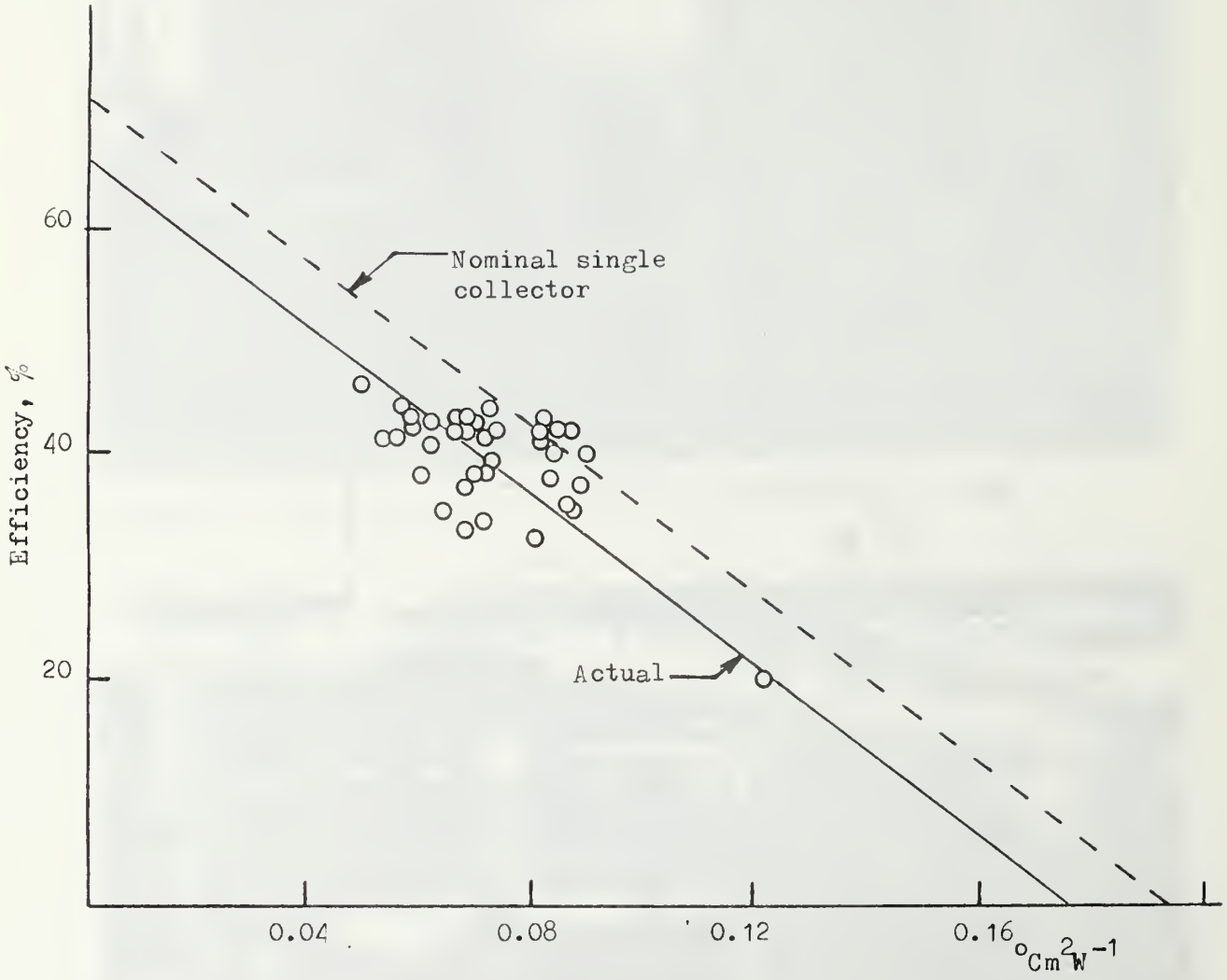

Figure 5. Collector array efficiency at quasi-steady condition

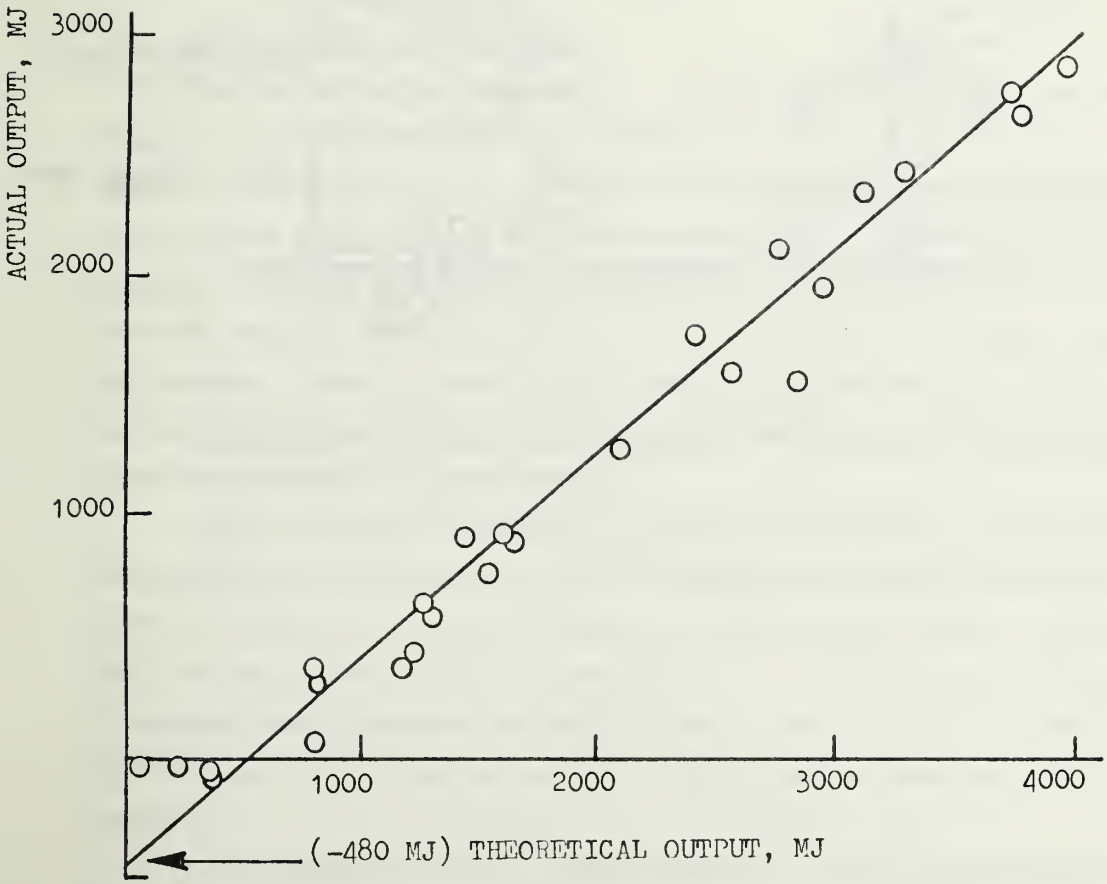

Figure 6. Comparison of daily total solar heat output

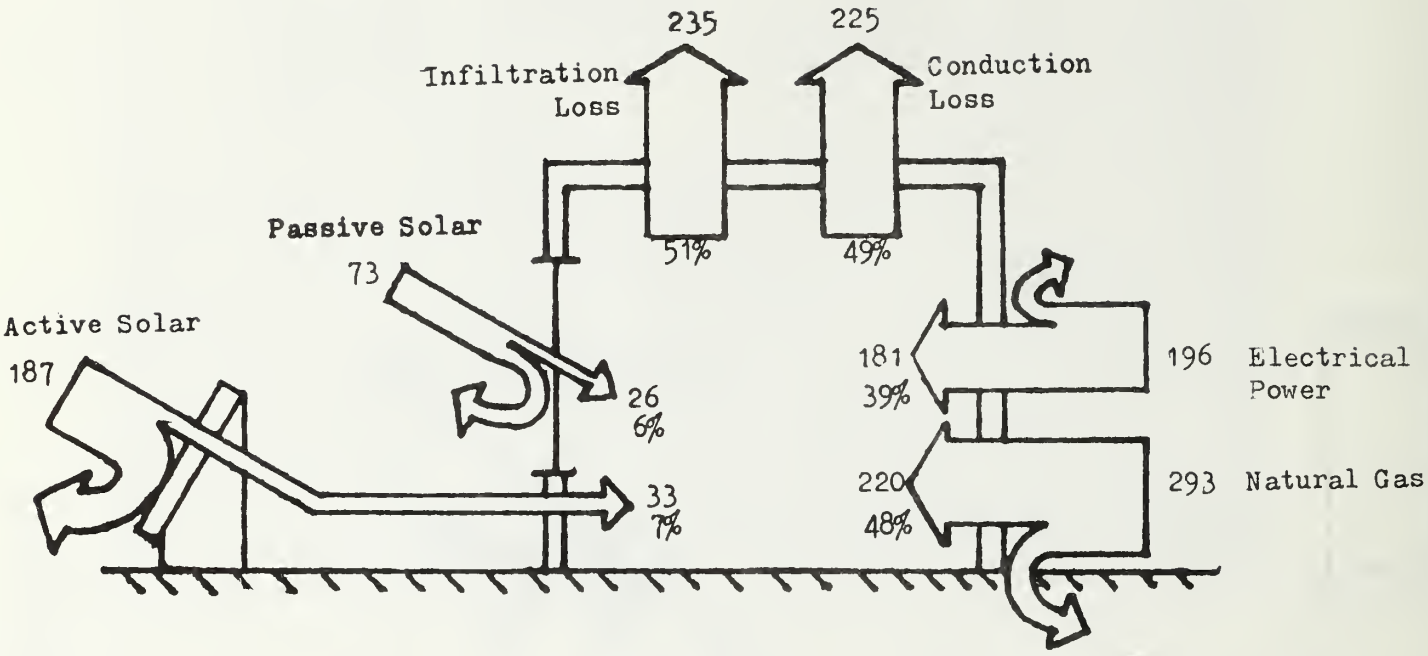

Figure 7. Building heat balance from January 19 to March 3, Gigajoules.

THERMAL PERFORMANCE OF THE BELGRADE JUNIOR HIGH SCHOOL SOLAR SYSTEM AND BUILDING

ABSTRACT

This paper presents thermal performance data on a liquid solar system which is part of the Belgrade Junior High School (B.J.H.S.) building. Solar collectors having an area of 72.6m^2 are arranged to provide heat to the domestic hot water (D.H.W.) system and to the building. Due to a variety of malfunctions, described in detail in this report, the solar system provided negligible net energy to the building.

1 SOLAR SYSTEM DESCRIPTION

The mechanical arrangement of the B.J.H.S. solar system is shown in Figure 1. Most of the solar equipment is located in a room in the basement of the building. The collectors are mounted in a vertical plane on the roof of the building and face true south. The control panel for the system is in the Boiler Room, located on the ground floor. Plumbing runs between the Solar Equipment Room and the Boiler Room average about 20 m in length. About 60 m of pipe is needed to connect the collectors to the solar heat storage tank. All pipes and tanks are insulated. Figure 2 shows photographs of the system.

The solar system schematic is shown in Figure 3. The main solar collector pump circulates a 50/50 ethelyne glycol/water solution through the collectors and a heat exchanger in the storage tank. The main pump and collector loop valve are controlled by a differential thermostat. A second pre-circulator collector pump is controlled by a photo cell sensor located at the collectors. This pump is supposed to turn on at sunrise.

The domestic hot water (DHW) system is also incorporated into the solar system. A pump circulates water from the DHW preheat tank through a heat exchanger in the solar storage tank. This pump is supposed to run if the storage tank temperature exceeds the DHW preheat tank temperature.

The service water passes through the DHW preheat tank and then into two natural gas fired DHW heaters. During the day a pump circulates hot water through the service loop so that hot water is instantly available at the point of use.

Heat is supplied to the building load by either the boilers or the

solar storage tank. The heat source is selected by a 3-way valve under system control. If solar heated water is available, the storage tank is connected to the load otherwise the boilers are connected to the load.

1.1 Instrumentation

The instrumentation lay-out is shown on the system schematic drawing in Figure 3. The instrumentation resources were focused primarily on components of the solar system. Temperatures in and out of the various heat exchangers were typically measured using Ad590 semiconductor probes mounted in thermal wells. The probes were covered with heat transfer paste to insure good thermal contact and the loads were oriented to reduce lead conduction errors. The protruding portions of the thermal wells were then insulated to reduce errors due to conduction.

Flow in the major heat exchange loops was measured several times during the monitoring period. A non-instrusive ultrasonic Doppler flow meter was used. No flow meters or orifice plates had been plumbed into the original system. The Doppler meter allowed us to sense flows without making extensive (and expensive) changes in the system plumbing.

The status (on and off) of several system components was sensed using a variety of probes. Clamp on ammeters indicated the status of the collector pre-circulation and DHW preheat circulation pumps. The positions of the control rods on the main collector valve and the 3-way (solar/boiler) mode valve were sensed with microswitches. Special mountings with temperature probes were placed on the flue of each gas fired DHW auxiliary heater. The sharp rise or drop in flue temperature indicated the on/off status of these devices. An LED optical isolator circuit was designed and built for each of the three gas fired boilers. The control voltage (28 vac) which turned the boilers on also powered the LED transducer. The data system sensed this light and converted the data into an "on" status. This optical isolation insured that the data system could never interfere electrically with the boiler controls.

Solar radiation was measured with a Li-Cor 200S transducer mounted in the plane of the solar collectors. After installation this sensor was calibrated, in place, against an Eppeley PSP reference pyranometer. This procedure insured that total errors in measuring insolation were within the accuracy of the transducer.

Ambient air temperature was measured near the solar collectors.

This probe was mounted inside a two-stage, aluminum, radiation shield. The estimated average radiation error was less than $\pm$ 1°C. The building air temperature was sensed in the main hallway of the building. The air temperature in the solar equipment room was also measured (for estimating stand-by tank losses).

1.2 Data Acquisition System

A DNR&C 40 channel data acquisition system based on a TRS-80 microcomputer was used. The arrangement of the transducers is documented in Table 1. A total of 22 channels of information was recorded.

The system scanned all channels each 5 seconds. Calculations and units conversion were performed on-line and displayed.

A special graphical display program was written which printed system data on an overlay on the face of the CRT. The overlay consisted of a system schematic similar to the one shown in Figure 3. This presentation contributed toward an understanding of the location of the measurements for the building occupants.

The data system averaged the instantaneous channel readings over periods of one hour. These hourly average values were stored on cassette along with the time-of-day. The cassette data was subsequently transferred to a floppy disk format on our office computer. Data processing programs including graphs and tables were used to summarize the performance of the solar system.

2 SOLAR SYSTEM OPERATIONAL FAULTS

2.1 List of Operational Faults

The solar system showed several operational faults in its behavior during the monitoring period. Many of these problems were related to improper operation of the system controls. The system was serviced several times during the monitoring period but the problems were never entirely eliminated. The combined effect of these problems was to reduce the net solar heat added to the building to approximately nothing. It is possible that the utility bills for operating the building would have to be lower if the solar system had been shut down.

The operation faults are listed below:

1) The 3 way solar/boiler mode valve would sometimes leak boiler heated water into the solar storage tank

2) The main collector pump ran 24 hours a day for several

weeks during the monitoring period

3) Faults 1) and 2) above occurred simultaneously during parts of February and March. The unfortunate result was this: The boilers were heating the solar storage tank. The collectors were simultaneously taking this energy and rejecting it to the atmosphere.

4) During its "best" periods the main collector circulation pump would turn on properly in the morning of a sunny day but would invariably run for about 2 hours after sundown. The thermal effect of this fault was to reject approximately 20-30% of the solar heat gained, during the day, back to the out-of-doors during the evening.

5) The pre-circulation pump ran all night during about 75% of the monitoring period. (It should come on at about sunrise and go off again at sunset.) At times an (apparent) leak in the main collector valve allowed the pre-circulation pump to take heat from the solar storage tank and reject it to the atmosphere at night.

6) The solar domestic hot water exchanger circulation pump ran continuously day and night during the monitoring period. (Ideally it should only run when the storage tank is warmer than the preheat tank.)

7) The parasitic energy, (electricity to run the solar system pumps) was between three to four times normal due to the problems above.

8) The domestic hot water would occasionally back flow from the auxiliary heaters into the preheat tank.

2.2 Detection and Analysis

The existence of several of the more subtle operational anomalies was first detected in the hourly data. Computer programs were written to graph the hour by hour values of system temperatures for the entire four-month monitoring period. Inspection of these graphs clearly showed the effects of leaking valves, unexpected back-flow, etc..

The steady-state fluid flows in the pipes were measured using an ultrasonic Doppler flowmeter. These measurements were made on several occasions for different system modes and the average results used for one-time flow constants in the data analysis. The leakage flows could

not be measured directly and would not be constant in time.

To analyze the data, energy balance equations were formulated for (a) the building, (b) the solar heat storage tank and (c) the DHW pre-heat tank. The entire hourly data base was then processed using these energy balance equations and the energy components and balance errors printed in tables. When large, consistant energy balance errors were detected, the models and the equations were modified and the analysis was repeated. After several iterations the average errors were minimized and the energy components were summarized.

The analysis of this system was particularly challenging due to (a) the large number of operational anomalies and (b) the fact that there was interaction between the anomalies. In past solar system monitoring we have often been able to reach a confidence of $\pm$ 10% or better on the average performance of the system components. The error bands on solar component performance are greater on this system.

2.3 Graphs Showing Solar System Faults

Figure 4 shows some system temperatures for three days in January. For the first two days the storage temperature decays due primarily to losses. A small amount of sun on the second day causes the main collector pump to come on. Since the collector outlet is nearly equal to the storage temperature there is no significant heat gained. The pump runs about 2 hours after sunset.

On the third, sunny day the main collector pump comes on and the storage temperature is noticably increased from before noon until an hour before sunset. The pump continues to run for about three hours after the collector outlet temperature drops below storage temperature. The solar system is taking heat out of storage for this period and the storage temperature drops.

Note how the collector inlet temperature drops to about 5°C above ambient air temperature at night. This drop is due to the pre-circulation pump running all night. As the fluid passes through the collectors it is cooled. An apparent leak in the main collector valve allows stored heat to be rejected.

Figure 5 shows another malfunction, about a month later, during

mid February. During this period the main collector pump was running 24 hours each day; the pump status is "on" and the collector outlet temperature is only a few degrees below the storage temperature at night. Since the collector is rejecting heat from the building to the ambient air (where temperature is around 0^{o}) we should expect the temperature of the solar storage to decrease.

The storage temperature at night does <u>not</u> decrease; it is constant! The explanation of this is obvious after inspecting the temperature of the fluid lines connecting the solar storage to the gas boilers. Although the valve between the boilers and the solar storage should be closed it is leaking significant amounts of boiler heated water into the storage tank. The boilers are supplying heat to solar storage, holding its temperature constant, while the collectors are pumping this heat out of the building. The system operated like this for several weeks during February and March.

Figure 6 shows another malfunction a month later during March. Three sunny days are shown. During the first two days the main collector pump does not turn on even though the collector outlet temperature exceeds the storage temperature by $50^{o}C$! After noon on the third sunny day the main pump comes on; marked by the abrupt decrease in collector outlet temperature.

During this period the storage tank gains heat due to an apparent leak in the main collector valve. This same leak also caused losses at night during times when the pre-circulation pump ran all night (much of the monitoring period). The penalties for this malfunction include lost heat and degradation of the collector fluid due to high temperatures.

Figure 7 shows the system temperatures during three days in April. The pre-circulation pump is operating properly. The main pump is irratic in its operation. During the first day, the boilers are leaking heat into the solar storage system. During the following two days the solar/boiler mode valve is properly closing when the system is in "boiler mode". Note the decrease in "building to storage" temperature on 4/9, showing that the valve is closed.

The graphs of the system behavior spanning the entire monitoring period illustrate a variety of faults primarily related to malfunctions

in the control system. The system controls were adjusted several times during the monitoring period. Proper operation of all systems was never achieved.

3 OVERALL PERFORMANCE OF SOLAR SYSTEM AND BUILDING

3.1 Actual Results

The hourly data was analyzed from the point of view of the entire building/solar system. The total solar system energy contribution to the building is summarized; i.e. heat used for the building and that used for heating are not separated (The DHW sub system is discussed in a separate section). Natural gas energy input and electrical energy input are not subdivided into their specific end uses. That was not a goal in this monitoring program. We would like to assess the role of solar energy input to the building as a percentage of the total energy required by the building.

The data for the monitoring period has been organized and presented in Table 2 to address this question. The first part of Table 2 shows the energy summary of the building over the 4 month monitoring period. (Data taken during early January and late May was rejected because it was incomplete.)

SOLAR AVAILABLE is the total solar energy striking the surface of the collectors. The SOLAR COLLECTED consists of solar energy that was delivered by the collectors to the solar storage tank and building during sunny days. The next entry HEAT REJECTED accounts for heat taken out of the building by the solar collectors. Heat was rejected when the collectors operated during the evening and all night. This rejected heat term combines solar heat rejected and boiler heat rejected (when the mode valve was leaking). Note that the solar system moved 22,000 MJ into the building and carried 17,000 MJ back out of the building. The net heat gain, a nominal 5,000 MJ, is about 1% of the building TOTAL load of 505,000 MJ.

The PUMP ENERGY is the parasitic electrical energy used to run the main collector pump and the pre-circulation pump. PUMP ENERGY amounted to 6,400 MJ or 29% of ACTIVE SOLAR. The pump energy for normal liquid solar systems is about 5% of the solar energy collected. The

high parasitic energy in this system related to the control anomalies discussed previously.

The uncertainty of the values for ACTIVE SOLAR and HEAT REJECTED are large ($\pm$ 50%) due to the strange and irratic behavior of the system. The average values show that the solar system contributed about 0% or nothing to the building. If the extreme "good" values are used we conclude that the solar system contributed 18,000 MJ or 3.5% to the buildings energy requirements. If the extreme "bad" values are used we find the solar system removed 20,500 MJ from the building. Taken either way we are talking about $\pm$ $100 worth of energy during the 4 month monitoring period. The system cost to the DNR&C program was about $100,000.

The PASSIVE SOLAR gain accounted for solar heat transmitted through the south-facing glass on the Belgrade J.H.S. building. The total south-facing aperature area was 18.6m^2 and a transmission factor of 0.7 was used. These factors multiplied by the vertical insolation provided a good measure of passive solar gain. The percentage of south-facing glazing on this building is about $\frac{1}{4}$ the south-facing glazing on a typical non-solar residence. The building thus has a less than average passive solar contribution; about 1% of the TOTAL LOAD.

The ELECTRICAL DISSIPATION (not measured hourly) was taken as 0.75 of the average electrical utility use of the building. The BOILER HEAT was calculated from a boiler rating multiplied by the measured on-time of the boilers. This value corresponds to the energy value of the natural gas entering the building multiplied by a 0.7 conversion efficiency factor.

The building heat loss factor was calculated and a variable infiltration rate added to account for daytime use and ventilation. The TOTAL LOAD each hour was calculated using this heat load factor multiplied by the measured temperature difference between the inside air and the ambient air.

The constants in the last three energy quantities are subject to some uncertainty. These constants were refined, based on the hourly, daily and overall heat balance relationships for the system. This iterative process practically guarantees that large errors are not present in the results.

The summary building energy analysis shows that this building shows little energy benefit, and perhaps a deficit, from the current active solar system. Since this poor performance is in part due to faulty system operation an additional performance projection is presented.

3.2 Calculated System Performance

This analysis assumes that the solar system, now installed on the building, is somehow adjusted to produce optimum performance. This hourly simulation was programmed on the computer using actual solar and temperature data measured on-site during the monitoring period. The collectors and controls were assumed to be operating normally and properly given the environmental conditions. The ELECTRICAL DISSIPATION, TOTAL LOAD and PASSIVE SOLAR were taken as the same as the real, monitored system.

The simulated, idealized solar system delivered 43,000 MJ of solar heat or 9% of the TOTAL LOAD. The parasitic pump energy was a nominal 5% of the heat produced. The BOILER HEAT is reduced by 38,000 MJ or about 10% during the monitoring period. The value of this solar heat would be about $250 at current prices. Note that if this solar heat was used only for hot water, given the current low water usage, the dollar value of the solar heat would be much less.

4 SOLAR DOMESTIC HOT WATER SUBSYSTEM

4.1 Graphs of Solar Hot Water System

Figure 8 shows the solar domestic hot water system operation during three days in April. The graphs show solar radiation, solar storage temperature, auxiliary gas DHW water operation and service water inlet temperature. When no water is used at the load (showers, sinks, etc.) there is no cold water drawn past the service water inlet temperature probe. This probe, with no flow, reads a temperature that is about equal to the storage temperature. This operation is shown on day 4/4 in Figure 8. This day is a Sunday and the school is closed and no water is being used.

Figure 8 for 4/5 and 4/6 show the effects of withdrawing hot water on the service water inlet temperature. The hourly average temperature

at the inlet is somewhere between the ground water temperature, about 10°C, and the preheat tank temperature and depends on water used. Since the ground water passes through pipes located inside the building it is preheated by the building interior air to a temperature approaching about 20°C. The amount of building preheat also depends on the rate at which water is used. The more water used, the lower the hourly average service water inlet temperature.

An important thermal feature of the DHW system was the circulation loop, Figure 3. A circulation pump would normally run between 6 AM and 4 PM. This pump circulated the hot water through the service loop so that hot water would be available, with no delay, at service points along the loop (showers, sinks, wash basins, etc.).

The loop was quite long (over 100m) and necessarily had a loss of heat along its length. Figure 8, Note 2, shows that the gas DHW heaters came on for about 30 minutes each morning when the circulation pump first turned on. This was the longest period of operation for the heaters during the entire day. This heat was used to "warm up" the circulation loop after being off all night. Note that the service water temperature shows that water is not being used; all the heat is going into the loop to get it up to service temperature.

Figure 9 shows data which implies that the circulation pump ran continuously for the three days. The evidence for this assumption is (a) the gas DHW heater ran periodically all night from 5/6 to 5/7 and all day on 5/8 and (b) the service water temperature shows that no water was used during these periods. (The 5/8 data was on Sunday and the school was empty).

No explanation is available as to why the circulation pump ran continuously during this period. The data did allow an accurate estimate of the stand-by losses of the circulation loop. Since no hot water was being used the entire output of the gas DHW heater was going into stand-by losses in the circulation loop.

The stand-by energy losses were much larger than the energy going into the load in this system. This can be seen by looking at the "on time" of the gas DHW heater in Figure 9. The "on time" during two normal school days when hot water is being used is not very much greater

than the "on time" on Sunday, or at night, when no hot water is used.

Figure 10 shows three days in April when hot water is being used. There is a small solar contribution during these days. During the afternoon of the sunny day on 4/2 the auxiliary heater does not come on as in the previous two days. This suggests a solar contribution. The inlet temperatures however show that little or no hot water was used at this time. Thus the solar contribution is negligible.

4.2 Solar DHW Summary

Figure 11 summarizes the performance of the Solar Hot Water System. The present DHW auxiliary heating system consumed about 9% of the natural gas entering the building. Most of this heat (80%) supplied line losses in the circulation loop. This means about 1% of the natural gas entering the building supplies usable hot water at the faucet.

The net useful solar gain was immeasurable. The net solar heat entering the preheat tank was of the same order as the stand-by losses of the tank. The circulation pump ran continuously, even when the solar storage was cooler than the DHW preheat tank; a control malfunction. The electric energy expended to run this pump exceeded the solar heat delivered. Given the range of measurement errors the solar energy contribution to DHW was between -2,200 and +10,000 MG during the monitoring period.

Translating this into the possible effects on the utility bills during the 4 month monitoring period the system may have increased the electric bill by $20 or reduced the natural gas bills by up to $50. This effect is on the order of 1% of the total utility bill.

If the solar DHW system were working perfectly the reduction in utility bills would still be only 1 or 2% given the low usage of hot water. This is because solar heated water is only transferred to the auxiliary tank when water is used. When no water is used, all auxiliary goes into supplying standby losses.

The data indicates that very little hot water is used at B.J.H.S.. (An employee said the boys showers were seldom used because the shower

area was uncomfortably cold due to a problem in the heating system.) The energy use of the DHW system is dominated by the losses in the circulation loop. These factors place stringent limits on the possible solar contribution of this system.

A Solar DHW system for a school is a questionable design concept. This is due to the fact that a typical solar DHW system produces about 40% of its annual heat output during June, July and August. Schools are not used at this time. Poor load matching limits the performance in this application.

5 CONCLUSIONS

The performance summary of the solar system is shown in Figure 12. There were solar gains but the solar system also caused losses approximately equal to the gains.

During the monitoring period the solar system did not significantly alter the fossil fuel energy use of the Belgrade Junior High School building. The main reason for the poor performance was the faulty operation of the system controls. If the system was operating perfectly it would provide a contribution approaching 9% of the current energy use of the building.

This system is relatively small, having only 72.2 m^2 of aperature. A residential system for heating water would typically have 6m^2 of collector aperature while a residential solar space heating system might have 35 m^2 of collector area. The solar system on this building is thus about the size of 2 normal residential space heating systems or 10 residential hot water systems. It cannot be expected to provide a very large portion of the energy for this large building serving several hundred occupants.

A <u>properly</u> operating system of this size would produce, during the school year, around $600 worth of energy at current prices. By the year 2000 a <u>properly</u> operating system of this size would have saved about $20,000, assuming 6% annual escalation in real fuel prices. The cost of the system was $103,610.

6 ACKNOWLEDGEMENTS

The cooperation and help of Ted Mangun was essential to the successful completion of this project. Ted helped us become familiar with the mechanical layout of the solar system, provided ladders and other tools while instrumenting the system, and shared his observations on the operation and performance of the system. His contributions are gratefully acknowledged.

Jerry Vanderpan, principal of Belgrade Junior High School, is acknowledged for his cooperation with this monitoring project by allowing easy access to the building.

Dick Lee and David Leavengood are acknowledged for their efforts to understand the malfunctions of the solar system.

TABLE 1

TRANSDUCER LOG

Belgrade Junior High School

TYPES:

S - SOLAR
T - TEMP
DT - DUCT TEMP
ST - STATUS
P - POWER

DISK #	RS #	PROBE #	TYPE	LOCATION AND MOUNTING
1	1	1	S	Solar radiation at midpoint of collectors
2	2	1	P(ST)	Status of precirculator pump
3	3	2	P(ST)	Status of DHW exchanger pump
4	4		ST	Main collector valve status 1 = open 0 = closed
6	6		ST	Boiler 1 & 2 status ∅ = off, 1= one on, 2 = both on
7	7		ST	Boiler 3 status 1 = on, ∅ = off
8	8		ST	SOLAR/BOILER MODE (Three way valve) Solar = 1 Boiler = ∅
9	9		Calc	COLLECTOR HEAT OUTPUT
13	10		ST	DHW Heater status 0 = off, 1 = one on, 2= both on
14	11		Calc	SOLAR HEAT TO DHW
17	12	12	T	DHW Preheat to solar storage exchanger
18	13	13	T	DHW Preheat from solar storage exchanger
19	14	14	T	Service water temperature
20	15	15	T	DHW SOLAR PREHEAT TANK OUT
21	16	16	T	Fluid temperature from solar collectors
22	17	17	T	Fluid temperature to solar collectors
23	18	18	T	Fluid temperature from building to solar storage
24	19	19	T	Fluid temperature from solar storage to building
25	20	20	T	Ambient air temperature
26	21	21	T	SOLAR STORAGE TEMPERATURE
29	22	22	T	Building air temperature
30	23	23	T	Mechanical room air temperature

TABLE 2

OVERALL SOLAR SYSTEM PERFORMANCE SUMMARY, Jan 26 - May 11, 1982

ACTUAL BUILDING PERFORMANCE

SOLAR AVAILABLE	SOLAR COLLECTED	HEAT REJECTED	PUMP ENERGY	PASSIVE SOLAR	ELECTRICAL DISSIPATION	BOILER HEAT	TOTAL LOAD
98,000	(1) (22,000)	(1) (-17,000)	(2) 6,400	5,000	(3) 137,000	(4) 358,000	(4) 505,000
		Ø%		1%	27%	71%	100%

CALCULATED PERFORMANCE IF SYSTEM WORKED NORMALLY

SOLAR AVAILABLE	SOLAR COLLECTED	HEAT REJECTED	PUMP ENERGY	PASSIVE SOLAR	ELECTRICAL DISSIPATION	BOILER HEAT	TOTAL LOAD
98,000	43,000	Ø	2,200	5,000	137,000	320,000	505,000
		9%		1%	27%	63%	100%

(1) ± 50%

(2) Main collector pump and pre-circulation pump, DHW pump not included (2,200 MJ)

(3) 0.75 recovery factor

(4) ± 20%

① Solar collectors
② Solar heat storage
③ Solar DHW preheat
④ Pumps
⑤ Solar control panel
⑥ Natural gas boilers
⑦ Natural gas DHW heaters

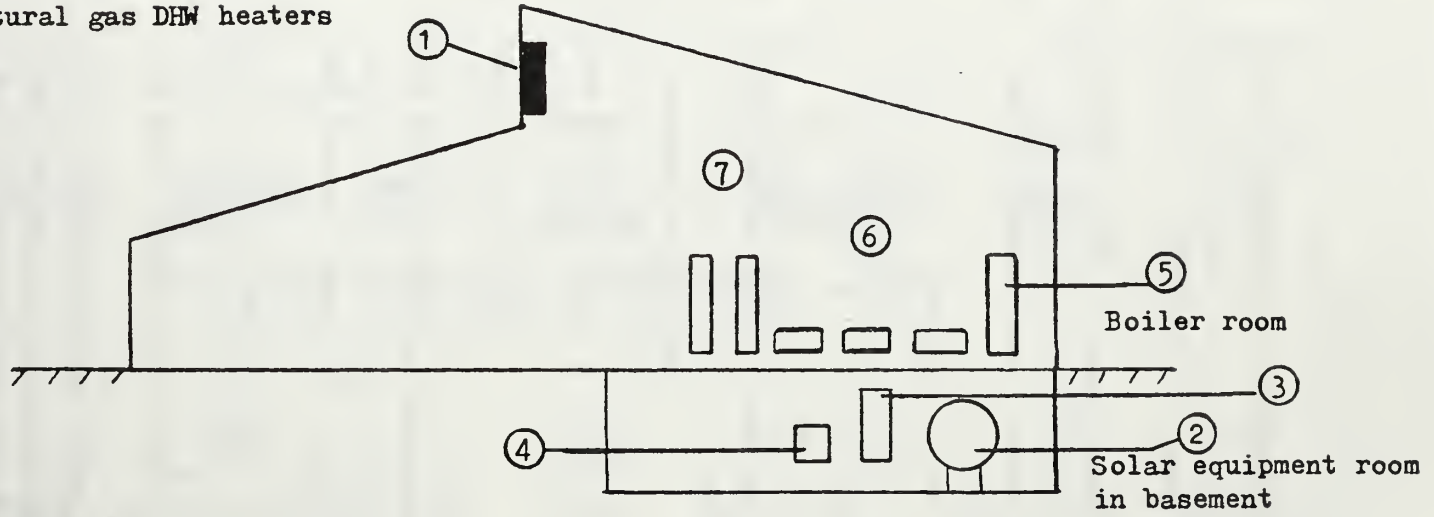

Figure 1: Schematic of B.J.H.S. Solar System arrangement

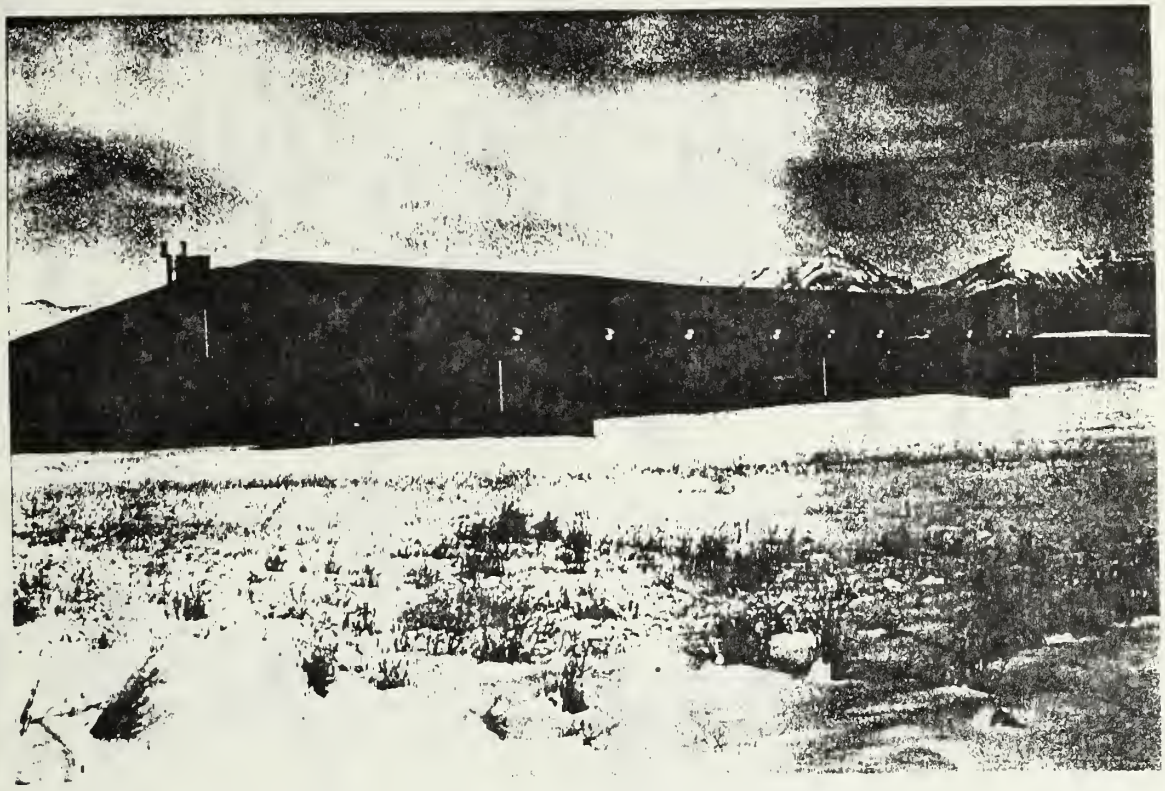

Exterior of building showing collectors

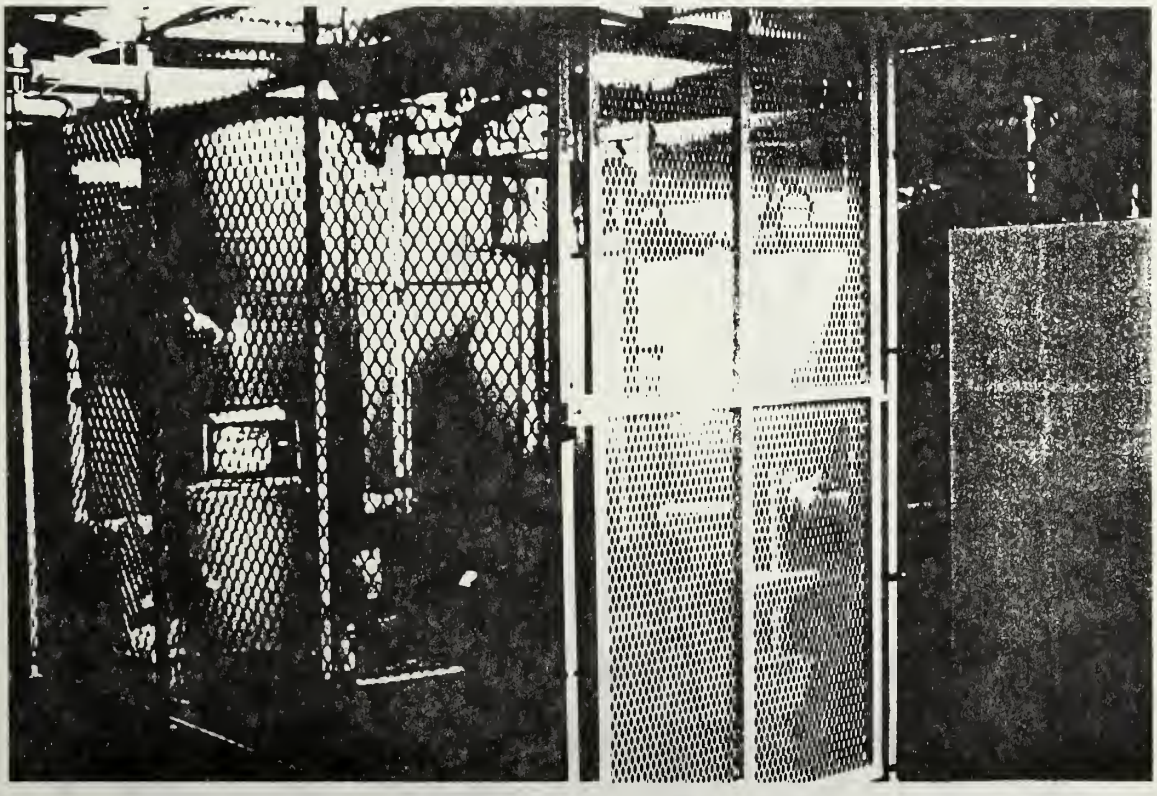

Solar equipment room

Figure 2: Belgrade Junior High School System

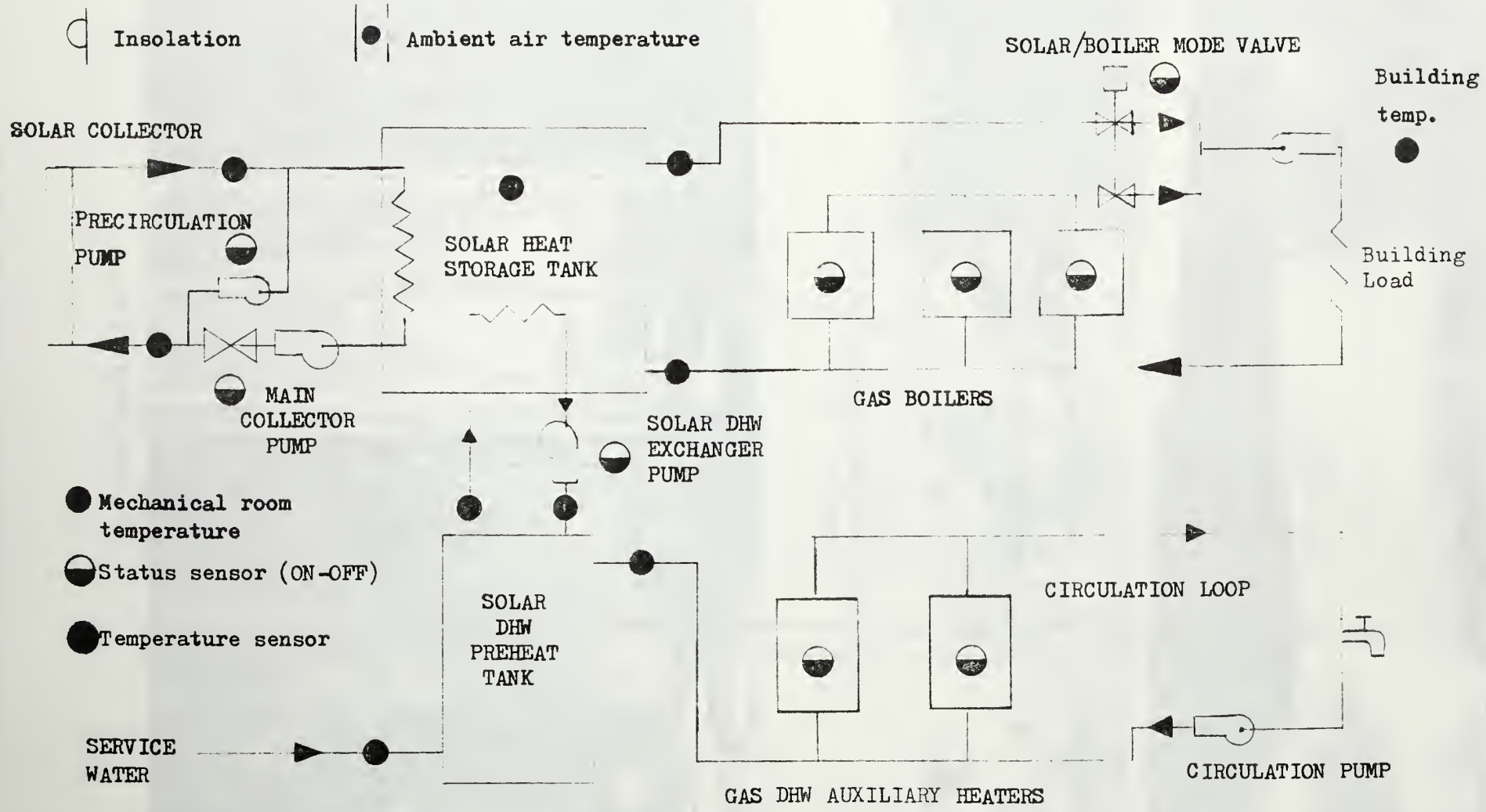

Figure 3: Schematic of Solar System showing instrumentation

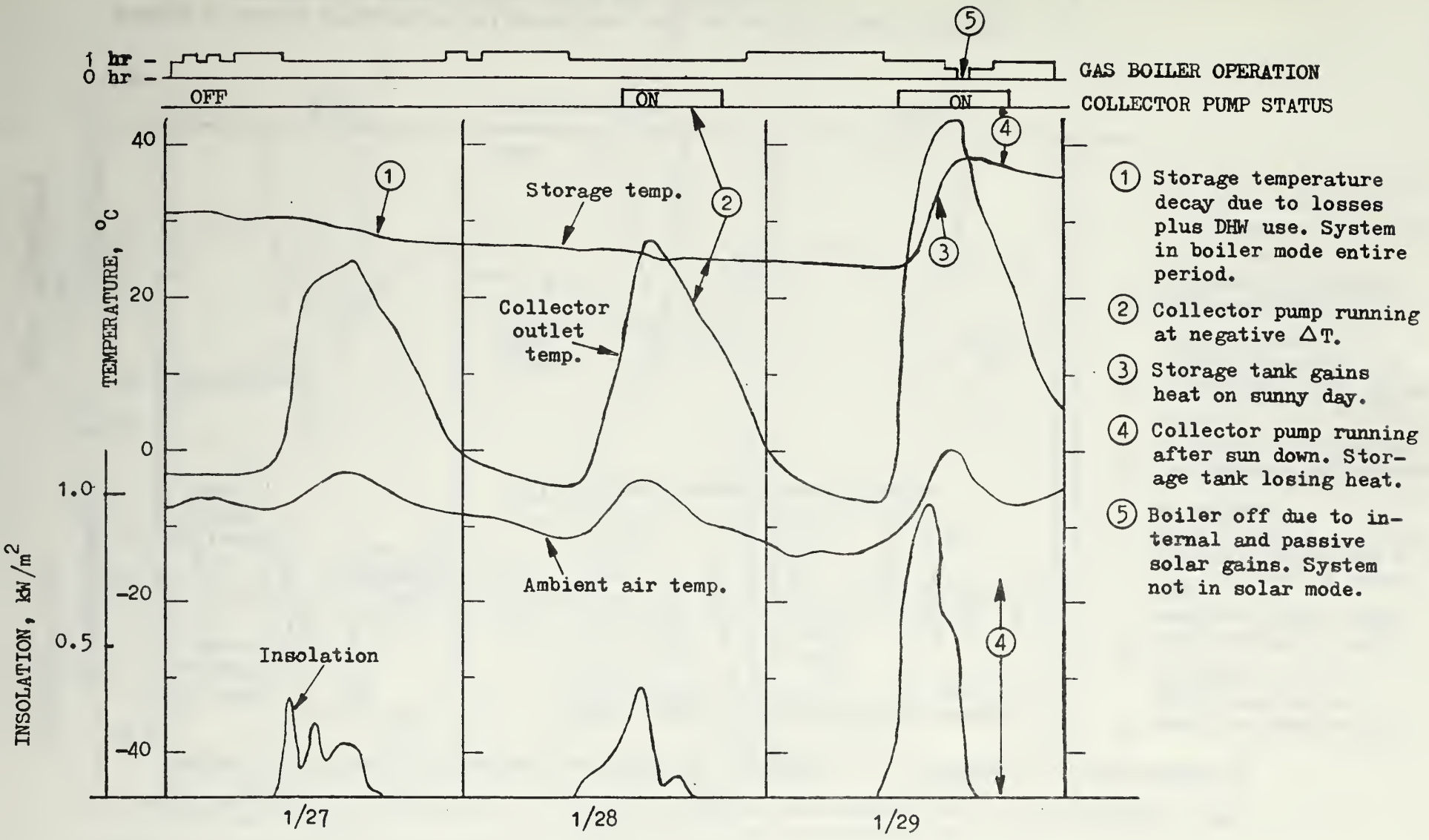

Figure 4: System response to faulty collector pump control.

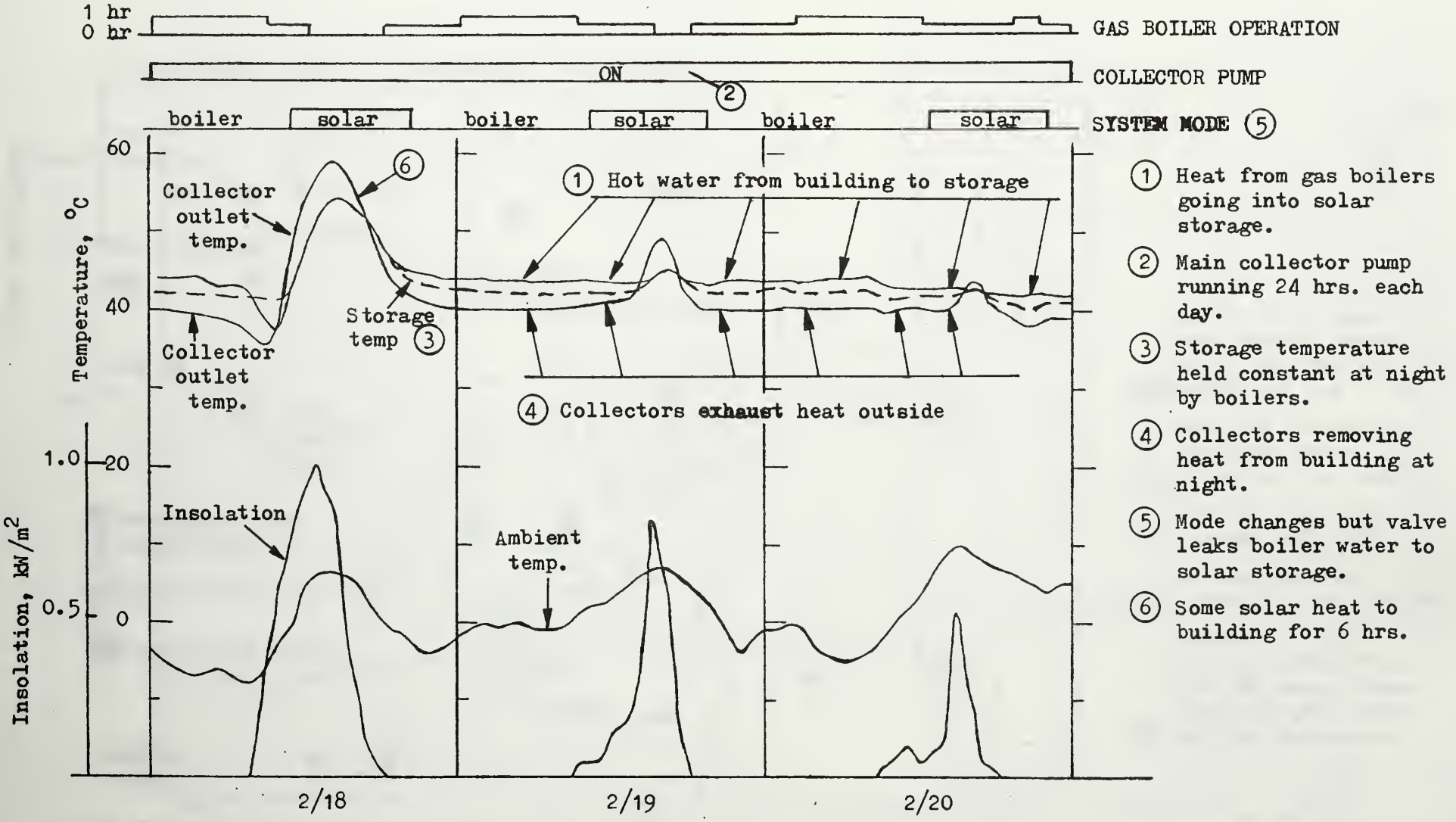

Figure 5: System response to collector pump running at night while heat is supplied to solar storage from gas boilers.

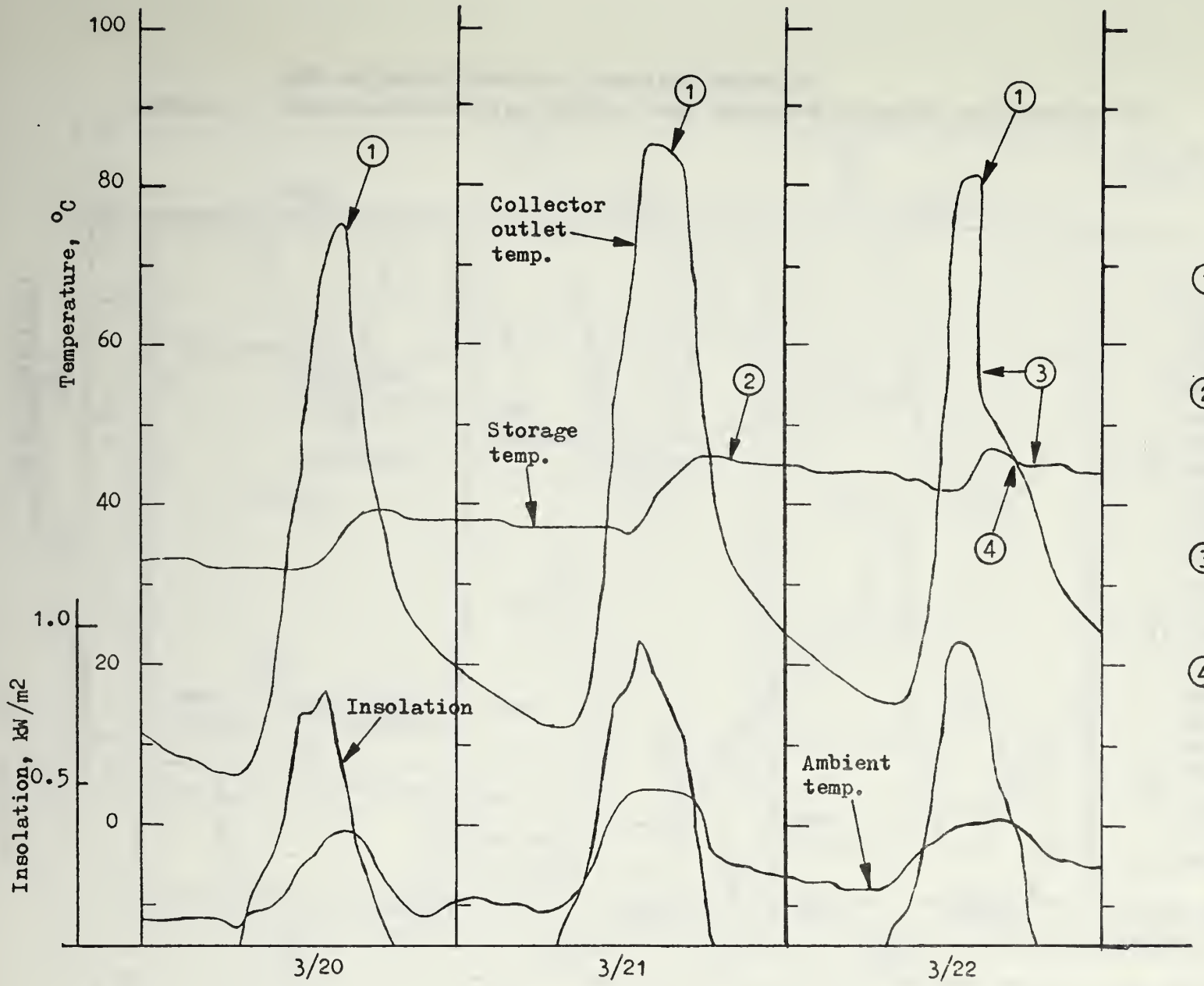

(1) High collector outlet temperatures because main collector pump is OFF.

(2) Storage gains heat from tickler pump due to extreme T. System in boiler mode so heat not delivered to building.

(3) Main collector pump turns ON for 3 hours at end of 3rd sunny day.

(4) System in solar mode for about 3 hours.

Figure 6: System response when main collector pump fails to operate on 3 sunny days.

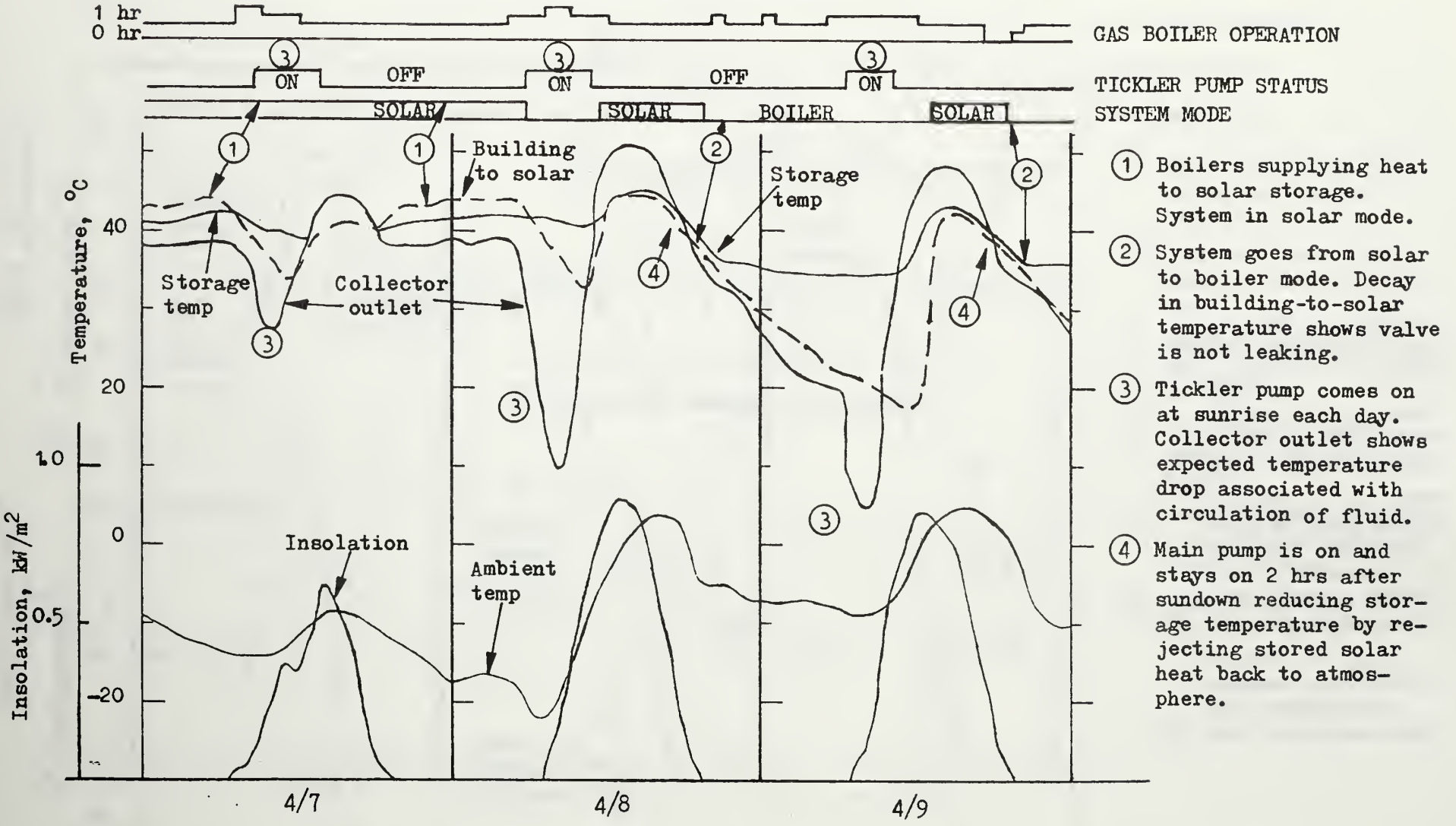

Figure 7: System response with tickler pump operating properly, mode control and main collector pump not operating properly.

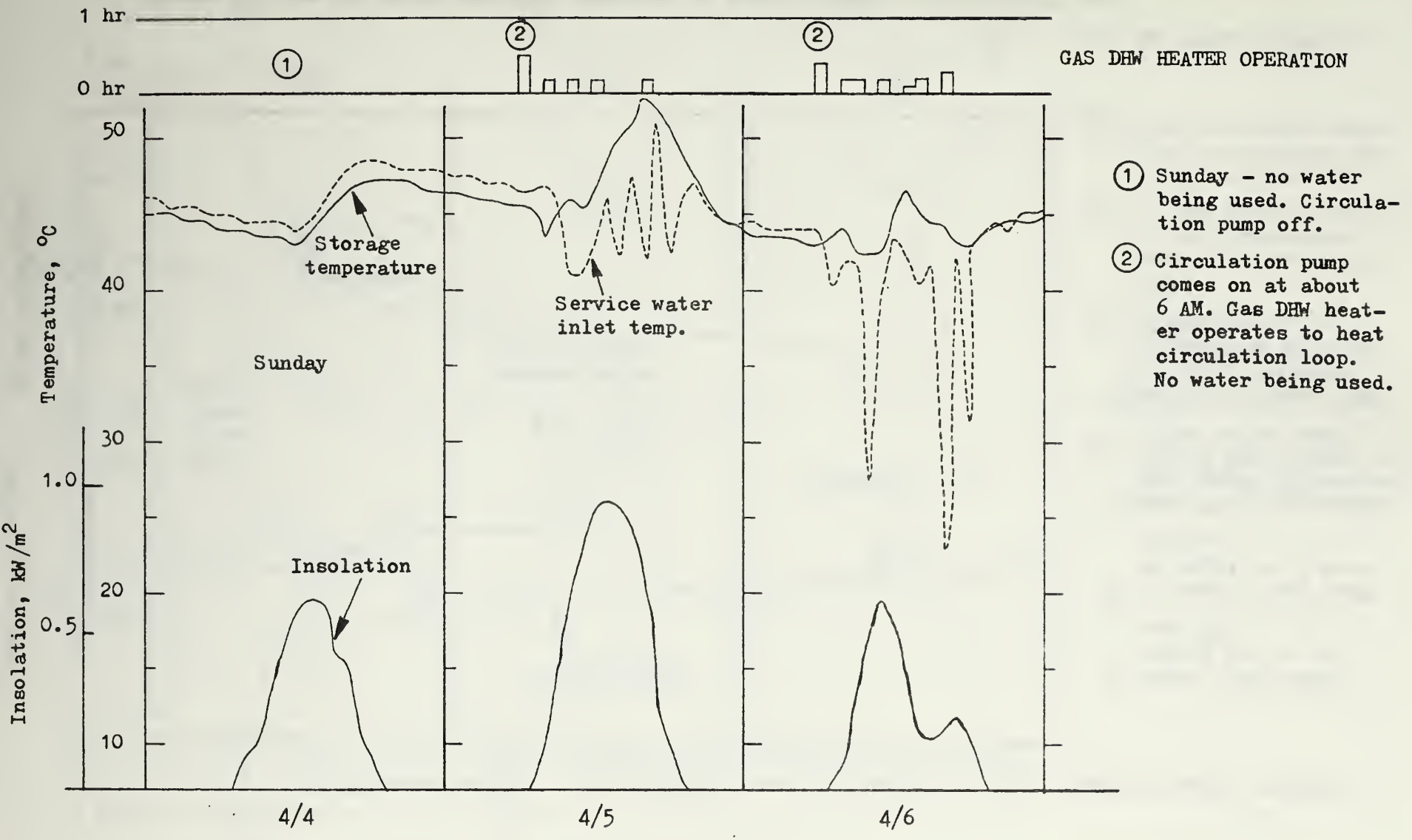

Figure 8: Operation with higher storage temperatures during sunny days.

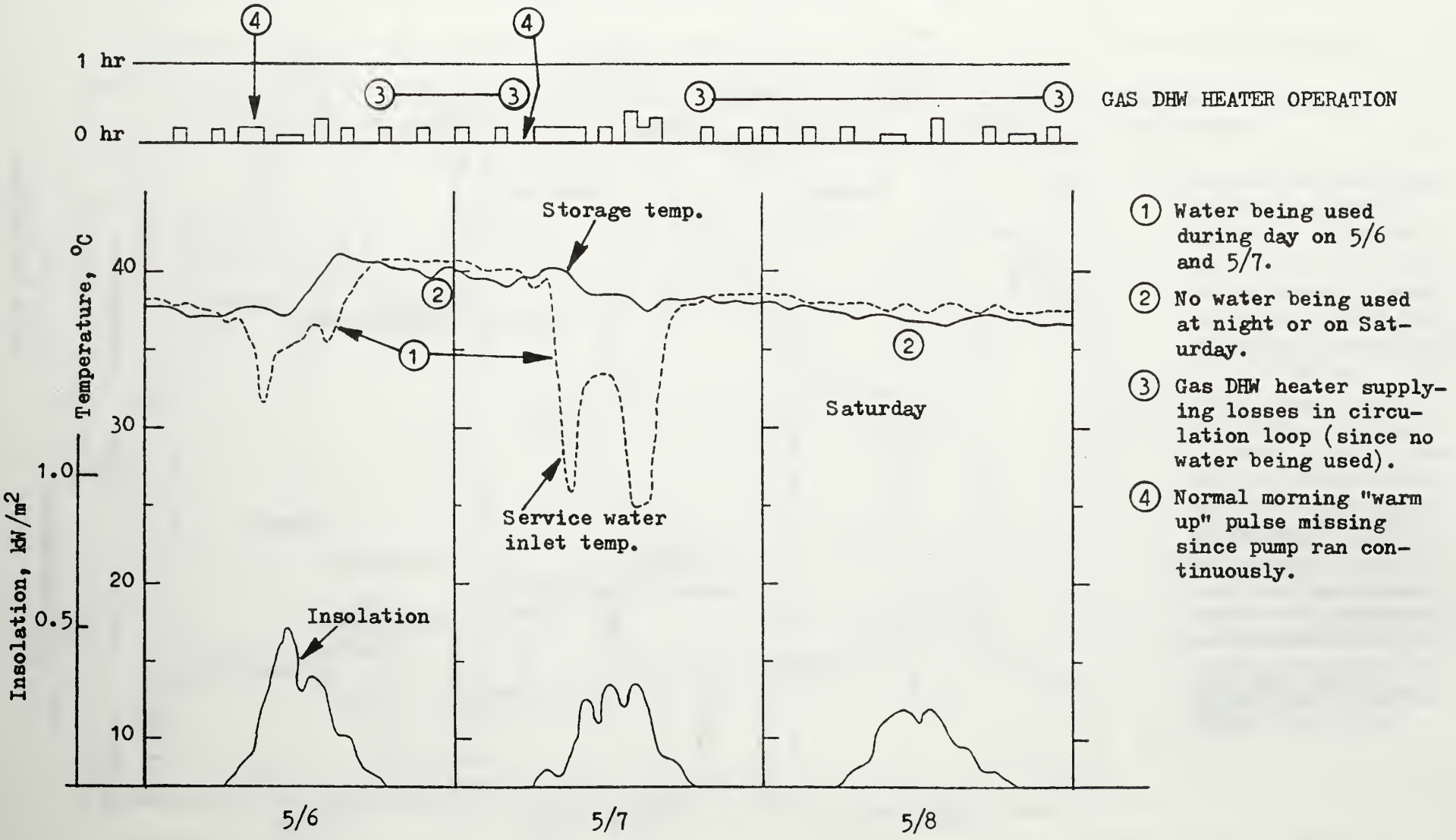

Figure 9: Gas DHW heater operates regularly to supply losses in circulation loop. Circulation pump on all night and weekend.

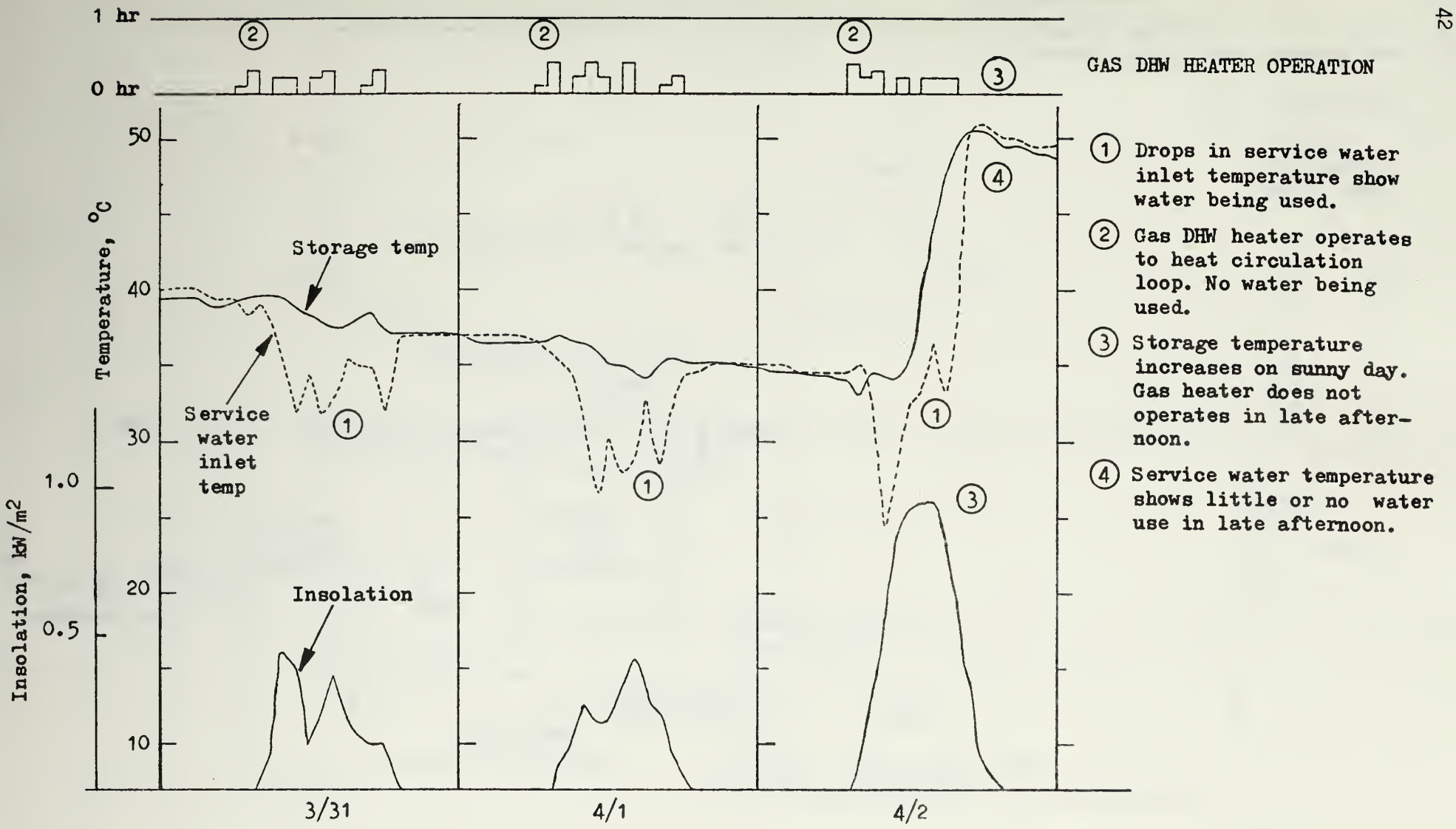

Figure 10: Operation with low storage temperature.

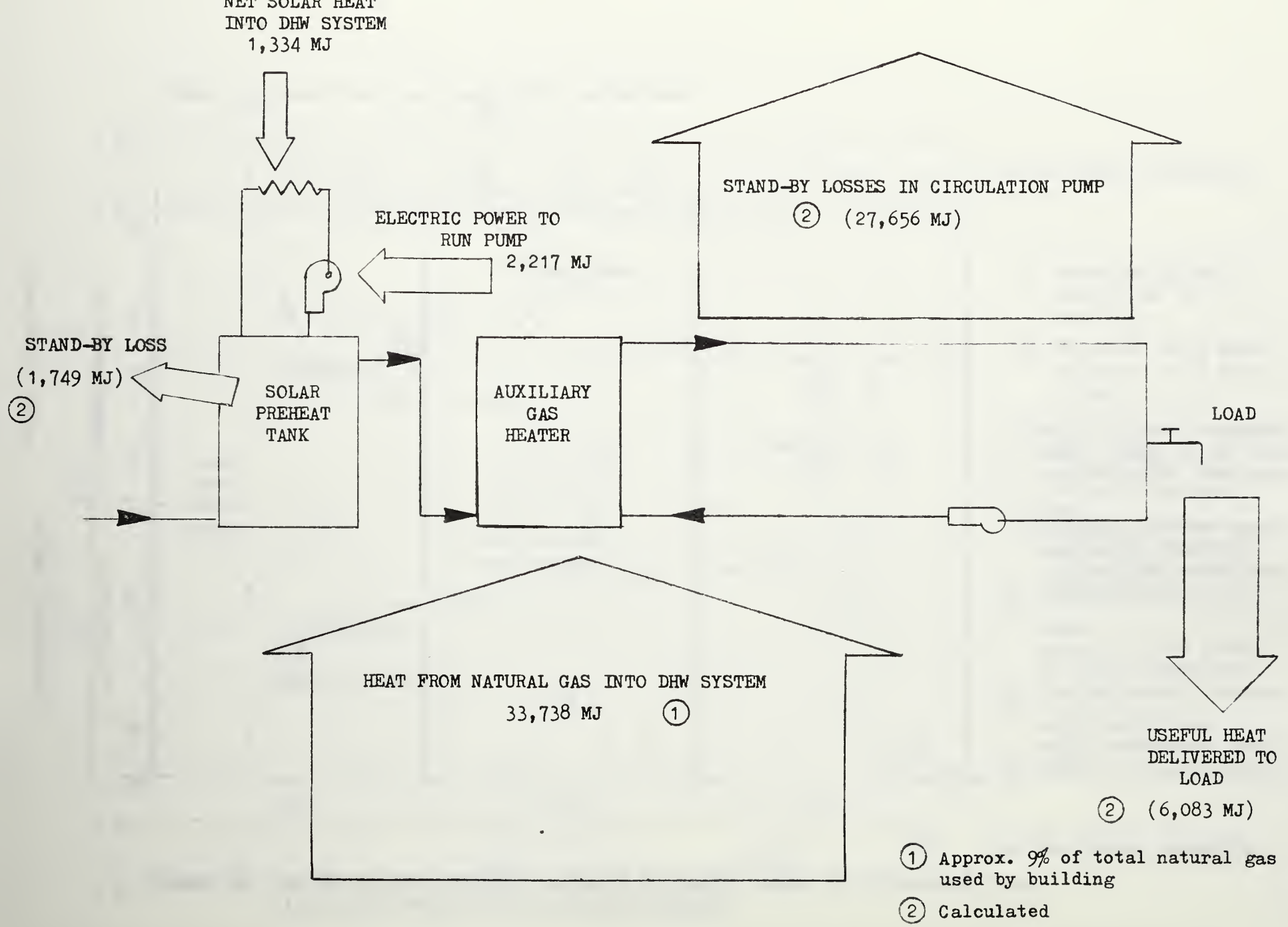

Figure 11: Summary performance of Solar Hot Water System during monitoring period, Jan. 26 to May 11, 1982

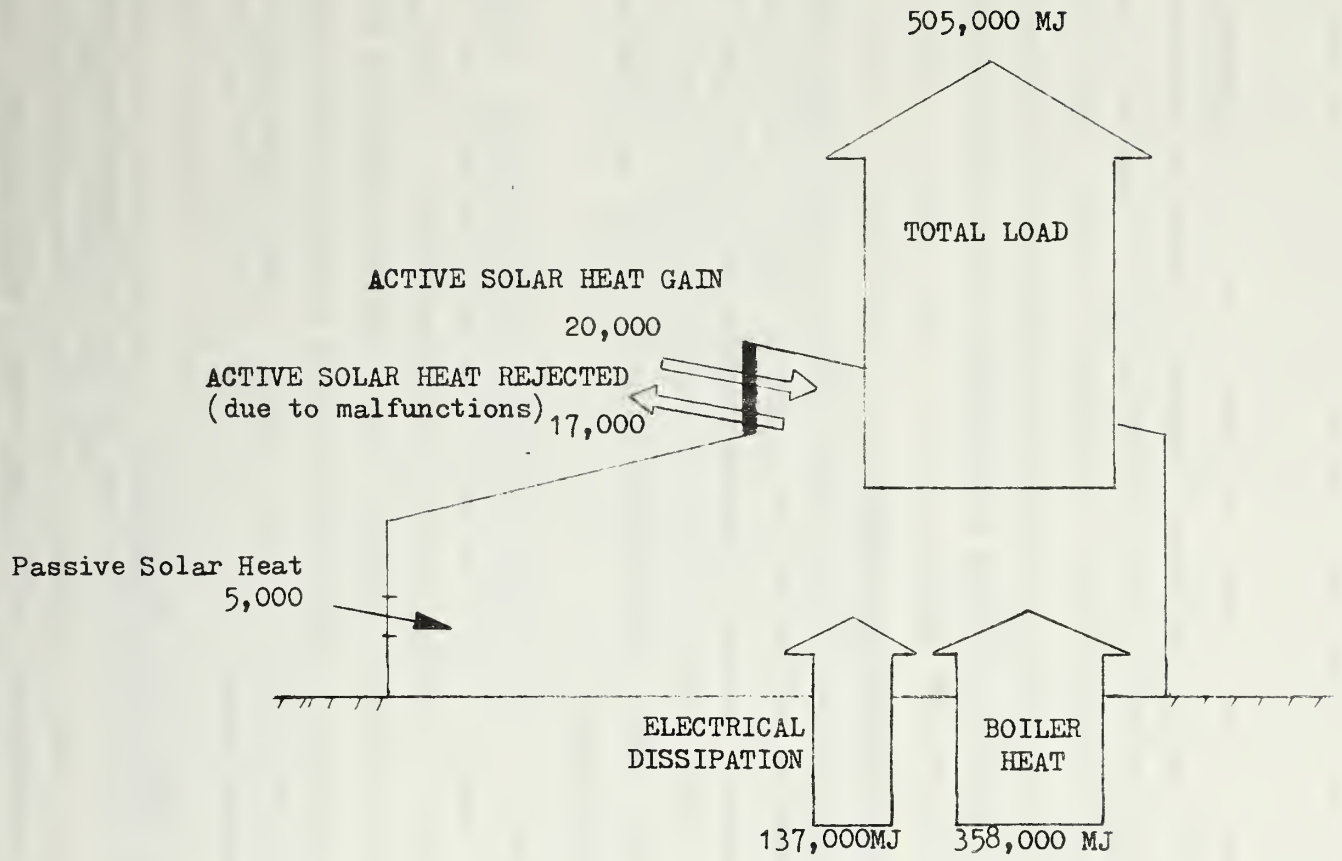

Figure 12: Energy flow summary for B.J.H.S. building

THERMAL PERFORMANCE OF A PASSIVE SOLAR DOUBLE ENVELOPE HOME

ABSTRACT

This paper presents thermal performance data on a double-shell or envelope passive solar residence. The space between the inner and outer shell was instrumented with home-made heated anemometers that were sensitive to air flows in the 0 to 0.5 m-sec^{-1} range. A partitioned heat balance on the inner and outer shell allowed conclusions to be drawn about the relative thermal contributions of the sun space, the air space and the crawl space.

1.0 DESCRIPTION OF THE HOUSE

The house discussed in this report was built about three years ago by Stan Wyatt and is currently owned and occupied by Jim and Barbara Darcy. The house is located near Bozeman, Montana at an altitude of about 1,520 m. There are typically 4,500 heating degree days per year in this region. The house faces 30 degrees west of south and has no significant shading.

The house is of wood frame construction and the overall design of the house closely parallels the early envelope house built near Lake Tahoe and described by Smith and Butler in Reference (1). A photograph of the house is shown in Figure 1. This house was carefully built and the construction, insulation and finish details are excellent. Auxiliary heat is supplied to the house by electric baseboard units and a woodburning stove.

2.0 INSTRUMENTATION AND HARDWARE

The data acquisition system used for the performance monitoring accepts 40 channels of analog input data. Data acquisition and storage is controlled by a Radio Shack TRS-80 microcomputer. Several of these systems have been used over the past three years to monitor 15 solar heating projects. The data system scans up to 40 channels, per-

forms a 12 bit A/D conversion, and processes and displays the data once each five seconds. The data is averaged over hourly periods and the averaged values are stored on cassette tape. This data is subsequently transferred to a larger microcomputer to produce summary reports. The data system accepts inputs from pyranometers or silicon cell radiometers, clamp-on ammeters, status switches, flow meters and temperature transducers. Figure 2 shows the data system located in the sunspace.

3.0 HEATED ANEMOMETERS

Early articles on the envelope design asserted that the purpose of the envelope construction was to allow air to flow by natural convection around the loop. The diagrams in Reference (1) indicated that during the day solar heated air in the sunspace would flow through the roof cavity, down the back wall cavity, through the crawl space where heat was stored in rocks, and then return to the sunspace. The literature asserted that during the night, stored solar heat was liberated from the rocks in the crawl space. Air would flow, by natural convection, up the real wall cavity, through the roof, and back to the sunspace. Diagrams depicting these natural convection loop flows have been reproduced many times in popular technical articles. Reference (1) specifically includes a section entitled, "The Positive Theory of Natural Physical Behavior". This section proposes to demonstrate the physical necessity of the natural convection loop flow based on Aristotle's Theory of Atoms and Newton's Theory of Gravity.

The technical literature includes a number of presentations of monitoring results on envelope houses, (2), (3), (4). Only a few experimentors have reported data on air flow measurements in the loop. This lack of data is unfortunate since the loop flow is supposed to be the basic mechanism of this design and is the reason for constructing the loop in the first place. The practical reason that this flow is seldom measured is that the associated instrumentation for measuring low velocity air flows is relatively expensive.

To measure air flow, we modified three of our normal temperature probes (Analog Devices AD590). A metal film resistor (0.12 W, 720 Ω) was bonded to the face of the AD590 and 12 vdc was applied to the resistor.

The equilibrium temperature of this device in zero velocity air flow is about 27°C above the ambient temperature. As the air velocity increases, the temperature difference, ΔT, decreases as shown in Figure 3. The equation

$$V = 0.006 \times (27.6 - \Delta T)^{0.5} \qquad [1]$$

closely fits the experimental data from Figure 3, where V is air velocity in m-sec^{-1}.

To use this device, both a heated probe and an unheated probe are placed in the region where air flow is to be measured. The data system samples the temperature of the heated probe and the unheated probe, calculates the difference, and substitutes that value into Equation [1].

Figure 4 illustrates the final results of this device. Shown on the abscissa are the reference velocities as indicated by a Model 1650 hot-wire anemometer produced by Thermal Systems, Incorporated. On the ordinate are values of velocity calculated from the measured ΔT's using Equation [1]. These readings are contained within an error band of less than .05 m-sec^{-1}.

Due to the thermal mass of the resistor and temperature transducer, several minutes are required for the device to come to thermal equilibrium when the air velocity is on the order of 0.1 to 0.5 m-sec^{-1}. This response is adequate for measuring hourly average flows. Each transducer pair was individually calibrated for a range of stagnation temperatures of 15 to 30°C. An expression in the form of Equation [1] fits the data over this range of stagnation temperatures to within .05 m-sec^{-1}.

4.0 INSTRUMENTATION LAYOUT

A schematic of the instrumentation layout is shown in Figure 5. Silicon cell solar radiometers were situated inside the glass on both the vertical and sloping sections of the sunspace. These radiometers were calibrated in place to agree with a recently calibrated Epply PSP pyranometer. Shaded temperature probes were mounted in the lower and upper sunspace and in the roof cavity as shown in Figure 5. Three pairs of heated anemometer probes were located at the midpoint of the channel in the north wall. These probes were distributed at three stations across the

north wall and located at a height of 2.5 m above the crawl space.

An air temperature probe was located at the midpoint of the crawl space and a second probe was buried to a depth of 10 cm in the rock storage floor of the crawl space. Ambient air temperature was sampled in a shaded location on the north side of the building. The clamp-on ammeters measured the total electrical current entering the house. A third clamp-on ammeter measured electric current through the domestic hot water heater located in the crawl space. These ammeters were calibrated on-site against the utility kWh meter.

The interior house air temperature was sampled at three locations, as indicated on the diagram. An additional temperature probe was mounted to an aluminum bracket which was attached to the wood stove in order to estimate the contribution of this device.

5.0 HEAT BALANCE

Separate heat balances were performed for the inner space and the loop space. The heat losses from each of the spaces were divided into elements consisting of the south wall, the roof, the north wall, the floor and the side walls. The heat conducted through each of these elements was assumed equal to a calculated U value multiplied by the measured hourly average temperature difference across the element. The south facing glazed elements in the outer shell were assumed to contribute a solar gain equal to the measured solar radiation multiplied by the appropriate glazed area. The solar gain through the windows in the south facing wall of the inner house was calculated by multiplying the measured vertical solar radiation into the sunspace by two factors to account for transmission loss and shading.

The heat added to the inner house due to electrical dissipation was taken as the measured total electrical input to the house reduced by 0.6 of the electrical energy going to the domestic hot water heater. The heat from the wood stove was estimated by multiplying the temperature of the stove minus a remote house air temperature by a suitable constant. This constant was determined by trial and error in order to achieve a heat balance. The stove drew combustion and circulation air from the crawl space. The infiltration losses of the

inner and outer shell were increased when the stove was used.

The outer shell was assumed to have electric gains equal to the stand-by losses of the domestic hot water heater plus 300 W to account for the dissipation from two freezers located in the sunspace. A heat storage term based on hourly air temperature changes was included in both the interior and the shell heat balance equations. The equation for the heat balance of the inner shell is:

$$Q_{electric} + Q_{wood} + Q_{solar} + Q_{stor} = Q_{loss}^{1}. \qquad [2]$$

The heat balance equation for the outer shell is:

$$Q_{solar} + Q_{electric} - Q_{loss}^{1'} + Q_{stor} = Q_{loss}^{2}. \qquad [3]$$

In these equations, Q_{loss} is the algebraic sum of the $U \times \Delta T$ for each element enclosing the space. Note that the heat losses from the inner space (except the side wall losses are heat gains into the shell, $Q_{loss}^{1'}$ in Equation [3]. These heat balances were calculated on an hourly basis, a daily average basis, and a monthly average basis.

The total electrical power entering the house as measured by the amp-clamp was compared to the utility bills for the month of January and the results agreed to within 2%. During the test period, there were several intervals of one to three days when little solar energy and little or no wood energy entered the building so that the house was heated primarily by electricity. These test periods can be viewed as coheating periods for which the energy input to the house is well known. The calculated heat loss coefficients and average infiltration rates for the house were adjusted to effect accurate hourly and daily heat balances during the coheating periods. Segments of data when the wood stove was the primary source of heat were then inspected. An empirical equation for wood stove heat was derived which produced satisfactory hourly and daily heat balances. The effective thermal storage masses in the interior and exterior shell were adjusted to smooth the hourly heat balances. The final value of storage mass selected was 3.5 kWh per degree Celsius air temperature change.

The iterations on the hourly, daily and monthly heat balance equations were repeated until there was less than 10% average error in the heat balances. The data was then summarized over the entire monitoring

period. Figure 6 shows the results of the total energy flow through each "element" of the structure for the months of January and February. The solar, electric and wood inputs into the inner and outer shell are depicted as large arrows. The conductive and infiltration losses are depicted by small arrows located near their respective elements.

Looking first at the inner shell, the largest heat losses are through (a) the floor, (b) the side walls and (c) the wall separating the inner house from the sun space. The loss in the floor is large because it is not insulated. The original design premise supposed that heat would be transferred from the crawl space into the house. This is clearly not the case. The sidewall losses are great because of the large ΔT existing across these walls. The loss from the inner house to the sunspace is large because this wall contains a relatively large area of glass.

Looking next at the outer shell, the largest heat losses are through the sunspace. The conductive loss of 3,238 kWh is actually greater than the solar gain of 3,164 kWh. The infiltration losses also appear quite large. The infiltration losses were not measured directly but were based on a constant 0.5 air changes per hour in the shell. This value was assumed to be accurate because of satisfactory heat balances on a majority of the days. We did notice an increase in heat loss on windy days which would be explained by an increased infiltration. Losses through the roof and north wall are small.

Figure 7 shows a summary of the average temperatures during January and February. The average daily maximum and minimum temperatures are also shown for the sunspace and the interior house, since these values help establish the relative success of a passive solar design. The sunspace shows large temperature swings as the space responds to large solar gains during the day and large losses through the uninsulated glass at night. The temperature swings in the upper part of the inner house average 4.8°C. This room is used as a master bedroom and has its own thermostatically controlled electric baseboard heaters. The temperature swings in the lower part of the house are considerably larger (10.8°C). The wood stove is located in this portion of the

house and there is a large area of glass in the wall dividing this room from the sunspace. When the occupants are not at home, they allow this space to cool off and when they come home they often build a fire in the wood stove, which produces relatively high temperatures. The temperature swings measured in this space, therefore, reflect the habits of the occupants and the use of wood heat, as well as the strong coupling to the sunspace.

The average temperature indicated by the probe buried 10 cm beneath the rocks in the crawl space was 11.0°C while the probe in the crawl space air averaged 10.8°C. This average temperature difference is slightly greater than the calibration accuracy of the probe, which is typically 0.1°C. This data could suggest either heat transferred up from the earth into the crawl space and/or heat radiated from the warm floor to the rocks. At this point there is inadequate data to draw conclusions. The amount of heat exchanged is small and is consequently of little importance to the performance of the house. The average temperature swing of the probe buried in the rocks in the crawl space was 0.7°C. From these data we can conclude that the rocks are not an important heat storage element in this system.

6.0 AIR FLOW MEASUREMENTS

During the two month monitoring period, there was no indication of air flow in the back wall greater than the resolution and accuracy of the measuring system. The anemometers registered a very small but measurable flow on days when the wind was blowing and on a few nights when the ambient temperature dropped to -20 to -30°C. On windy days, these readings were apparently due to increased infiltration and drafts driven by the wind. On extremely cold nights, a small "apparent flow" was judged to be due to radiation from the heated probe to the walls.

Any air flow in the loop would have to be driven by a thermal gradient existing between the air in the sunspace and the air in the north wall. Figure 7 shows that for the two-month period, the average temperature gradient between the lower sunspace and the north wall was less than 1°C. Hourly data also showed only small gradients here.

The driving force for flow appears small. This evidence agrees with the anemometer measurements.

Don Aitken has suggested that sometimes the air is not "smart" enough to follow the arrows drawn by architects or solar entrepreneurs. It appears what we have here is a case of dumb air. This shortcoming may be due to the effect of altitude or perhaps the lack of air pollution.

7.0 THE ROLE OF THE LOOP

The roof and rear walls of both the inner and outer shell contain equal amounts of insulation. If the "loop" or air space had been closed off from the sunspace and the crawl space (or eliminated entirely), the average temperature at this mid-point would have been about half-way between the interior air and exterior air temperatures, or 8 to 9°C, during the monitoring period. The average temperatures measured in the air space were 12.5°C in the north wall and 15.5°C in the roof cavity. This data implies that the inner shell losses through the roof and north wall were less than the hypothetical "no space" wall and that the corresponding outer shell losses were greater than the "no space" wall. The data also raises the following questions: Why is this air space warmer? Where does the heat come from? Does this heat come from the sun?

Figure 6 shows that the conduction and infiltration losses of the sunspace exceed the solar gain. Thus the shell does not, on the average, receive a net solar gain. The heat conducted up from the earth into the crawl space was estimated at 284 MJ. Even if this crude estimate is doubled, its magnitude is still small compared to most of the remaining energy fluxes in the system. Thus, the air in the shell is not primarily heated by contact with the earth.

Figure 6 shows that losses from the inner shell through the uninsulated floor are 1,426 MJ. The losses through the south wall of the inner shell total 655 MJ, primarily due to the large areas of glass. We conclude that the heat losses through the floor and south wall of the inner shell are the primary sources for heating the air in the loop to

a temperature above the "no space" condition.

8.0 INSOLATION COMPARISON

During the period from January 6 to March 3, the daily average transmitted insolation at the envelope house site was 2.19 $kWh\text{-}m^{-2}$ on the vertical plane and 1.89 $kWh\text{-}m^{-2}$ on the 59° tilted plane, Figure 7. I initially thought there must be an error in the results, but a calibration check of the transducers showed them to be accurate. We had collected comparative data in Bozeman for 60° and 90° insolation during the previous winter for two south-facing transducers. This data showed the average 90° insolation to be about 0.88 times the 60° insolation.

There are three points which help to explain this data: (a) The house is oriented 30° west of true south so the relative azimuth angle of the glazing becomes zero at about 2:30 p.m. in January. At this hour, the angle of incidence for both glazings is nearly the same (13 to 17°). For the remainder of the afternoon, the angle of incidence of the vertical glazing is less than the slanted glazing. (b) The ground in front of the glazing slopes down at about 5 to 10° and was always snow covered during the monitoring period. These conditions would produce a large reflected radiation component (estimated to be up to 25% of the total insolation transmitted through the vertical glazing). (c) The slant glazing is occasionally covered with snow for part or all of the day. The vertical glazing is almost never snow covered.

9.0 CONCLUSIONS

(1) The anemometers measured no air flow in the loop greater than 0.05 $m\text{-}sec^{-1}$ (their limit of resolution).

(2) Heat losses from the sunspace were greater than the solar gains during the monitoring period, January and February.

(3) The air space in the roof and north wall was warmer than a hypothetical "no space" roof or wall. This feature was not a net benefit since this heat came primarily from losses through the floor and south wall of the inner house.

(4) The crawl space contributed a small apparent heat flux from the earth. The crawl space was not an important thermal storage element.

(5) Temperatures in the sunspace were always above freezing, making this area suitable for growing plants. The attached sunspace provides spectacular views and is, in my opinion, a visually attractive feature. The sunspace would certainly provide a net solar gain during the spring and fall when ambient temperatures and insolation are greater.

10.0 REFERENCES

(1) Smith, T. and Butler, L.P., The Energy Producing House, Tahoe City, California, 1979.

(2) Jones, R. F., et.al., Case Study of the Mastin Double-Envelope House, Brookhaven National Laboratory Associated Universities, Inc., Upton, New York, for the Department of Energy and Environment, May, 1981.

(3) Chen, B., et. al., "Performance Results of the Tom Smith Double Shell Residence, Lake Tahoe, California," Proceedings of the 5th National Passive Solar Conference, Amherst, Massachusetts, October, 1980.

(4) Akridge, J. M. and Benton, C. C., "Performance Study of a Thermal Envelope House - Final Report, Phase I," College of Architecture, Georgia Institute of Technology, May, 1980.

Figure 1: The Darcy/Wyatt envelope house

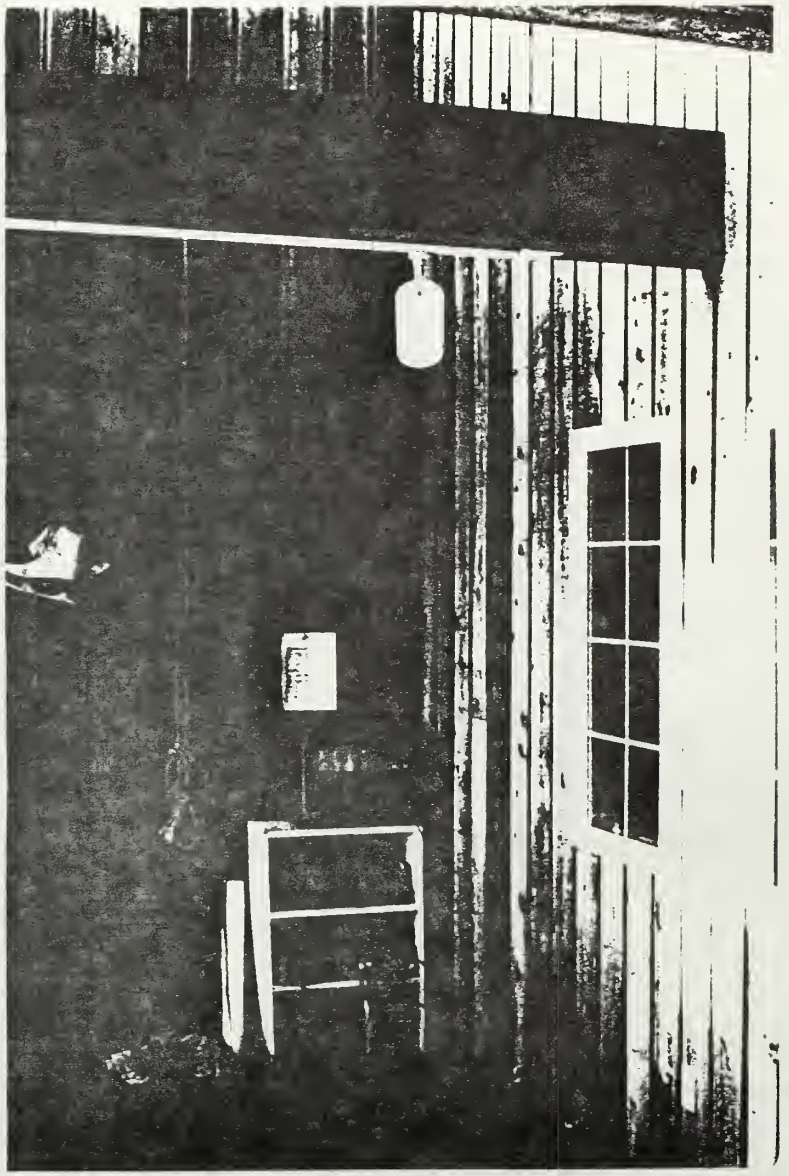

Figure 2: Data acquisition system in sunspace

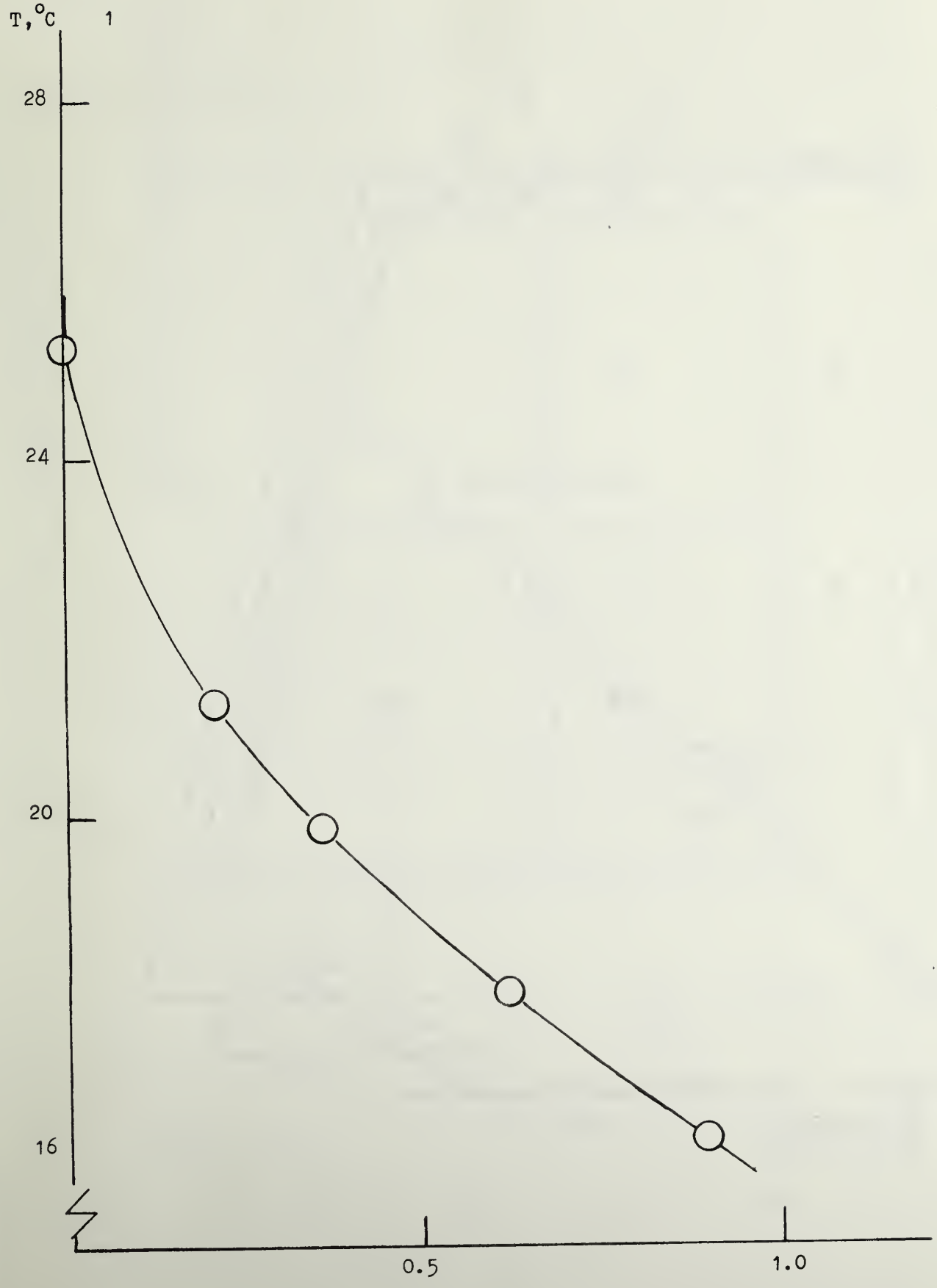

Figure 3. Cooling characteristic of heated probe.

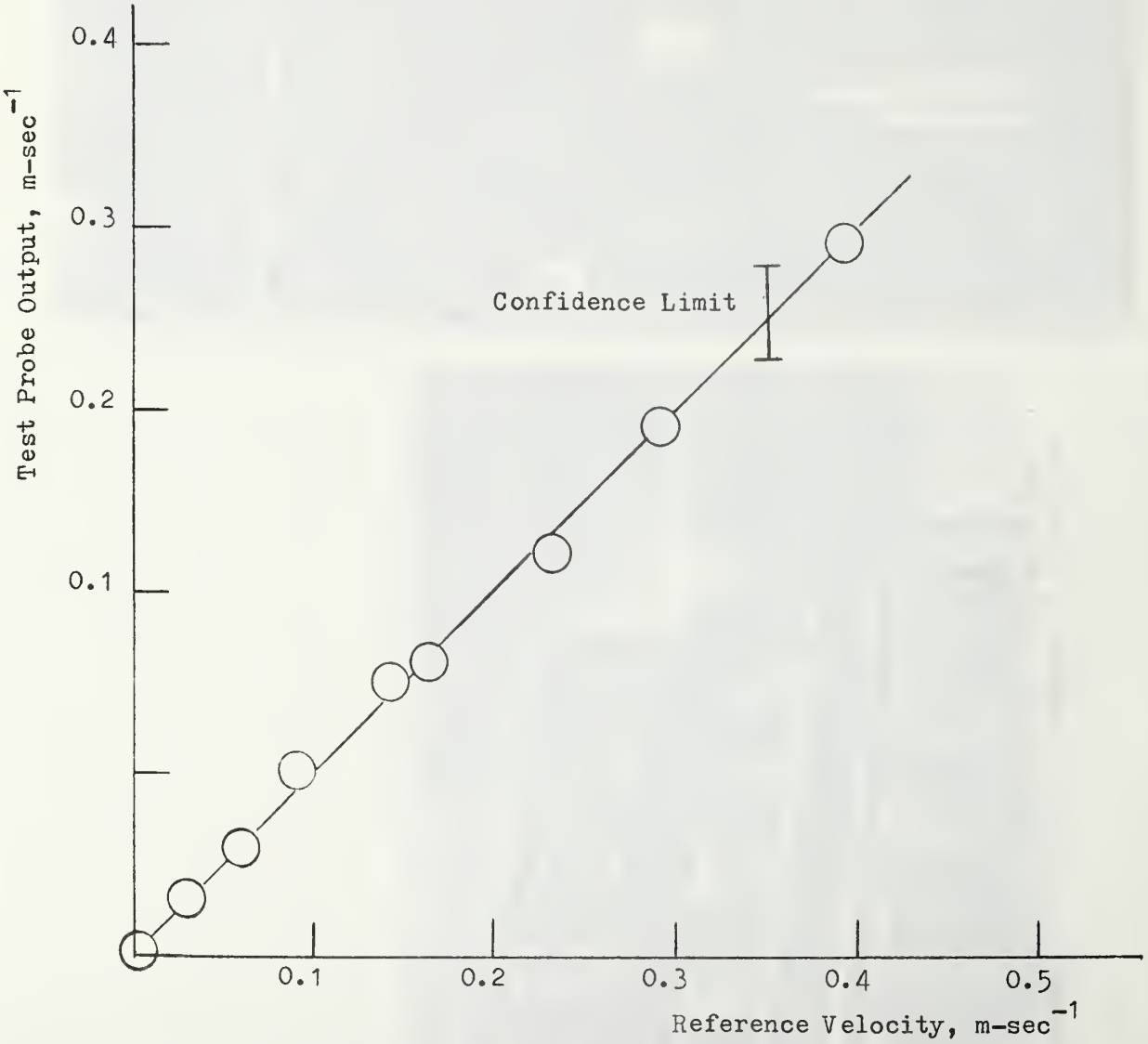

Figure 4. Overall performance of anemometers.

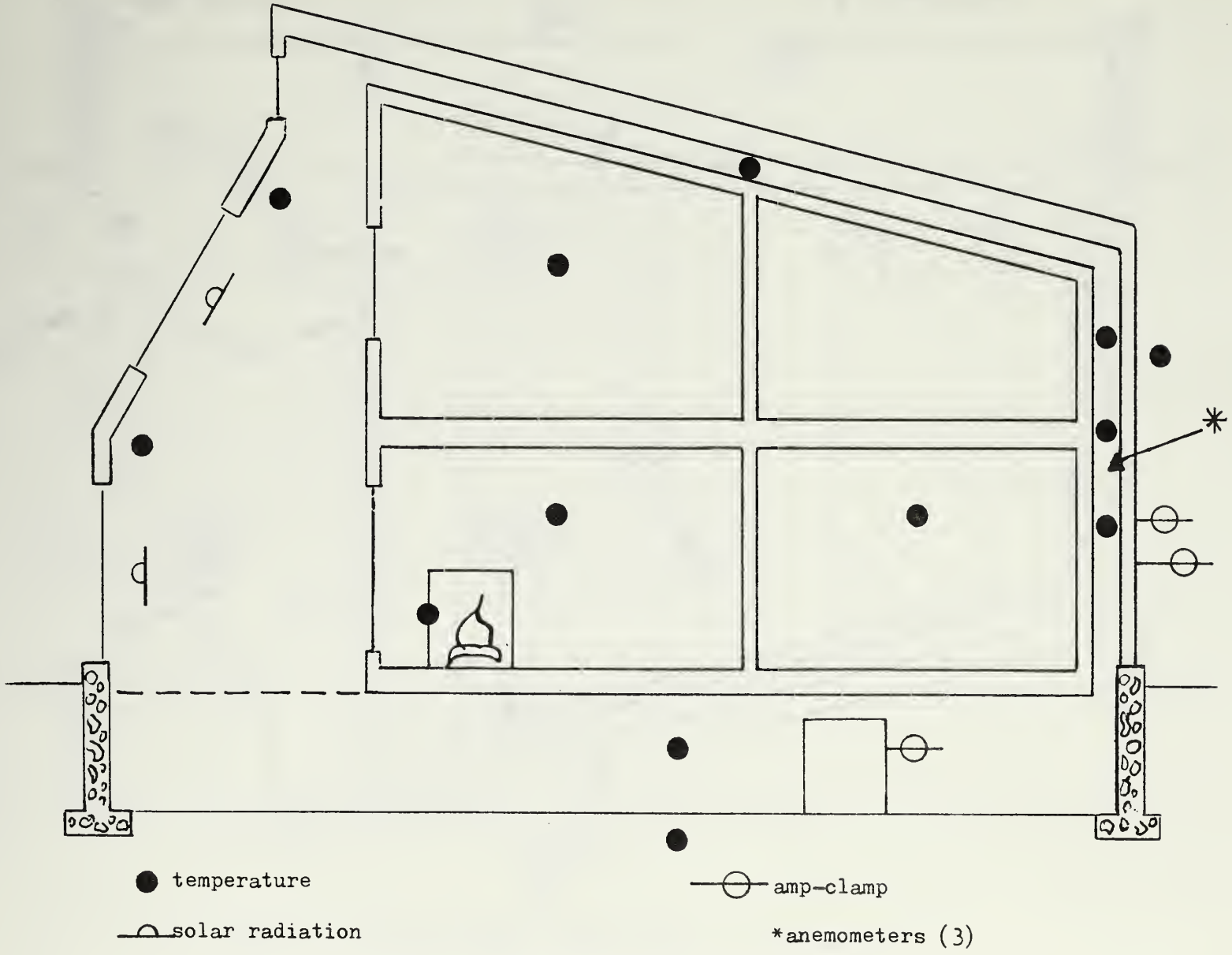

Figure 5. Instrumentation layout.

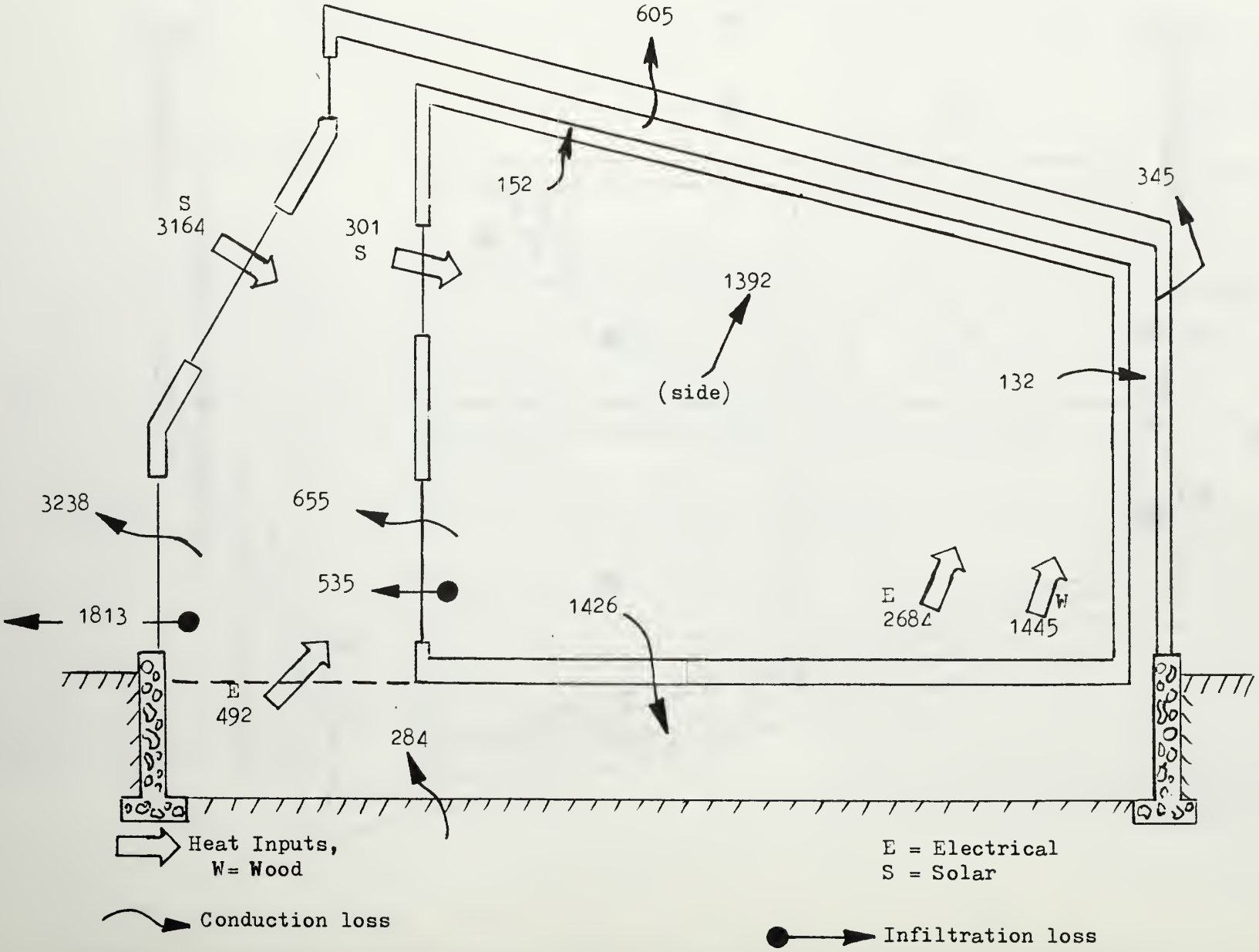

Figure 6. Distribution of total heat inputs and losses for the period from 1/6 to 3/3.

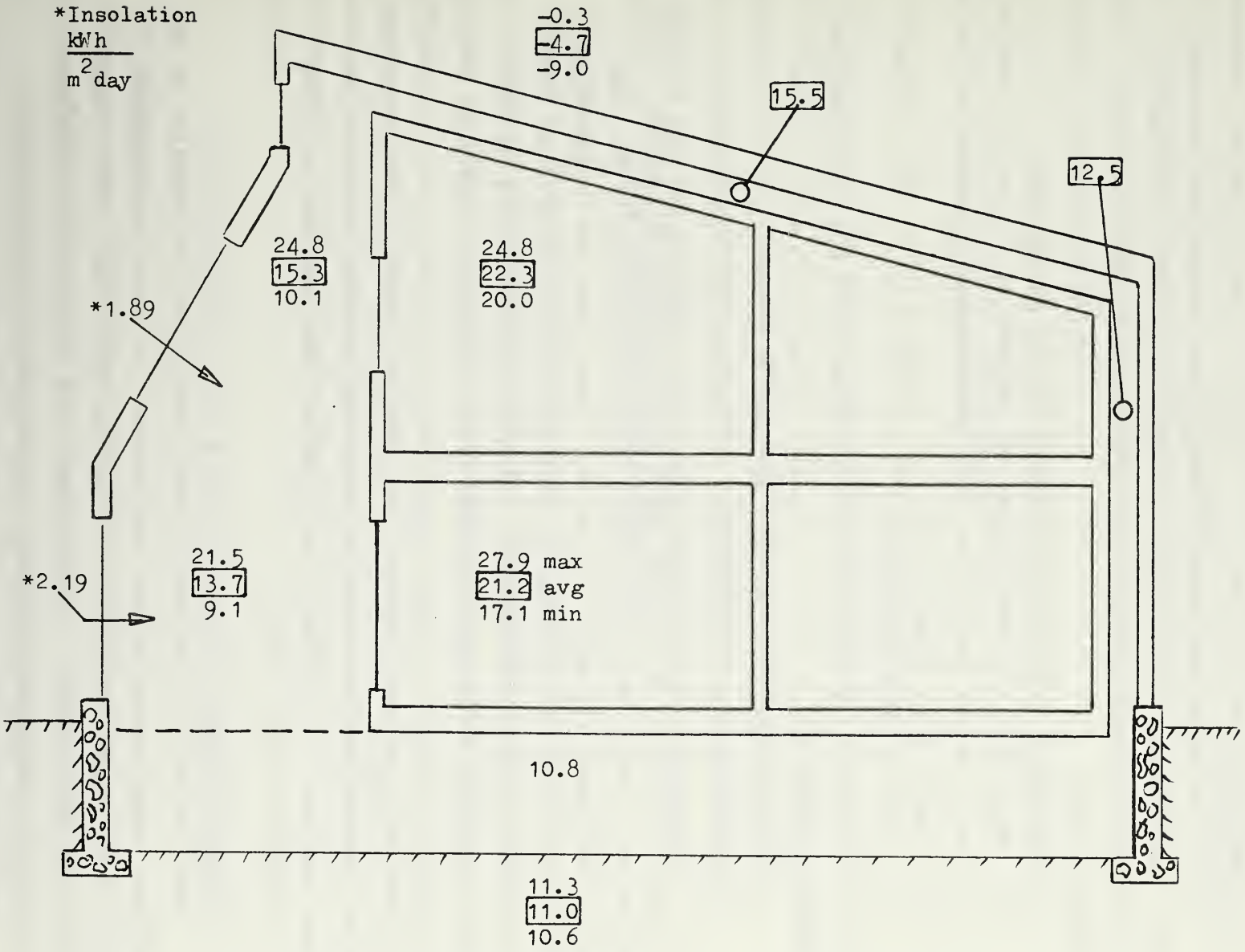

Figure 7. Daily average temperatures, °C, 1/6 to 3/3.

CLASS C SURVEY PROJECTS

1.0 Introduction

Six solar systems were surveyed using Class C methods and estimates made of their thermal performance. The input data for the performance was primarily collected during an on-site visit and consisted of the following items:

(a) Utility bill records for natural gas and electricity
(b) Other auxiliary fuel records and estimates
(c) Solar system description, size, principals of operation
(d) Owners data, comments, etc.
(e) Data for load calculations

The on-site data was supplemented with monthly, yearly and average environmental values for

(a) Solar radiation near site (DNR&C, SIMM program)
(b) Temperatures and degree-days (National Weather Service)

The data was analyzed to estimate how much solar energy each system would deliver on an annual basis. The error bands on these results are large due to the fragmentary nature of the input data. Past work for DNR&C in which solar systems were carefully and thoroughly instrumented has shown a variety of performance anomalies. Every active-air solar system monitored had serious leaks and unexpected modes of behavior. There are several documented examples in these reports where the system would effectively pump hot air out of the structure. The results of this Class C performance survey have suggested that some of the systems surveyed have some operational problems. The mechanism and nature of these problems could only be established with more data.

2.0 Analysis Method

The first step in the analysis was to define the load supplied by the auxiliary energy system and the solar system. For solar space heating projects the heated envelope was measured and insulation levels documented during the on-site visit. An ASHRAE heat load calculation was performed and combined with annual degree-day data to predict TOTAL HEAT LOAD.

The fossil (utility bills) and solid fuel records were processed and summarized to estimate net AUXILIARY HEAT INPUT. Typical conversion efficiencies were assigned to the individual energy conversion devices.

The theoretical thermal performance of each solar system was calculated using standard f-chart design methods for the average environmental conditions. The manufacturers collector efficiency curve was used when available. Site-built collectors were classified and proto typical efficiency curves for that design were input to f-chart. This calculation produced an estimate of SOLAR HEAT INPUT for the system, assuming the system was performing perfectly.

The law of conservation of energy demands that the inputs must equal the outputs. Formulated in terms of the energy quantities defined for these systems the energy balance equation is

SOLAR HEAT INPUT + AUXILIARY HEAT INPUT = TOTAL HEAT LOAD

This equation formed a test which was used to identify errors and make refined estimates of the energy components. Since no component was independently measured to high accuracy the results are necessarily subject to unknown errors. The results for each project were reviewed using all the data that was available and we think they represent "reasonable estimates" or a "best effort" given the limited data.

3.0 Presentation

Each of the Class C monitoring projects is described with solar system schematics and photographs. The heat load calculations are presented and a narrative description of the project and interpretation is included.

An average ANNUAL SUMMARY table for each project illustrates our best estimate of the average energy load, solar energy and auxiliary energy contributions. A solar fraction is presented for each project which is defined as:

SOLAR FRACTION = SOLAR ENERGY/TOTAL HEAT LOAD

4.0 Acknowledgements

The cooperation of the owners of all the solar projects is gratefully acknowledged. They shared their time, opinions and data which enabled us to do this work. They have clearly invested large amounts of work, money, thought and enthusiasm in their projects. Their tenacity in pursuing novel and individualistic solar designs is admirable.

Jim Baerg is acknowledged for collecting the site data, writing the

narrative descriptions and contributing to the interpretation of the data. His long experience with owner built solar energy systems and his thoughtful intuition was very valuable in accessing the performance of these projects.

HORIZON LODGE SYSTEM

The Horizon Lodge, a 84 unit Retirement Complex, in Conrad, MT., has a large solar domestic hot water heating system. This system consists of 4 racks(1,000 ft^2) of Sunworks collectors mounted on the building roof, two 800 gallon storage tanks, shell and tube heat exchanger, plumbing lines, and controlls mounted in a converted utility room on the main floor. The system was professionally installed and used off the shelf components. Engineering was by Drapes Engineering of Great Falls, MT.

Of all the solar systems investigated, this system has fewer obvious problems. One problem area is heat loss from the uninsulated pipes, within the building. The exterior piping on the roof is insulated but the foam insulation is deteriorating, has gaps around the fittings and does not cover the numerous valves.

A water meter measured the hot water used and another meter measured the MCF of natural gas consumed by the auxiliary water heater. A short-term performance test by Drapes Engineering in August 1979 showed a solar contribution of 35% and a boiler efficiency of 69%.

We conducted a similar analysis spanning a time period of 1332 days between 8/31/79 and 4/28/83. Over this period 1,650 x 10^6Btu of natural gas heat was used and 1,830 x 10^6Btu of energy was required to heat the water. Simple subtraction implies that 174 x 10^6Btu of solar energy was used. The expected solar contribution calculated using f-chart is 166 x 10^6Btu/year or 605 x 10^6Btu over the 1,332 day sample period. This data implies that the solar system is less than 1/3 as efficient as it should be.

The system includes a circulation loop to insure that hot water is readily available at the point of use. This is normal design procedure in large buildings. An approximate analysis shows that the heat losses from this circulation loop could be on the order of 400 x 10^6Btu over the sample period. If this loss is added to the load the implied solar energy is much closer to the f-chart prediction.

Observations of the storage tank temperature show a typical peak of 125°F. The collector array should provide a 52°F temperature rise on an average sunny day if no water was used. These observations thus seem reasonable for a working solar system. The hot water is primarily used in the morning which would tend to reduce the overall efficiency of the solar system.

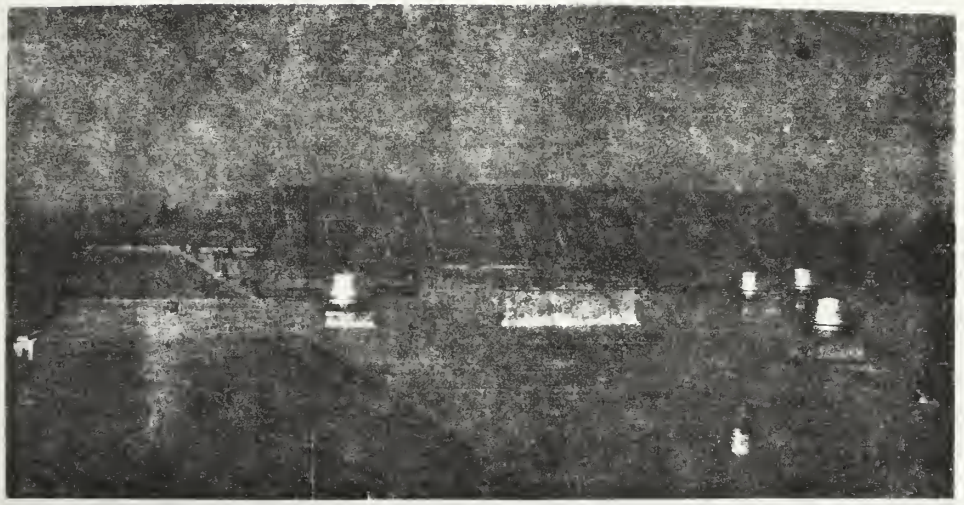

Collector array on roof

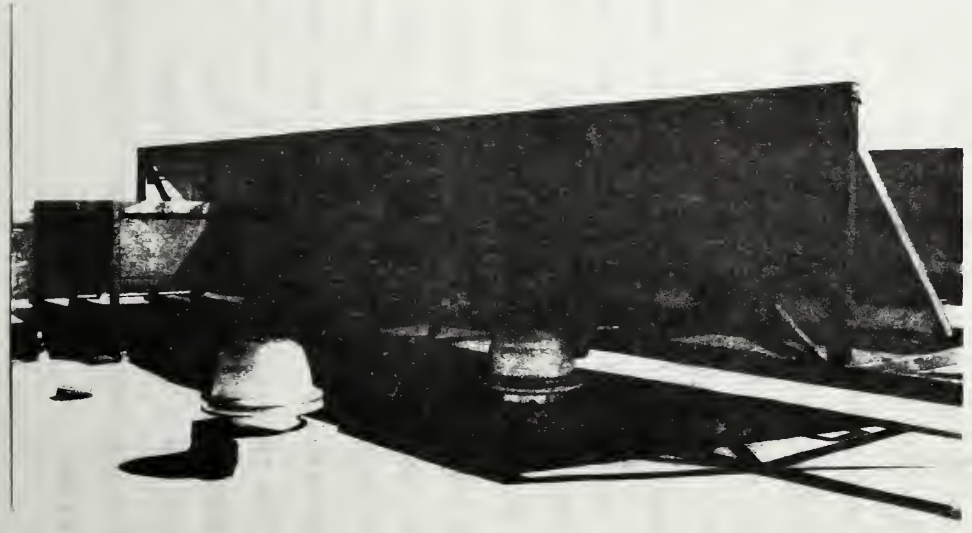

Dissipator for temperatures over 212°F

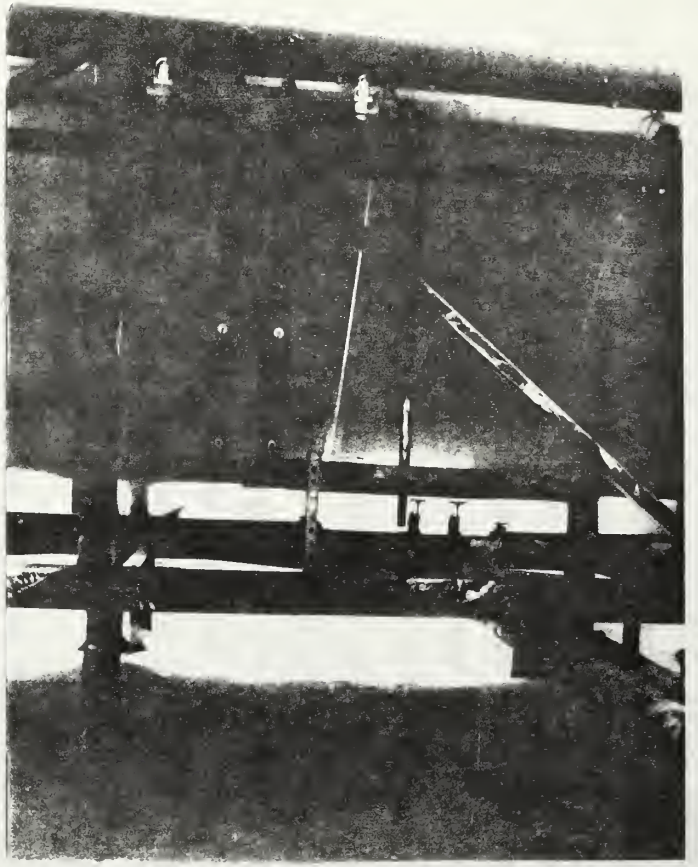

Photo showing insulation on manifold piping

Horizon Lodge System

An accurate and final assessment of the solar system is not possible due to incomplete data. The data available imply a year round solar contribution of at least 10%. The calculated annual contribution to the hot water load is 38%. The actual load will exceed this hot water load by the amount of the losses which are presently unknown.

Improving system efficiency necessitates a thorough monitoring. Major Caldwell, the building administrator also recommends separating the apartment hot water which needs only 120°F water from the cafeteria which needs 140°F to 180°F water. The cafeteria would need a separate heater to raise the water to use temperature. This should lower energy consumption therby raising the annual solar fraction.

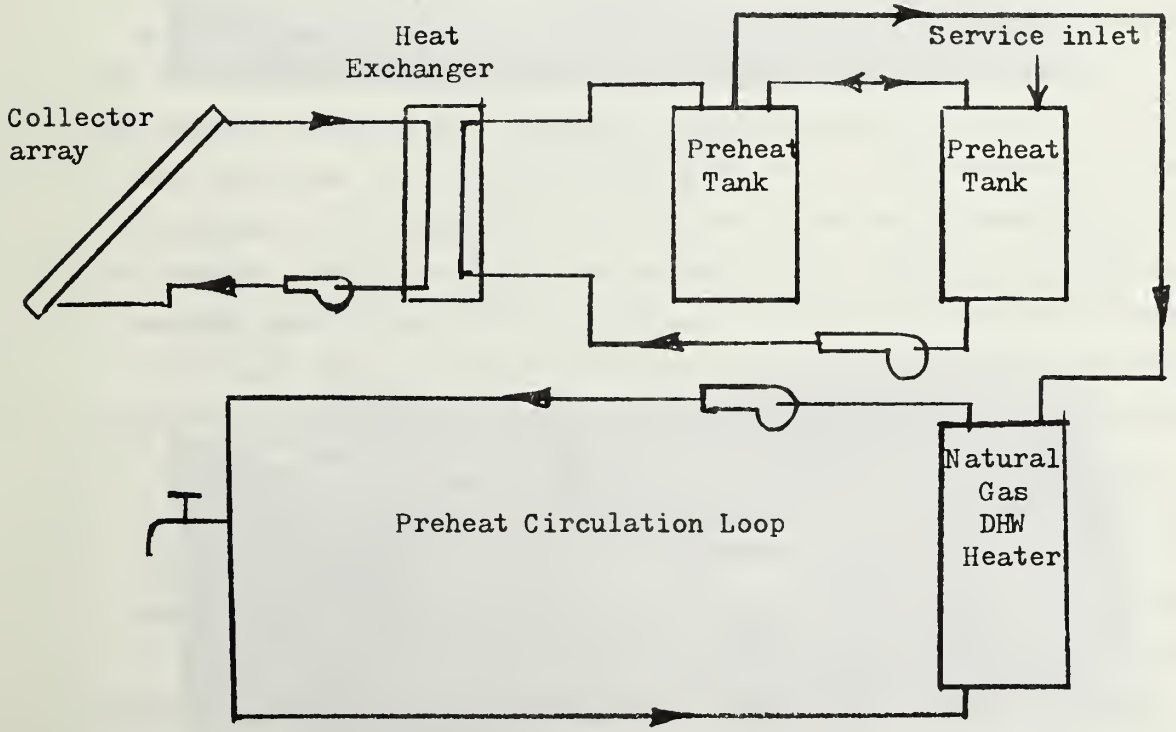

3.6 YEAR SUMMARY	
HOT WATER LOAD	1,830 x 10^6 Btu*
NATURAL GAS HEAT	1,650 x 10^6 Btu
SOLAR HEAT	174 x 10^6 Btu*

* see text

JOHN ALLENMEIER SYSTEM

John Allenmeier constructed a air collector system for space heating using a renewable energy grant fund. This system consists of 360ft^2 of single glazed collector mounted on a sloped surface which is the south wall of his garage. A 4' x 4' x 30' rock storage bin is located under the floor of his garage and two, 18" by 22' long culverts duct air underground to the finished basement of his house.

The collector absorber uses black metal shavings which came from a manufacturing facility in Havre. Chicken wire holds the shavings in place. The glazing cover is 1 layer of FRP. The backing of the collector is a layer of fiberboard sheathing and 2" of 150 cyanuriate (thermax) which has numerous gaps. The ducting is neither insulated nor duct taped. The culvert is insulated with 2" of polystrene.

Hot air is either directed to the house via the culverts or dumped in the top of the rock bin. This bin has 2" of polystyrene insulation on the sides, none on the top (hottest area) or bottom. The garage, although well insulated, is unheated and has a leaky 16' garage door on the windy west side. A lot of heat is probably lost through air leaks in the ducting and via conduction through the 4" slab on top of storage. Mr. Allenmeier experiences a maximum of 2 hours of useful heat from the storage system.

Within the house, the inlet and outlet are side by side which probably results in short circuiting of distribution, sending warmer air back to the collectors.

There is a 3/4 - 1" air space between the metal shavings and the glazing. Probably much of the air passes on top of the shavings rather than through them. A second layer of glazing should improve performance substantially.

No data was available on the solar system itself. Since the house is electrically heated the auxiliary energy use is well measured. When this is compared to the calculated heat load a negligible contribution remains.

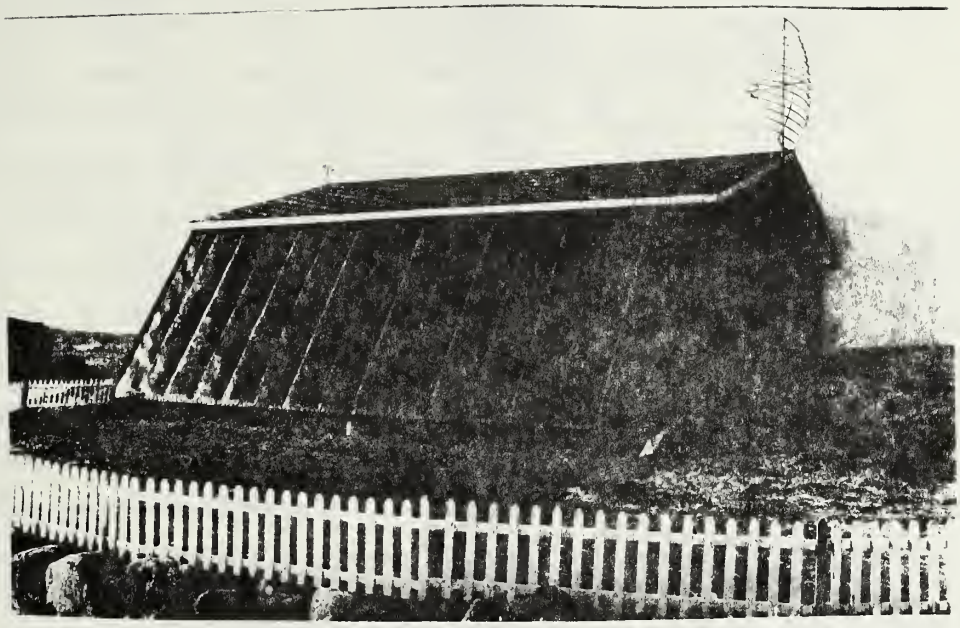

Solar Collector

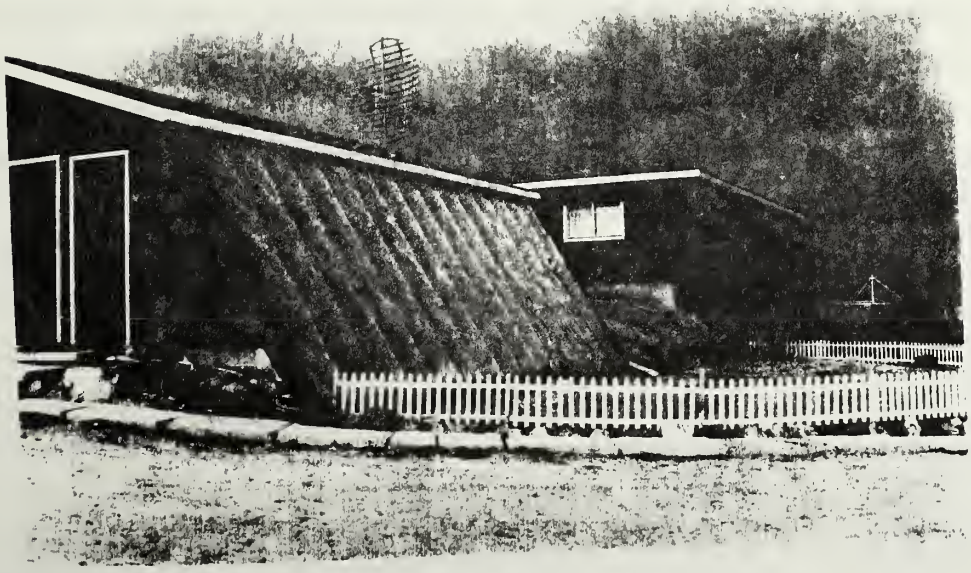

Collector next to house

John Allenmeier System

JOHN ALLENMEIER SYSTEM

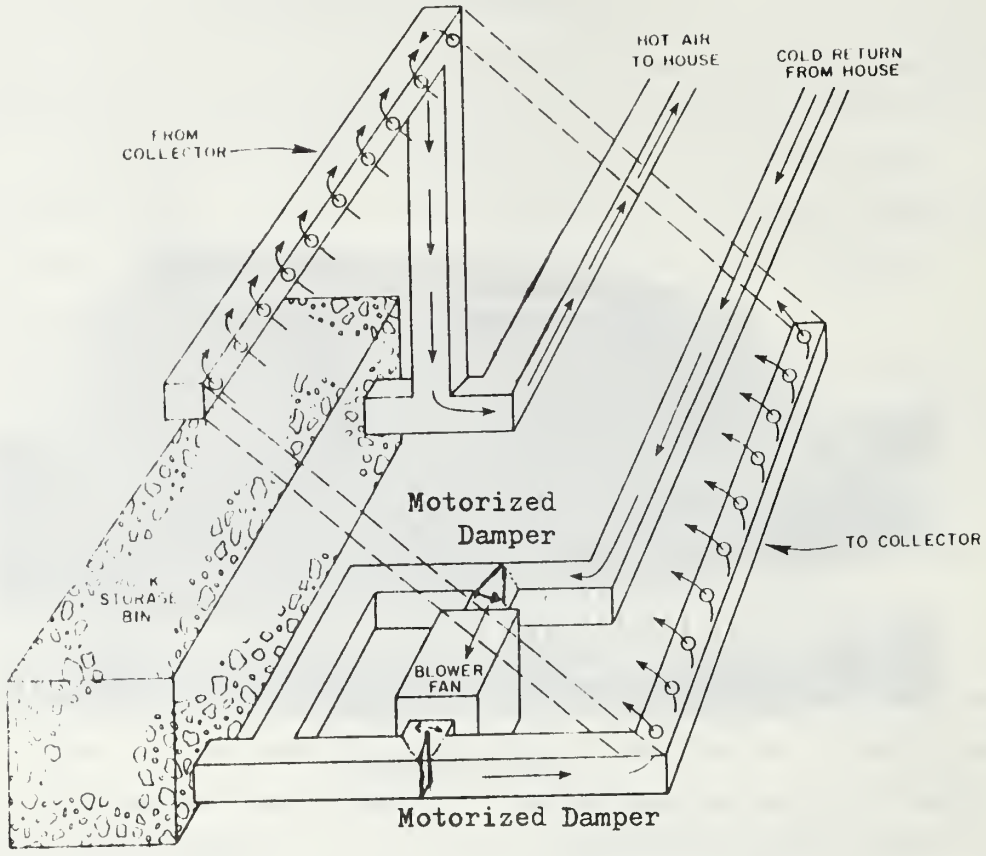

ANNUAL SUMMARY	
TOTAL HEAT LOAD	110 x 10^6 Btu
ELECTRICAL HEAT	108 x 10^6 Btu
SOLAR HEAT	8 x 10^6 Btu

JAMES COONS SYSTEM

James Coons has a 600ft^2 hydronic solar system on his house - the main rack of collectors are flush mounted on the roof/wall of the living area with a smaller bank on the roof. Two 1,000 gallon storage tanks in the basement have fin-tube heat exchangers which transfer heat out of the collector/glycol loop into storage. Collection into and distribution out of the tanks is separately controlled in an attempt to maintain high temperatures to drive a water-to-air heat exchanger for heat distribution to the house. A 25 gallon tank inside one of the 1,000 gallon storage tanks is used for DHW preheat.

Backup heat is via a Carrier air-to-air heat pump which uses outside air. Although the off the shelf componets were professionally installed, Mr. Coons spent considerable time working on this system including the control of distribution systems. Insulation of the pipes and tanks are moderately well done.

Mr. Coons has maintained twice daily records of weather and tank temperatures. While simple calculations would predict 60°F temperature rise within one 1,000 gallon tank on a mild sunny day, the usual performance is often much less than 20°F. Sometimes no temperature increase is noted, insufficient heat exchanger sizing is one possible explanation. It is also possible that the upper bank of collectors is not receiving circulating fluid. Outgassing against the cover plates on this bank due to stagnation temperatures does reduce sunlight onto the absorber. It is also noted that one collector on the main bank has a shattered inner glazing (tempered low iron glass). In the winter a pine tree @24° west of south shades the lower bank for 1-2 hours daily. Collector orientation is 17° west of south.

Because the solar system does not achieve usable temperatures during the winter (except for some DHW preheat), and because the COP for the air-to-air heat pump is at its lowest in the winter, Mr. Coons experiences to sharp a rise in utility cost in these months. Since the tank only reaches max temperature of 140°F in the swing months, the solar system contribution is probably less than the design goal of 61 x 10^{6}Btu/year.

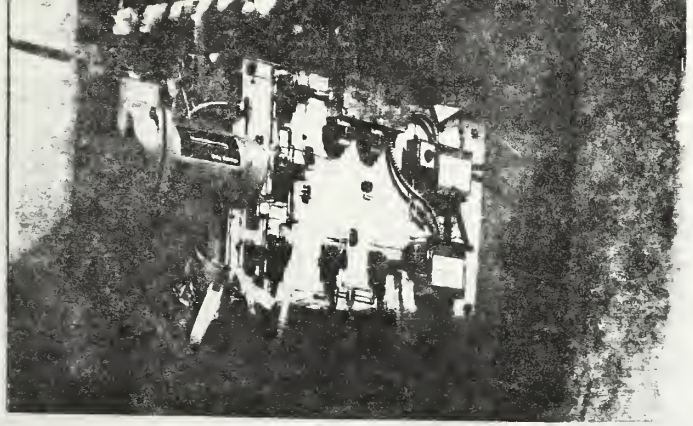

Controls

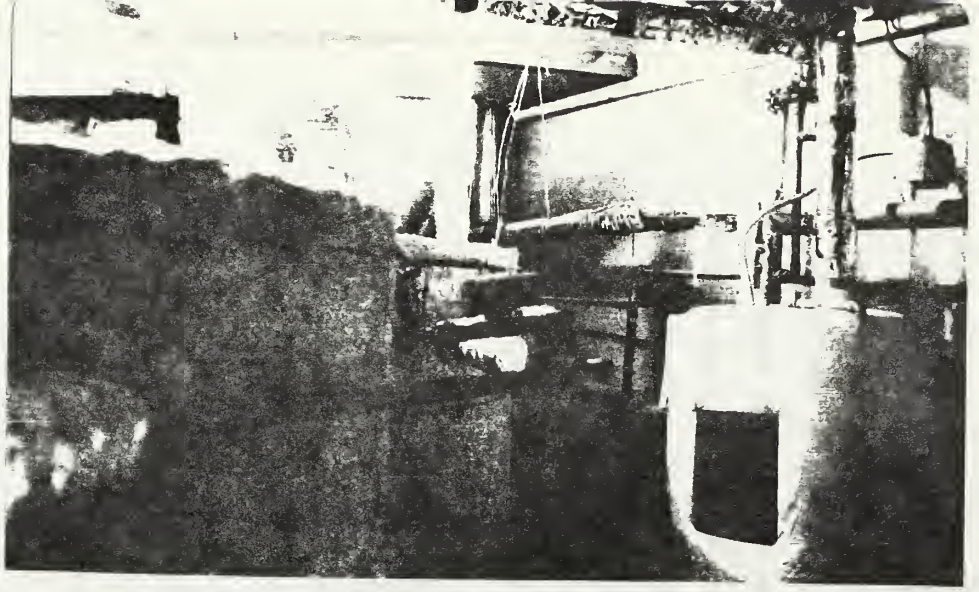

Heat storage tanks and DHW heater

Main Collector Array

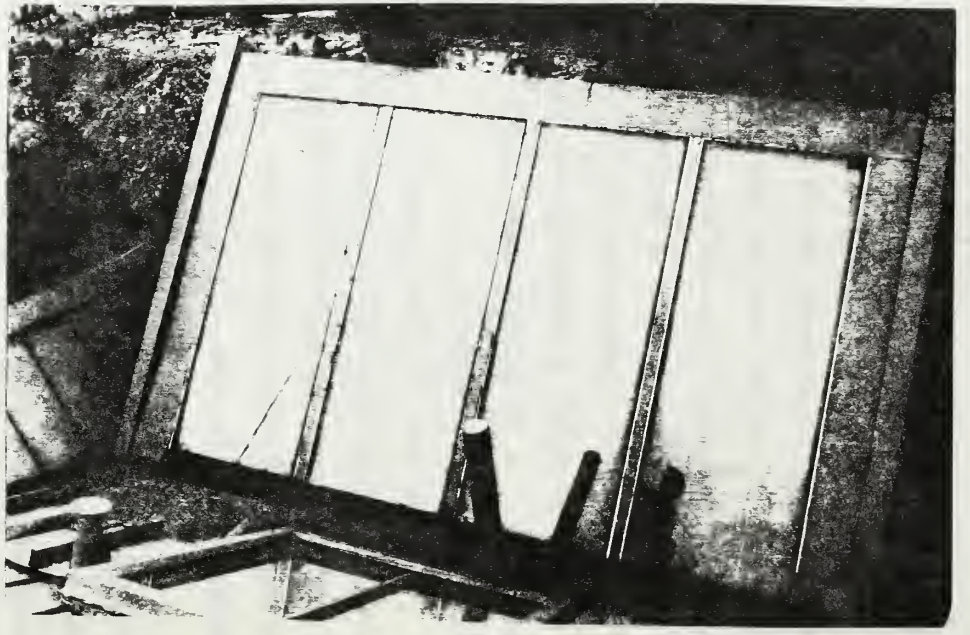

Roof mounted collectors

James Coons System

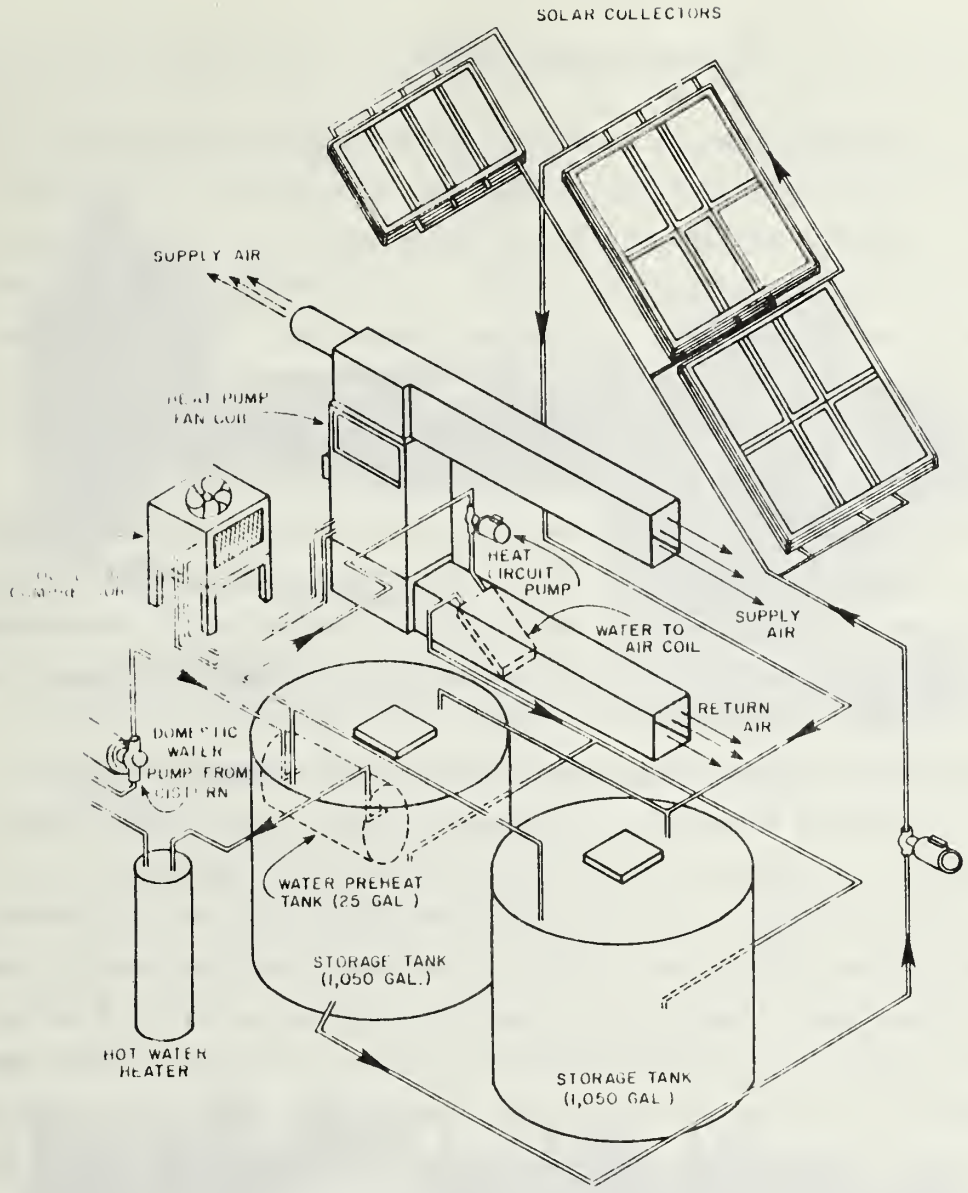

ANNUAL SUMMARY	
TOTAL HEAT LOAD	172×10^6 Btu
ELECTRIC HEAT	111×10^6 Btu
HEAT PUMP ADD	24×10^6 Btu
SOLAR HEAT	37×10^6 Btu
SOLAR FRACTION	22%

CLARK MacDONALD SYSTEM

This solar system consists of 200ft^2 hydronic solar collectors manufactured by Dick Dill of Stevensville, MT. The glycol circulation fluid delivers heat to storage via a heat exchanger in a well insulated 1,000 gallon tank also manufactured by Dill. A $4\frac{1}{2}$ ton water to air heat pump was installed between the existing gas furnace and a new, water-to-air heat exchanger. The existing duct work supplies heat to the house. A 30 gallon tank submerged in the heat storage tank is used for preheating domestic hot water.

A lack of pipe insulation coupled with the low specific heat of glycol and heat exchanger inefficiencies would lower overall efficiency. Between March 1 and April 9, 1980 recorded data showed a daily 10-14°F temperature rise in storage. Calculations show a temperature rise of 15-20° is expected during this period.

Mr. MacDonald replaced the malfunctioning solar thermostat with a timer which he adjusts seasonally for length of day. This change would greatly diminish the seasonal contribution of the solar system.

In the fall of 1980, a rebuilt wood fired boiler was set up behind the house to assist the collectors. Chunks of railroad ties are burnt to heat the solar storage tank. There is no record of the amount of wood burned. Although this boiler is old and unsophisticated, it provides a large share of the house heat. The water to air heat pump failed after the second season. Mr. MacDonald has been unable to get the contractor to fix it. Without the heat pump, storage temperatures must be maintained at 110°F to use the water to air heat exchanger for distribution.

Clark MacDonald subsequently added 232ft^2 of home-built, air collectors to the south wall of his house. They are constructed of 2 layers of FRP with an absorber/baffle plate and insulation behind the glazing. A fan circulates hot air through the basement which is open to the main floor via the stair well. The occupant felt that this system worked quite well, effectively heating the house. The air collector system is removed during the summer so the flower bed underneath can be used.

Recommended system improvements include: Differential themostat replacement, pipe insulation, and fixing the heat pump.

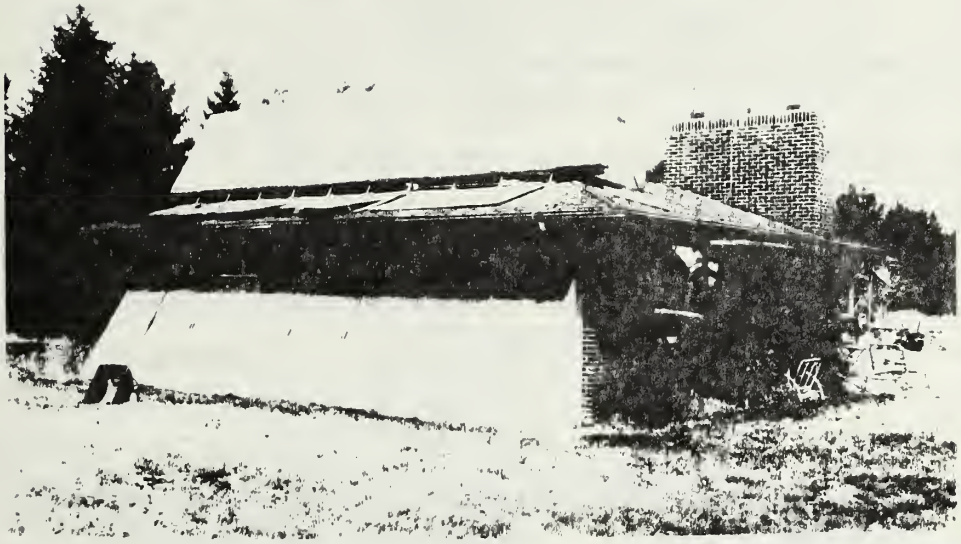

Liquid collectors mounted on roof and connected to thermal storage

Air collectors mounted on ground - hot air circulated through basement

CLARK MacDONALD SYSTEM

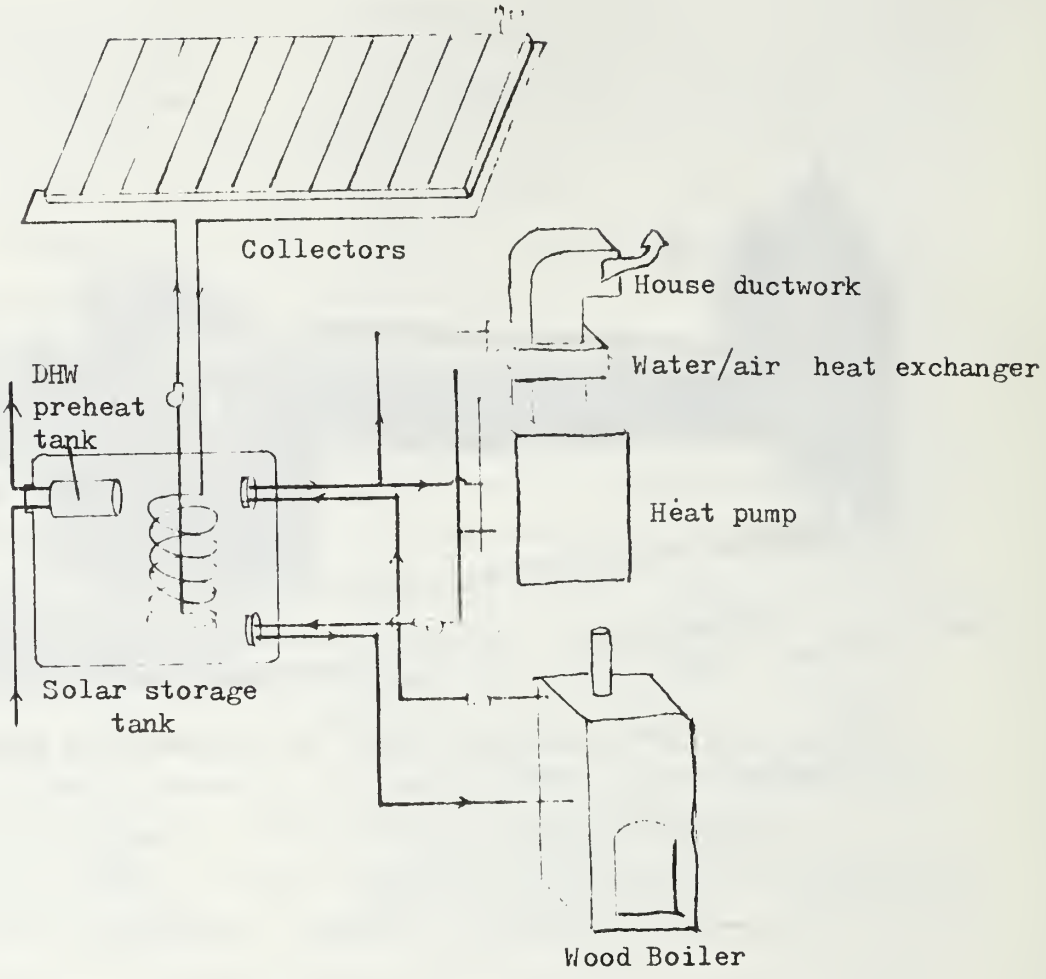

ANNUAL SUMMARY		
TOTAL HEAT LOAD	180×10^6 Btu	
GAS HEAT	40×10^6	*
ELECTRIC HEAT	30×10^6	
WOOD HEAT	75×10^6	*
SOLAR HEAT (liquid)	15×10^6	*
SOLAR HEAT (air)	20×10^6	*

*expected error $\pm 20 \times 10^6$ Btu due to lack of data

JOHN MacDONALD SYSTEM

John MacDonald added a 360 ft^2 liquid collector array to his existing heating system. The existing system includes a commercial wood fired boiler feeding a 1,500 gallon storage tank. Approximately 10 cords of wood are burned per year. Distribution is via commercial sized fin tube baseboards in the house and a hydronic radiant slab in the basement. Back up heat is a 140 Amp electric boiler.

John MacDonald is an accomplished craftsman. The existing heating system, which he installed, is of professional quality. However the solar system suffers from design and materials problems. Since an early failure, the collectors have not been used until recently. Originally mounted below the house and connected to storage via a glycol loop and external heat exchanger - plumbing leaks and low collection efficiencies led to discontinuance of their use.

The homebuilt collectors suffered severe degredation from weather and stagnation temperatures (see photographs). The butyl sealant in the insulated glass units melted down during stagnation, breaking the glass seals. Styrene insulation has suffered melt down.

Mr. MacDonald moved the collectors above the house and constructed a drain back system using water as collection fluid. This was done in the fall of 1982. Because of drawback problems the collectors froze and burst in many places in November 1982. These leaks were fixed and modifications to the drawback plumbing were made at that time. At this time the major work needed to fix the system is to rebuild the glazing on the collectors. Currently there exists $\frac{1}{2}$ - 1" gaps between the glass and collector frame. Until this is done, very low collector efficiency is expected.

One design flaw which should be changed is the buried plumbing line to the house. The two copper lines lay side by side in 4" PVC pipe without insulation between them. The collector loop inlet and outlet are both on the bottom of the storage tank. Until the collectors are rebuilt and achieve higher temperatures this connection is probably better than diluting the higher temperatures produced by the boiler which are at the top of the tank. The tank usually maintains 40-50° temperature stratification unless the boiler pump is on. Usually the boiler/storage loop thermosyphens.

When the collectors are fixed, the solar system should produce approximately 45 x 10^6Btu/year, approximately 24% of the house heating load. Current electrical consumption averages 100 x 10^6Btu/year and wood heat supplies are estimated 81 x 10^6Btu/year. Since the collectors have not operated over the sunny period there is no solar contribution.

Collector array

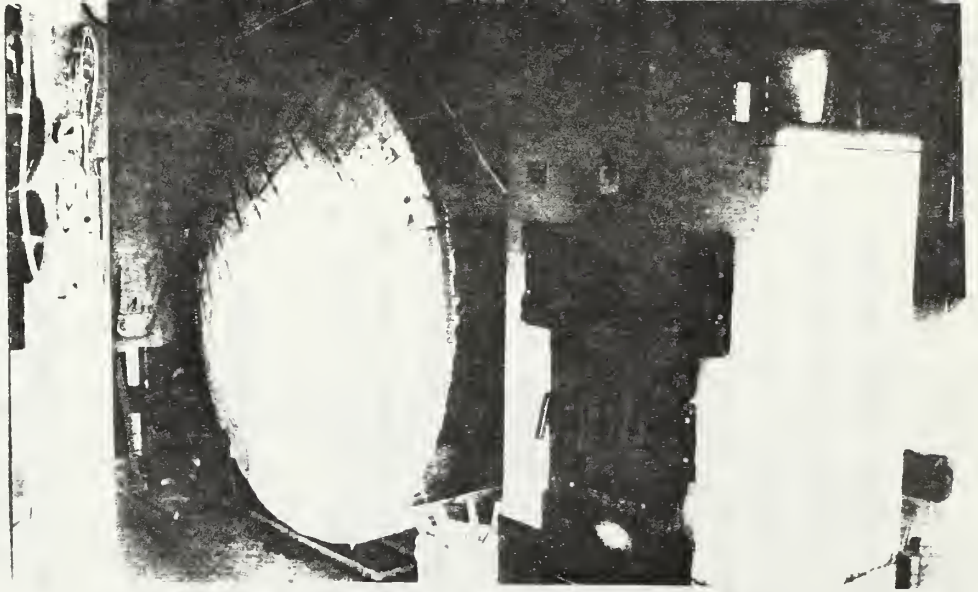

Heat storage tank and wood boiler

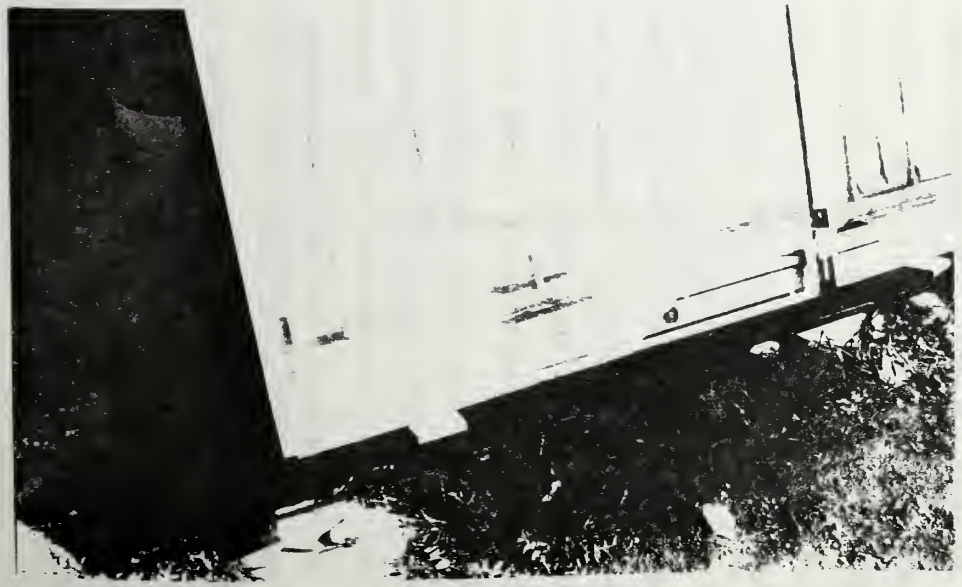

Loose cover plates

Buried drainback tank and plumbing lines to house

John MacDonald System

JOHN MacDONALD SYSTEM

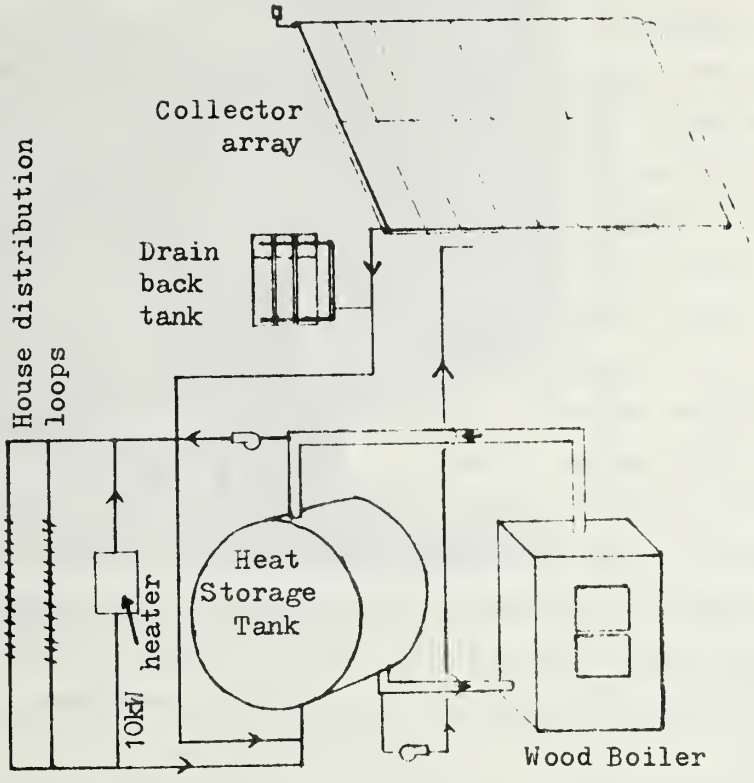

ANNUAL SUMMARY	
TOTAL HEAT LOAD	181 x 10^6Btu
ELECTRIC HEAT	100 x 10^6Btu
WOOD HEAT	81 x 10^6Btu
SOLAR HEAT	ø
SOLAR FRACTION	ø

JAMES TAYLOR SYSTEM

James Taylor modified a south wall and the roof of his pre-cut house during construction to include two arrays of air collectors on the house. Integrated into the solar system is a rock storage bin, air-to-air heat pump drawing air off rock storage, wood fired furnace and DHW preheat.

The 426ft^2 of low cost collectors consist of double glazed FRP, a 24" air space and a flat black back wall insulated to R-33. Ducting and baffling is very simple - aluminum baffles were added later, but do not force air against the absorber. Standard absorber design objectives include using the baffles to "wash" the absorber with circulating air to increase collector efficiency. Because of the large air space (24") and the single inlet and outlet the heat transfer is less than optimum implying a low collector efficiency. The lower collector includes a $2\frac{1}{2}$' x 20' DHW absorber section consisting of copper pipes imbedded in mortar. This loop is a glycol based thermosyphen loop to a 100 gallon tank. Mr. Taylor believes that glycol circulation is very slow and pumping would improve performance.

Temperature levels in the rock storage as recorded via thermocouples buried in the rock bed are much lower than anticipated. This is possibly due to both low collector efficiences, duct leaks, and ducting short circuiting via damper leaks in the rock storage plenum. This data indicates some major system problem.

The heat pump loop seems to work as designed. The wood furnace is seldom used as Mr. Taylor uses a modified fireplace in the house to provide backup heat. Mr. Taylor plans to rebuild the rock bed storage. A different absorber, and baffle system in the collectors would probably be helpful. Additional monitoring and analysis would be helpful in pinpointing problems.

Hot air distribution is accomplished using the crawl space as a plenum with perimeter registers. DNR&C detailed monitoring data on the Mattson crawl space plenum (Bozeman, 1979) showed very high losses due to air leakage and conduction. Mattson has subsequently replaced the plenum with a duct system. The analysis of the Taylor data showed that auxiliary energy inputs alone (no solar contribution) far exceeded the calculated heat load of the building. We conclude that either the plenum system or the active solar system is increasing the load through losses due to leaks.

Solar collectors

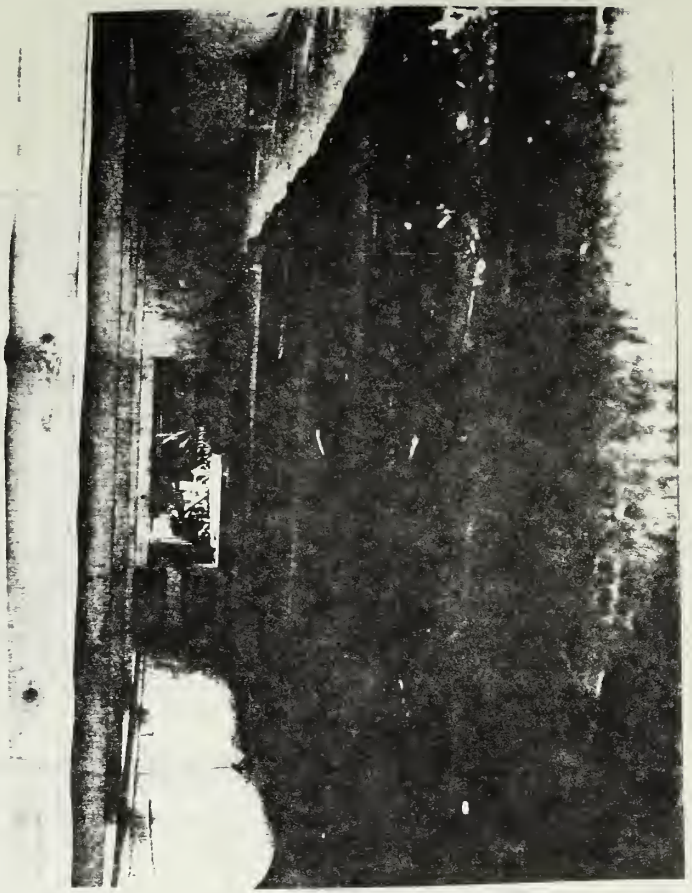

Collector plenum showing inlet and outlet duct

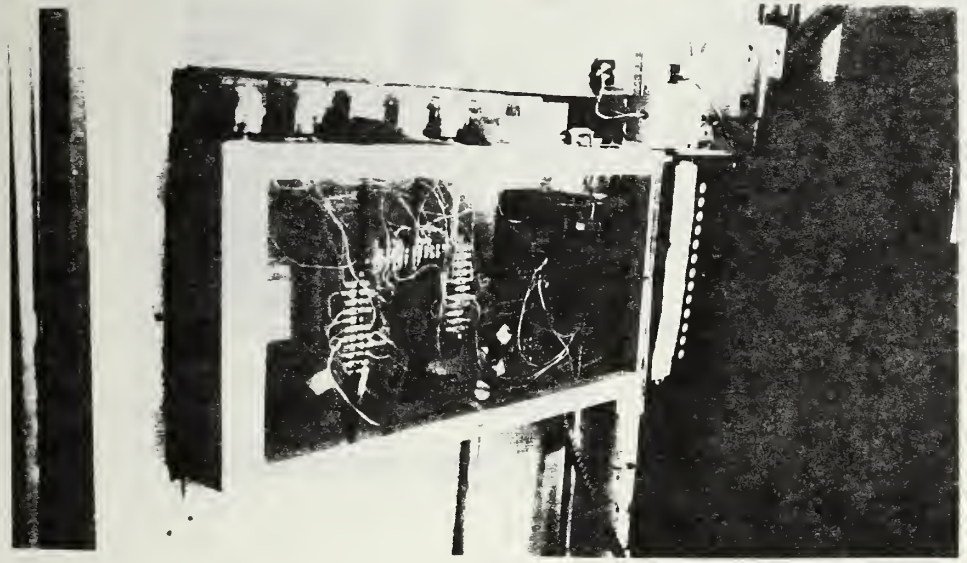

Control Panel

James Taylor System

JAMES TAYLOR SYSTEM

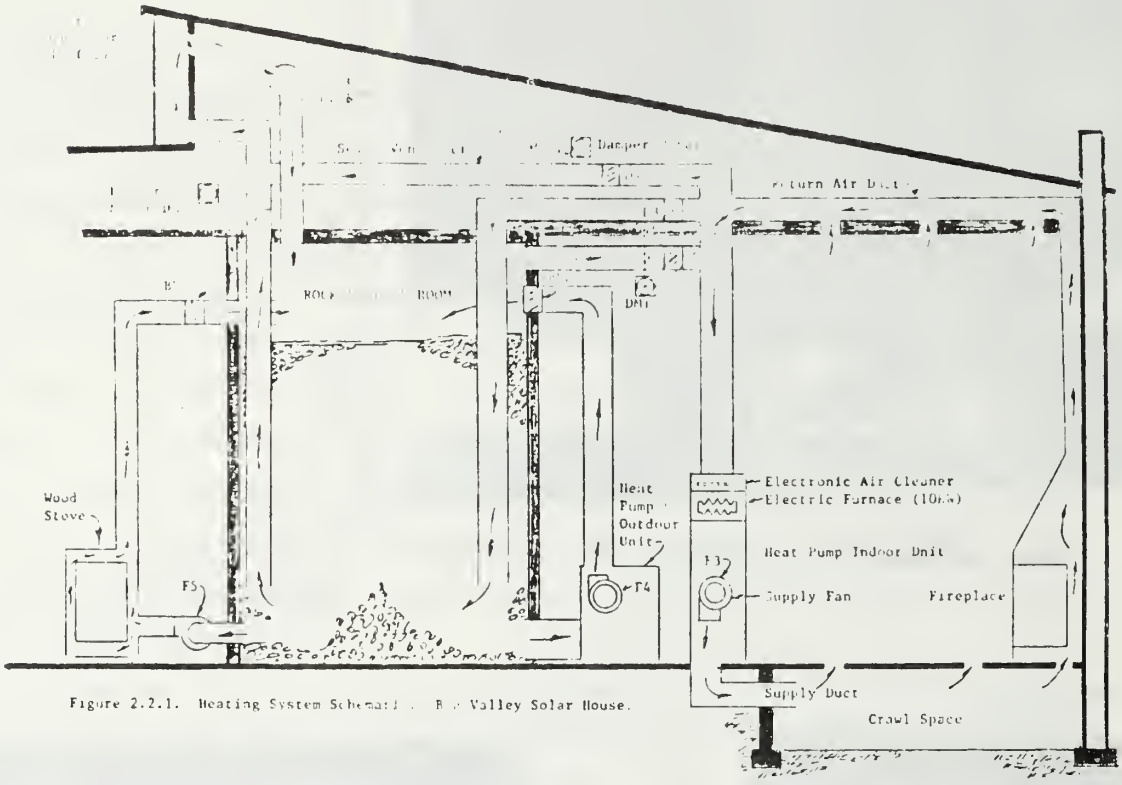

Figure 2.2.1. Heating System Schematic - Blue Valley Solar House.

ANNUAL SUMMARY	
TOTAL HEAT LOAD	115×10^6 Btu
ELECTRIC HEAT	91×10^6 Btu
WOOD HEAT	38×10^6 Btu
PASSIVE SOLAR	10×10^6 Btu
ACTIVE SOLAR + EXTRA LOSSES	-24×10^6 Btu

Progress in Solar Energy Copyright 1982 by American Section of the International Solar Energy Society, Inc. Printed in U.S.A.

0731-860X/82/0501-0691$3.00

THERMAL PERFORMANCE OF AN ENVELOPE HOUSE IN A COLD CLIMATE

Charles W. Fowlkes, Ph.D., P.E.
Fowlkes Engineering
31 Gardner Park Drive
Bozeman, Montana 59715

ABSTRACT

This paper presents thermal performance data on a double-shell or envelope passive solar residence. The space between the inner and outer shell was instrumented with home-made heated anemometers that were sensitive to air flows in the 0 to 0.5 m-sec^{-1} range. A partitioned heat balance on the inner and outer shell allowed conclusions to be drawn about the relative thermal contributions of the sun space, the air space and the crawl space.

1. DESCRIPTION OF THE HOUSE

The house discussed in this report was built about three years ago by Stan Wyatt and is currently owned and occupied by Jim and Barbara Darcy. The house is located near Bozeman, Montana at an altitude of about 1,520 m. There are typically 4,500 heating degree days per year in this region. The house faces 30 degrees west of south and has no significant shading.

The house is of wood frame construction and the overall design of the house closely parallels the early envelope house built near Lake Tahoe and described by Smith and Butler in Reference (1). A photograph of the house is shown in Figure 1. This house was carefully built and the construction, insulation and finish details are excellent. Auxiliary heat is supplied to the house by electric baseboard units and a wood-burning stove.

Fig. 1. The Darcy/Wyatt envelope house.

2. INSTRUMENTATION AND HARDWARE

The data acquisition system used for the performance monitoring accepts 40 channels of analog input data. Data acquisition and storage is controlled by a Radio Shack TRS-80 microcomputer. Several of these systems have been used over the past three years to monitor 15 solar heating projects. The data system scans up to 40 channels, performs a 12 bit A/D conversion, and processes and displays the data once each five seconds. The data is averaged over hourly periods and the averaged values are stored on cassette tape. This data is subsequently transferred to a larger microcomputer to produce summary reports. The data system accepts inputs from pyranometers or silicon cell radiometers, clamp-on ammeters, status switches, flow

Fig. 2. Data acquisition system in sunspace.

Ed. Note: A list of metric-English-metric conversion values appears immediately preceding the Author Index.

meters and temperature transducers. Figure 2 shows the data system located in the sunspace.

3. HEATED ANEMOMETERS

Early articles on the envelope design asserted that the purpose of the envelope construction was to allow air to flow by natural convection around the loop. The diagrams in Reference (1) indicated that during the day solar heated air in the sunspace would flow through the roof cavity, down the back wall cavity, through the crawl space where heat was stored in rocks, and then return to the sunspace. The literature asserted that during the night, stored solar heat was liberated from the rocks in the crawl space. Air would flow, by natural convection, up the rear wall cavity, through the roof, and back to the sunspace. Diagrams depicting these natural convection loop flows have been reproduced many times in popular technical articles. Reference (1) specifically includes a section entitled, "The Positive Theory of Natural Physical Behavior". This section proposes to demonstrate the physical necessity of the natural convection loop flow based on Aristotle's Theory of Atoms and Newton's Theory of Gravity.

The technical literature includes a number of presentations of monitoring results on envelope houses, (2), (3), (4). Only a few experimentors have reported data on air flow measurements in the loop. This lack of data is unfortunate since the loop flow is supposed to be the basic mechanism of this design and is the reason for constructing the loop in the first place. The practical reason that this flow is seldom measured is that the associated instrumentation for measuring low velocity air flows is relatively expensive.

To measure air flow, we modified three of our normal temperature probes (Analog Devices AD590). A metal film resistor (0.12 W, 720 Ω) was bonded to the face of the AD590 and 12 vdc was applied to the resistor. The equilibrium temperature of this device in zero velocity air flow is about 27° C above the ambient temperature. As the air velocity increases, the temperature difference, ΔT, decreases as shown in Figure 3. The equation

$$V = 0.006 \times (27.6 - \Delta T)^{0.5} \qquad [1]$$

closely fits the experimental data from Figure 3, where V is air velocity in $m\text{-}sec^{-1}$.

To use this device, both a heated probe and an unheated probe are placed in the region where air flow is to be measured. The data system samples the temperature of the heated probe and the unheated probe, calculates the difference, and substitutes that value into Equation [1].

Figure 4 illustrates the final results of this device. Shown on the abscissa are the reference velocities as indicated by a Model 1650 hot-wire anemometer produced by Thermal Systems, Incorporated. On the ordinate are values of velocity calculated from the measured ΔT's using Equation [1]. These readings are contained within an error band of less than .05 $m\text{-}sec^{-1}$.

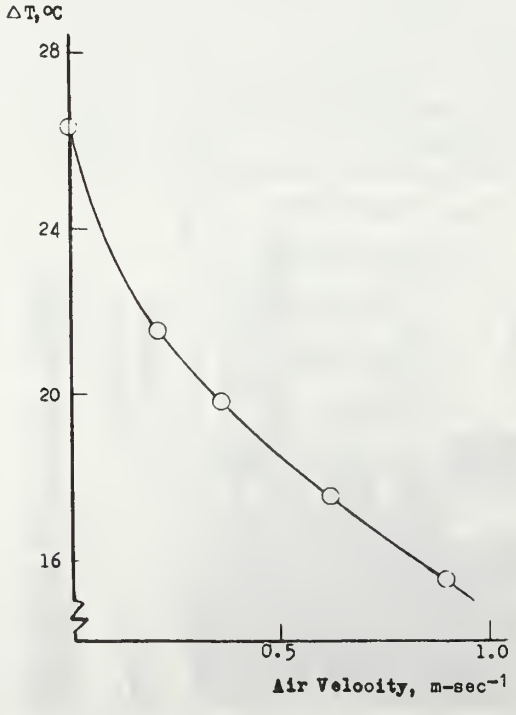

Fig. 3. Cooling characteristic of heated probe.

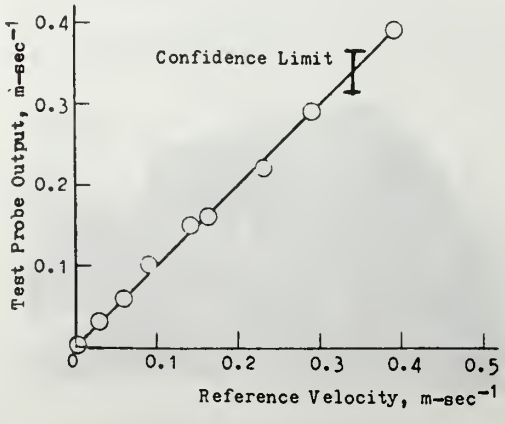

Fig. 4. Overall performance of anemometers.

Due to the thsrmal mass of the resistor and temperature transducer, several minutss are requirsd for the dsvice to coms to thsrmal equilibrium when the air velocity is on the order of 0.1 to 0.5 m-sec^{-1}. This response is adsquats for msasuring hourly averags flows. Each transducsr pair was individually calibratsd for a range of stagnation temperatures of 15 to 30° C. An exprssion in the form of Equation [1] fits ths data over this range of stagnation temperaturss to within .05 m-sec^{-1}.

4. INSTRUMENTATION LAYOUT

A schematic of the instrumsntation layout is shown in Figure 5. Silicon cell solar radio-

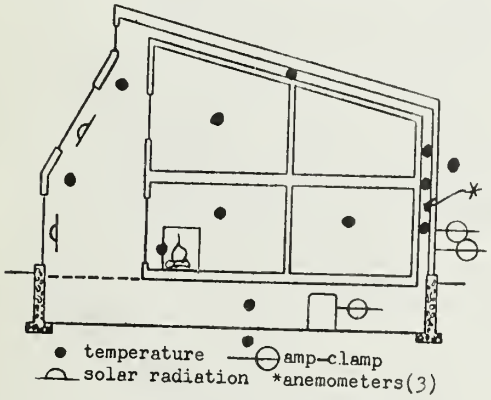

Fig. 5. Instrumentation layout.

meters were situated inside the glass on both the vertical and sloping sections of the sunspace. These radiometers were calibratsd in place to agree with a recently calibrated Eppley PSP pyranometer. Shaded temperature probes were mounted in the lower and upper sunspace and in the roof cavity as shown in Figure 5. Three pairs of heated anemometer probes were located at the midpoint of the channel in the north wall. These probes were distributed at three stations across the north wall and located at a height of 2.5 m above the crawl space.

An air temperature probe was located at the midpoint of the crawl space and a second probe was buried to a depth of 10 cm in the rock storage floor of the crawl space. Ambient air temperature was sampled in a shaded location on the north side of the building. Two clamp-on ammeters measured the total electrical current entering the house. A third clamp-on ammeter measured electric current through the domestic hot water heater located in the crawl space. These ammeters were calibrated on-site against the utility kWh meter.

The interior house air temperature was sampled at three locations, as indicated on the diagram. An additional temperature probe was mounted to an aluminum bracket which was attached to the wood stove in order to estimate the contribution of this device.

5. HEAT BALANCE

Separate heat balances were performed for the inner space and the loop space. The heat losses from each of the spaces were divided into elements consisting of the south wall, the roof, the north wall, the floor and the side walls. The heat conducted through each of these elements was assumed equal to a calculated U value multiplied by the measured hourly average temperature difference across the element. The south facing glazed elements in the outer shell were assumed to contribute a solar gain equal to the measured solar radiation multiplied by the appropriate glazed area. The solar gain through the windows in the south facing wall of the inner house was calculated by multiplying the measured vertical solar radiation into the sunspace by two factors to account for transmission loss and shading.

The heat added to the inner house due to electrical dissipation was taken as the measured total electrical input to the house reduced by 0.6 of the electrical energy going to the domestic hot water heater. The heat from the wood stove was estimated by multiplying the temperature of the stove minus a remote house air temperature by a suitable constant. This constant was determined by trial and error in order to achieve a heat balance. The stove drew combustion and circulation air from the crawl space. The infiltration losses of the inner and outer shell were increased when the stove was used.

The outer shell was assumed to have electric gains equal to the standby losses of the domestic hot water heater plus 300 W to account for the dissipation from two freezers located in the sunspace. A heat storage term based on hourly air temperature changes was included in both the interior and the shell heat balance equations. The equation for the heat balance of the inner shell is:

$$Q_{electric} + Q_{wood} + Q_{solar} + Q_{stor} = Q_{loss}{}^{1}. \quad [2]$$

The heat balance equation for the outer shell is:

$$Q_{solar} + Q_{electric} - Q_{loss}{}^{1'} + Q_{stor} = Q_{loss}{}^{2}. \quad [3]$$

In these equations, Q_{loss} is the algebraic sum of the $U \times \Delta T$ for each element enclosing the space. Note that the heat losses from

the inner space (except the side wall losses) are heat gains into the shell, $Q_{loss}{}'$ in Equation [3]. These heat balances were calculated on an hourly basis, a daily average basis, and a monthly average basis.

The total electrical power entering the house as measured by the amp-clamp was compared to the utility bills for the month of January and the results agreed to within 2%. During the test period, there were several intervals of one to three days when little solar energy and little or no wood energy entered the building so that the house was heated primarily by electricity. These test periods can be viewed as coheating periods for which the energy input to the house is well known. The calculated heat loss coefficients and average infiltration rates for the house were adjusted to effect accurate hourly and daily heat balances during the coheating periods. Segments of data when the wood stove was the primary source of heat were then inspected. An empirical equation for wood stove heat was derived which produced satisfactory hourly and daily heat balances. The effective thermal storage masses in the interior and exterior shell were adjusted to smooth the hourly heat balances. The final value of storage mass selected was 3.5 kWh per degree Celsius air temperature change.

The iterations on the hourly, daily and monthly heat balance equations were repeated until there was less than 10% average error in the heat balances. The data was then summarized over the entire monitoring period. Figure 6 shows the results of the total energy flow through each "element" of the structure for the months of January and February. The solar, electric and wood inputs into the inner and outer shell are depicted as large arrows. The conductive and infiltration losses are depicted by small arrows located near their respective elements.

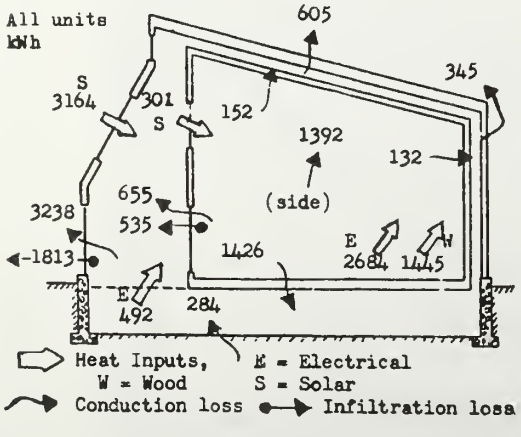

Fig. 6. Distribution of total heat inputs and losses for the period from 1/6 to 3/3.

Looking first at the inner shell, the largest heat losses are through (a) the floor, (b) the side walls and (c) the wall separating the inner house from the sun space. The loss in the floor is large because it is not insulated. The original design premise supposed that heat would be transferred from the crawl space into the house. This is clearly not the case. The sidewall losses are great because of the large ΔT existing across these walls. The loss from the inner house to the sunspace is large because this wall contains a relatively large area of glass.

Looking next at the outer shell, the largest heat losses are through the sunspace. The conductive loss of 3,238 kWh is actually greater than the solar gain of 3,164 kWh. The infiltration losses also appear quite large. The infiltration losses were not measured directly but were based on a constant 0.5 air changes per hour in the shell. This value was assumed to be accurate because of satisfactory heat balances on a majority of the days. We did notice an increase in heat loss on windy days which would be explained by an increased infiltration. Losses through the roof and north wall are small.

Figure 7 shows a summary of the average temperatures during January and February. The average daily maximum and minimum temperatures are also shown for the sunspace and the interior house, since these values help establish the relative success of a passive solar design. The sunspace shows large temperature swings as the space responds to large solar gains during the day and large losses through the uninsulated glass at night. The temperature swings in the upper part of the inner house average 4.8°C. This room is used as a master bedroom and has its own thermostatically controlled electric baseboard heaters. The

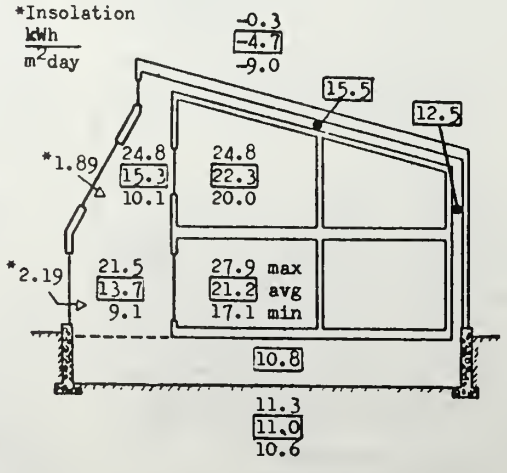

Fig. 7. Daily average temperatures, °C, 1/6 to 3/3.

temperature swings in the lower part of the house are considerably larger (10.8° C). The wood stove is located in this portion of the house and there is a large area of glass in the wall dividing this room from the sunspace. When the occupants are not at home, they allow this space to cool off and when they come home they often build a fire in the wood stove, which produces relatively high temperatures. The temperature swings measured in this space, therefore, reflect the habits of the occupants and the use of wood heat, as well as the strong coupling to the sunspace.

The average temperature indicated by the probe buried 10 cm beneath the rocks in the crawl space was 11.0° C while the probe in the crawl space air averaged 10.8° C. This average temperature difference is slightly greater than the calibration accuracy of the probe, which is typically 0.1° C. This data could suggest either heat transferred up from the earth into the crawl space and/or heat radiated from the warm floor to the rocks. At this point there is inadequate data to draw conclusions. The amount of heat exchanged is small and is consequently of little importance to the performance of the house. The average temperature swing of the probe buried in the rocks in the crawl space was 0.7° C. From these data we can conclude that the rocks are not an important heat storage element in this system.

6. AIR FLOW MEASUREMENTS

During the two month monitoring period, there was no indication of air flow in the back wall greater than the resolution and accuracy of the measuring system. The anemometers registered a very small but measurable flow on days when the wind was blowing and on a few nights when the ambient temperature dropped to -20 to -30° C. On windy days, these readings were apparently due to increased infiltration and drafts driven by the wind. On extremely cold nights, a small "apparent flow" was judged to be due to radiation from the heated probe to the walls.

Any air flow in the loop would have to be driven by a thermal gradient existing between the air in the sunspace and the air in the north wall. Figure 7 shows that for the two-month period, the average temperature gradient between the lower sunspace and the north wall was less than 1° C. Hourly data also showed only small gradients here. The driving force for flow appears small. This evidence agrees with the anemometer measurements.

Dr. Donald W. Aitken (Center for Solar Energy Applications, San Jose State University) has suggested that sometimes the air is not "smart" enough to follow the arrows drawn by architects or solar entrepreneurs. It appears what we have here is a case of dumb air. This shortcoming may be due to the effect of altitude or perhaps the lack of air pollution.

7. THE ROLE OF THE LOOP

The roof and rear walls of both the inner and outer shell contain equal amounts of insulation. If the "loop" or air space had been closed off from the sunspace and the crawl space (or eliminated entirely), the average temperature at this mid-point would have been about half-way between the interior air and exterior air temperatures, or 8 to 9° C, during the monitoring period. The average temperatures measured in the air space were 12.5° C in the north wall and 15.5° C in the roof cavity. This data implies that the inner shell losses through the roof and north wall were less than the hypothetical "no space" wall and that the corresponding outer shell losses were greater than the "no space" wall. The data also raises the following questions: Why is this air space warmer? Where does the heat come from? Does this heat come from the sun?

Figure 6 shows that the conduction and infiltration losses of the sunspace exceed the solar gain. Thus the shell does not, on the average, receive a net solar gain. The heat conducted up from the earth into the crawl space was estimated at 284 MJ. Even if this crude estimate is doubled, its magnitude is still small compared to most of the remaining energy fluxes in the system. Thus, the air in the shell is not primarily heated by contact with the earth.

Figure 6 shows that losses from the inner shell through the uninsulated floor are 1,426 MJ. The losses through the south wall of the inner shell total 655 MJ, primarily due to the large areas of glass. We conclude that the heat losses through the floor and south wall of the inner shell are the primary sources for heating the air in the loop to a temperature above the "no space" condition.

8. INSOLATION COMPARISON

During the period from January 6 to March 3, the daily average transmitted insolation at the envelope house site was 2.19 $kWh\text{-}m^{-2}$ on the vertical plane and 1.89 $kWh\text{-}m^{-2}$ on the 59° tilted plane, Figure 7. I initially thought there must be an error in the results, but a calibration check of the transducers showed them to be accurate. We had collected comparative data in Bozeman for 60° and 90° insolation during the previous winter for two south-facing transducers. This data showed the average 90° insolation to be about 0.88 times the 60° insolation.

There are three points which help to explain this data: (a) The house is oriented 30° west of true south so the relative azimuth

angle of the glazing becomes zero at about 2:30 p.m. in January. At this hour, the angle of incidence for both glazings is nearly the same (13 to 17°). For the remainder of the afternoon, the angle of incidence of the vertical glazing is less than the slanted glazing; (b) the ground in front of the glazing slopes down at about 5 to 10° and was always snow covered during the monitoring period. These conditions would produce a large reflected radiation component (estimated to be up to 25% of the total insolation transmitted through the vertical glazing); (c) the slant glazing is occasionally covered with snow for part or all of the day. The vertical glazing is almost never snow covered.

9. CONCLUSIONS

(1) The anemometers measured no air flow in the loop greater than 0.05 $m\text{-}sec^{-1}$ (their limit of resolution).

(2) Heat losses from the sunspace were greater than the solar gains during the monitoring period, January and February.

(3) The air space in the roof and north wall was warmer than a hypothetical "no space" roof or wall. This feature was not a net benefit since this heat came primarily from losses through the floor and south wall of the inner house.

(4) The crawl space contributed a small apparent heat flux from the earth. The crawl space was not an important thermal storage element.

(5) Temperatures in the sunspace were always above freezing, making this area suitable for growing plants. The attached sunspace provides spectacular views and is, in my opinion, a visually attractive feature. The sunspace would certainly provide a net solar gain during the spring and fall when ambient temperatures and insolation are greater.

10. ACKNOWLEDGEMENTS

I would like to express my gratitude to the owners of this envelope house, Jim and Barbara Darcy, for their cooperation with this monitoring project. When approached for permission to instrument their house, their response was, "If this information will help anyone, go right ahead."

The work described in this paper was supported by a grant from the Alternative Renewable Energy Sources Program of the Montana Department of Natural Resources and Conservation. This grant program derives operating revenue from a severence tax on coal mined in Montana and is dedicated to promoting "research, development and demonstration of renewable energy resources". The cooperation and support of Rick Itami, Van Jamison and Mike Chapman are acknowledged.

Several members of the staff at Fowlkes Engineering have contributed to this project. Dennis Stillwaggon helped instrument the house and Sharon Kleingartner helped prepare graphics. Jody Martinson typed and edited this paper.

11.0 REFERENCES

(1) Smith, T. and Butler, L. P., The Energy Producing House, Tahoe City, California, 1979.

(2) Jones, R. F., et. al., Case Study of the Mastin Double-Envelope House, Brookhaven National Laboratory Associated Universities, Inc., Upton, New York, for the Department of Energy and Environment, May, 1981.

(3) Chen, B., et. al., "Performance Results of the Tom Smith Double Shell Residence, Lake Tahoe, California," Proceedings of the 5th National Passive Solar Conference, Amherst, Massachusetts, October, 1980.

(4) Akridge, J. M. and Benton, C. C., "Performance Study of a Thermal Envelope House - Final Report, Phase I," College of Architecture, Georgia Institute of Technology, May, 1980.

Progress in Solar Energy. Copyright 1982 by American Section of the International Solar Energy Society, Inc. Printed in U.S.A.

0731-860X/82/0501-0489$3.00

THERMAL PERFORMANCE MONITORING OF A COMMERCIAL BUILDING AT THE CLASS B LEVEL

Charless W. Fowlkes, Ph.D., P.E.
Fowlkes Engineering
31 Gardner Park Drive
Bozeman, Montana 59715

ABSTRACT

This paper reports thermal performance data gathered on a 5,300 m^2 office building incorporating an active solar collector heating system. The data resulted from the application of low cost instrumentation applied to selected measurement sites. Data on the thermal performance of the building system is presented. Thermal capacity effects and line losses due to the remote location of the collector array significantly reduced the performance of this solar system.

1. INTRODUCTION

The project covered in this report is located in Bozeman, Montana, at an altitude of 1,520 m^2. There are typically 4,500 heating degree days per year. The temperatures in January average -8° C and will often drop to -20° C for periods of several days. Solar radiation on a 60° tilted collector surface will average 3.8 $kWh\text{-}m^{-2}$ per day during the winter season. This building was completed in September, 1979, and is the home office of the Life of Montana Insurance Company. The company president, Herb Richards, received a demonstration grant from DOE for $208,000 and a demonstration grant from the Montana Department of Natural Resources Renewable Energy Program for $59,500. According to the operating engineer, Ivan Newnham, the total system cost is estimated as $303,000, or $840-$m^{-2}$ of collector area.

2. DESCRIPTION OF BUILDING

A photograph of the building is shown in Figure 1. The three story building has a total floor area of 5,300 m^2. The walls contain large areas of glass comprising 47% of the total wall area. Auxiliary heat is provided by a natural gas fired hot water boiler. Heat is distributed to the building through five air handlers, each located in a separate zone. The space between the drop ceiling and the structural ceiling is used as a return plenum for the air handlers for the purpose of circulating heat dissipated by the lighting fixtures.

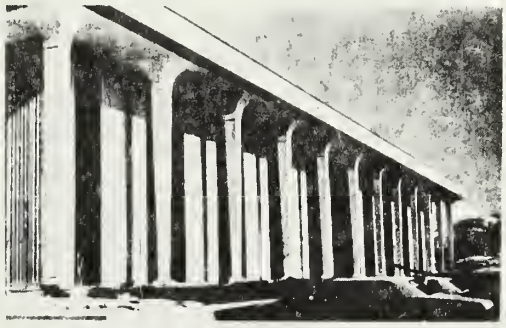

Fig. 1. South side of building

The active collector array is located at ground level at about 120 m from the building, Figure 2. Two hundred ten collector panels are tilted at 60° and face about 22° west of true south. The collectors are double glazed with low-iron glass and use selective surface absorber plates.

The collector fluid, a 50/50 ethylene glycol-water mixture, is circulated through buried

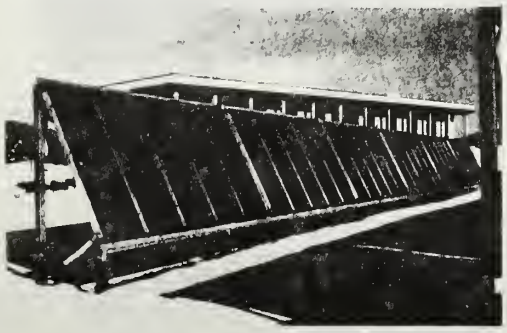

Fig. 2. One bank of collectors

insulated pipes to a heat exchanger in the basement of the building. Water circulates through the other side of the heat exchanger to two 11,300 l heat storage tanks. The collector loop contains about 2,600 l of fluid. The collectors are controlled by a differential thermostat. A second, adjustable thermostat in the building connects the solar storage tanks to the building circulation system, if the storage temperature is above the set point (normally 49° C). All of the solar system piping is well insulated and the mechanical equipment and controls are in excellent condition.

3. DATA ACQUISITION SYSTEM

The data acquisition system used to monitor this building is shown in the photo in Figure 3. This is one of three home-made data systems constructed three years ago and subsequently used to monitor 15 solar heating projects. A Radio Shack TRS-80 microcomputer controls the data acquisition. The instrumentation interface contains a 12 bit A/D converter, and a real time clock. There are 40 input channels with integrated signal conditioning for temperature probes, flow meters, clamp-on ammeters, pyranometers and status switches. Up to 40 channels are sampled and processed each five seconds and hourly averages are stored on cassette tape.

Fig. 3. Heat storage tanks and data acquisition system

4. INSTRUMENTATION LAYOUT

The instrumentation layout is shown on the schematic diagram in Figure 4. Solar radiation was sensed by a Li-Cor 200S radiometer mounted in the plane of the collector array at mid-height. An ambient air temperature probe was mounted in the shade of the collectors and another probe was mounted in the thermal well containing the differential control transducer at the collector array. Extension leads from these remote transducers ran 130 m through an underground conduit to the data acquisition system located in the

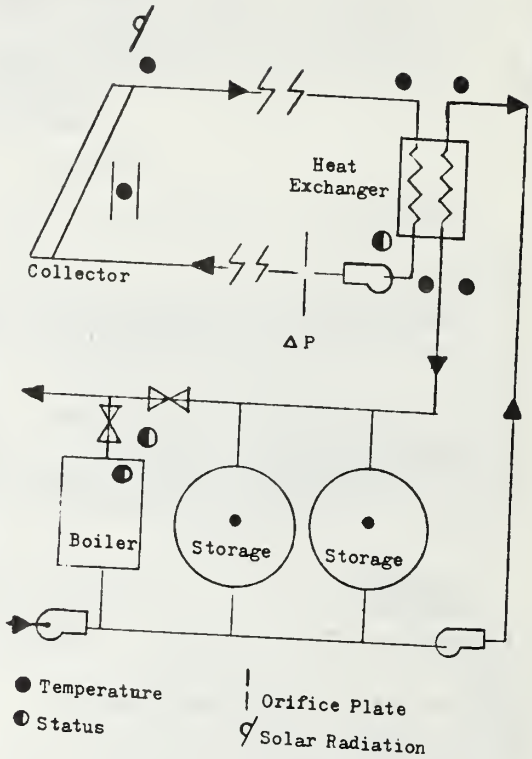

Fig. 4. Instrumentation layout

mechanical room. Fluid temperatures in the solar system were measured by Analog Devices AD-590F probes inserted in the wells in the fluid. Two special probes having stems approximately 1 m long measured the temperature near the center of the heat storage tanks.

Flow in the collector loop was measured by interfacing a differential pressure transducer to an existing orifice plate. The pressure transducer was calibrated on site. The calibration of the orifice plate was provided by the manufacturer, as well as the correction curve to account for the glycol-water mixture. A status switch was connected to the gas valve of the auxiliary boiler, allowing the data system to accumulate boiler on-time. Another status switch was attached to the valve which selects either boiler heat or solar heat for the building. The air temperature within the building was measured at five different locations. A pulse-initiating, watt-hour meter was also interfaced to the data system at a later date.

The temperature transducers were individually calibrated using a precision thermometer and an ice-point reference. The relative accuracy of the temperature transducers was 0.1° C (the resolution of the data system). The absolute accuracy is better than 0.5° C.

This relative accuracy is needed because the temperature differentials through the heat exchanger are typically only a few degrees Celsius.

Being uncertain of the effect of 130 m of lead wire, the Li-Cor radiometer was calibrated on-site after the entire system was connected. A recently calibrated Eppley PSP was used for the reference. The data system has performed quite well in the electrically noisy environment of the mechanical equipment room. The system has run continuously for three months with only a few hours of lost data.

5. STEADY-STATE COLLECTOR PERFORMANCE

The collectors are partially shaded in the early morning and late afternoon in the middle of the winter. This shading should have little effect on the overall collector performance. The average flow through the collector array is 0.0148 $l\text{-}sec^{-1}\text{-}m^{-2}$ and storage volume is 62.8 $l\text{-}m^{-2}$. These values are well within the range of recommended design parameters.

The data base from mid-January through the end of February was scanned to identify periods when the circulation pump was on for a full hour. A total of 39 hours on 13 different days satisfied this requirement. The hourly collector array efficiency was calculated by dividing the total solar heat output by the aperture area and the radiant flux. The corresponding value of collector inlet temperature minus ambient temperature divided by the solar flux was also calculated. The inlet temperature and heat output were measured at the heat exchanger. This procedure debits the collector performance for the line losses between the heat exchanger and the collectors.

These results are plotted in Figure 5. A dashed curve having a y-intercept of 0.73 and an x-intercept of 0.196 $^{o}C\text{-}m^{-2}\text{-}W^{-1}$ represents the expected performance of a single collector of the type in this array. On the average, experimental points fall below the single collector efficiency curve. This reduced efficiency is typical of collector arrays and is primarily due to heat losses in the manifold lines. A second curve has been drawn which passes approximately through the center of the experimental points. This data indicates that the average, steady-state performance of the array is about 7% below the expected performance of a single collector.

6. DAILY AVERAGE COLLECTOR PERFORMANCE

Although steady-state performance departed only slightly from ideal collector performance, the daily and monthly collector performance was clearly below expectations.

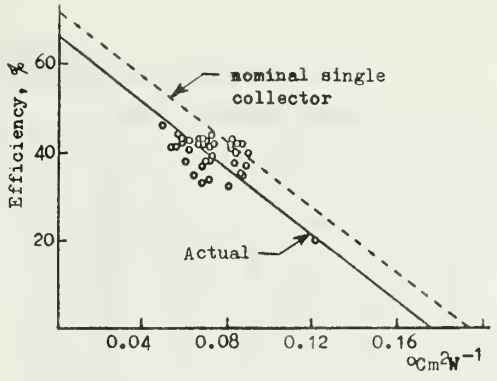

Fig. 5. Collector array efficiency at quasi-steady-state condition

Hourly data for the month of February was inspected to identify the cause of the reduced solar output. The collector performance curve shown in Figure 5 was used as a basis of comparison. The abscissa of the lower curve in Figure 5 was calculated each hour using measured insolation, ambient temperature and an inlet temperature equal to the current storage temperature. The calculated array efficiency was multiplied by the measured solar radiation to arrive at an "ideal" collector heat output. The calculated output of the ideal collector was compared to the measured solar heat output for each hour in February.

Table 1 shows typical measured hourly performance data for February 24 and calculated "ideal" collector performance. The first line in the Table shows that the "ideal" collector would have collected a small amount of heat (104 MJ) while the real collector did not turn on. During the period between 10:00 and 11:00 a.m., the real collector was on an average of 0.2 hour. Its negative heat output indicates that heat was removed from the solar storage tanks. During the same time, the ideal collector delivered 337 MJ. This difference reflects the solar heat being used to warm the fluid and piping in the collector loop. During the next hour, the actual solar system delivered 456 MJ while the "ideal" system delivered 509 MJ.

This comparison indicates the collector loop was warmed up and most of the solar heat was being delivered to the heat exchanger. During the rest of the day, the hourly performance of the real and "ideal" collector agree quite closely.

An overall performance summary for this day shows that the real collector delivered 2,667 MJ while the "ideal" collector delivered 3,149 MJ. On this day, the output of the "ideal" collector was 480 MJ greater than the output of the actual collector. The daily total heat output of the real collector array

TABLE 1
HOURLY COLLECTOR DATA COMPARISON FOR FEBRUARY 24, 1982

	Actual Collector Array									Ideal Collector			Diff
HR	Insol kW-m^{-2}	Tamb °C	Tin °C	Tout °C	Xin °C	Xout °C	Con Hrs	Eff %	Qout MJ	Tin °C	Eff %	Qout MJ	Δ Qout MJ
10	0.48	-7.4	29.8	41.1	39.9	39.8	0	0	0	56.3	17	104	-104
11	0.71	-1.3	45.6	44.4	53.7	48.9	0.2	-2	-7	55.0	36	337	-344
12	0.90	0.6	61.0	69.2	54.8	58.1	1.0	38	456	55.1	43	509	-53
13	0.99	-1.2	64.4	73.7	57.0	60.9	1.0	42	559	57.4	44	566	-7
14	1.02	0.8	68.0	77.1	60.2	64.4	1.0	43	595	60.6	44	586	10
15	0.93	1.9	70.3	78.4	63.5	67.3	1.0	42	524	63.9	41	498	26
16	0.80	1.7	70.7	76.7	65.6	68.5	1.0	36	388	65.8	36	376	11
17	0.58	-1.0	69.9	74.0	66.5	68.4	0.5	17	153	65.9	23	174	-21
TOTAL									2667			3149	-480

for the month of February are plotted in Figure 6. A straight line drawn through the data points intersects the actual output axis at about -480 MJ. This data shows that the actual solar heat output is offset about 480 MJ below the ideal output.

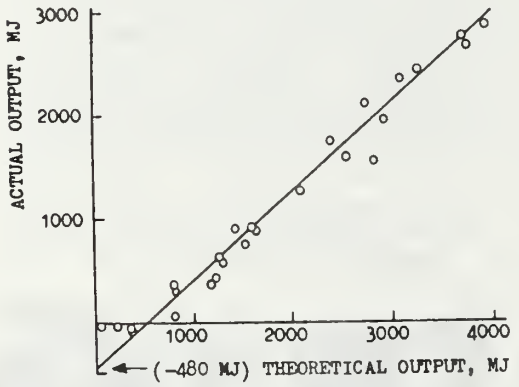

Fig. 6. Comparison of daily total solar heat output

7. HEAT CAPACITY OF THE COLLECTOR LOOP

We looked next at the pipes and manifold which connect the collectors to the heat exchanger. This loop contains about 2,650 l of fluid. We divided this piping into an underground portion and an above ground portion. The underground portion of the piping was estimated to contain 1,300 l of fluid in copper pipes having a mass of approximately 900 kg. Thermal mass of the underground piping is 4.5 MJ-°C^{-1}. The above ground portion of the loop, which includes the manifold and the absorber plates, contains about 1,000 l of fluid, while the pipes and absorber plates have a mass of about 2,400 kg. The overall thermal capacity of the above ground portion of the loop is, therefore, about 4.5 MJ-°C^{-1}.

Each day when the collectors operate, the fluid temperature reaches 60 - 70° C. Each night, the above ground fluid and pipe comes to equilibrium with the ambient temperature while the underground pipe and fluid comes to an equilibrium temperature of approximately 20° C. On the average day in February, the above-ground fluid, manifold and collector plate assemblies were raised from -4.8° C to 65° C, requiring 280 MJ of energy each day that the collector operated. The underground portions of the line similarly required about 203 MJ per operating day. The total heat required each collector operating day is estimated at 483 MJ. This value agrees very closely with the intercept of the actual vs. ideal performance shown in Figure 6.

8. COLLECTOR PERFORMANCE SUMMARY

The parasitic power for the solar collector system for the month of February was 1,541 MJ or about 5% of the delivered solar heat. This power is the sum of electricity used by the solar circulating pump and the storage tank circulating pump. During the month of February, the solar collectors delivered 20.3% of the incident solar radiation to the building; a total of 29,895 MJ. During the same period, the "ideal" collector would have delivered 41,600 MJ to the building. The collectors were on during 24 days in February. If the heat capacity of the piping and collector system is 480 MJ per day, the resulting heat lost would be 11,500 MJ. This is very close to the difference between the "ideal" collector and the measured collector performance.

9. BUILDING PERFORMANCE

This building receives heat from the auxiliary gas boiler, electrical dissipation or internal gains, and active solar gains. The monitoring data for the period from mid-January to early March was formulated into an hourly building

heat balance. To estimate the amount of heat delivered by the natural gas furnace, we compared the amount of natural gas entering the building between January 18 and February 16 (251.7 Mcf) to the total hours of on-time for the gas furnace (162.4 hrs). Using a heating value supplied by the utility company and a conversion efficiency of 75%, we estimated the boiler output as 1,061 MJ-hr^{-1}.

This building uses between 36,000 and 55,000 kWh of electricity per month. During the period covered in this report, the building was using 38,000 kWh per month. About 2,800 kWh of this electricity is used for architectural lighting outside the building during the night. This means 35,200 kWh were being dissipated in the building each month. An hourly load schedule was devised which assigned 300 MJ-hr^{-1} internal gains during the daytime and 52 MJ-hr^{-1} dissipation during the night. (A pulse-initiating kWh meter was interfaced to the data system in March. Initial results showed that the daytime hourly consumption was slightly higher than 300 MJ-hr^{-1}.) The heat loss of the envelope was calculated using normal ASHRAE procedures assuming an infiltration rate of 0.76 air changes per hour during the day and 0.2 air changes per hour during the night. The daily average load coefficient used for the building was 18 MJ-hr^{-1}-°C^{-1}.

The building contains large areas of south facing glass (195 m^2). This heat absorbing glass has a transmission of 0.35 at normal incidence. To calculate the passive solar gain, the insolation measured on the tilted collectors was multiplied by a shading factor of 0.8, a transmission factor of 0.35, and an angle correction factor of 0.9. This value multiplied by the total area of windows was assumed to represent passive solar gain. The shading coefficient in this calculation is judged conservative and no allowance is made for reflected radiation onto the vertical glazing, which is significant at these latitudes. The estimated passive solar gain may, therefore, be conservative by 10 - 20%.

The active solar heat entering the building was measured at the interface between the collector loop and the heat exchanger. Since practically all of this solar heat is dissipated into the building, only the timing is unknown. To determine when the solar heat enters the building, we constructed a heat balance based on temperature changes of the fluid in the storage tanks. The temperature of the storage tanks at the beginning and end of the hour of interest were interpolated by fitting a second-order polynomial through the three temperature data points centered around the hour of interest. This curve was differentiated to determine the average rate of temperature change of the storage tanks during that hour. This value multiplied by the thermal mass produced an hourly stored energy change.

The hourly solar energy delivered to the building was calculated by subtracting the solar heat delivered by the solar collectors from the stored energy change. This procedure credits the building with heat losses from the storage tanks, which is justified, since the tanks are located within the heated envelope. This procedure for calculating solar heat added to the building is a little crude on an hour-by-hour basis, but the errors tend to average out. For a time period spanning six weeks, the total measured solar heat delivered by the collectors was 32,606 MJ while the solar heat calculated from storage tank temperature changes was 32,993 MJ. This comparison indicates that no large errors are incurred by using this calculation method.

The entire hourly data base was processed using the heat balance procedure on which the summation of all the inputs were compared to the calculated heat loss (based upon an assumed infiltration factor, a conductive factor and a measured ΔT). The thermostat in this building is set back during the night. In the evening when the thermostat is set back, the building "coasts" for several hours and then in the morning when the thermostat is advanced, the furnace runs for almost the entire hour to catch up. The initial hourly heat balances showed the need of a building heat storage term in the heat balance. We devised a heat storage term for the building based upon the air temperature in the building.

The building has an estimated thermal mass of 700 MJ-°C^{-1}, but this thermal mass is weakly coupled to the air. To account for this weak coupling, we devised a thermal storage model which had a memory of five hours. The air temperature differences occurring during any given hour is placed in a bin. During each of five succeeding hours, the temperature difference in this bin is sequentially reduced by one-half. For any given hour, the heat stored in the building mass is calculated by multiplying a thermal mass constant by the sum of the ΔT contributions of these five bins. This is a fairly simple algorithm to program and it seems to smooth out the effects of large temperature transients on the building heat balance.

The hourly base from January 19 to March 3 was evaluated using an hourly energy balance which included electrical inputs, gas boiler inputs, passive solar inputs, active solar inputs and building storage exchanges balanced against building losses. Acceptable hourly, daily and monthly heat balances define the overall accuracy of the data and the suitability of the assumptions. The final results of these calculations are shown in Figure 7. The active solar collectors contribute a total of 33 GJ, the passive

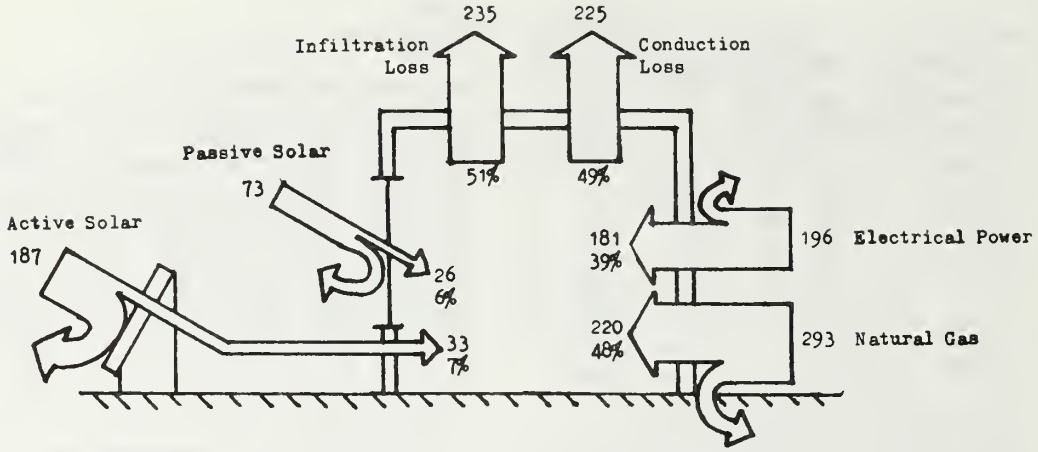

Fig. 7. Building heat balance from January 19 to March 3, Gigajoules

solar gains total 26 GJ, the electrical dissipation is 181 GJ and the heat supplied by the natural gas boiler is 220 GJ. The total heat losses during this period are 225 GJ from conduction through the skin of the building and 235 GJ due to infiltration (natural and forced). Data in Reference (1) shows that the environmental solar radiation and temperatures were typical during the monitoring period.

10. CONCLUSIONS

(1) At thermal equilibrium, the collectors performed to within about 7% of the expected, single collector performance. This reduction in performance is characteristic of practical active solar heating systems.

(2) The remote location of the collectors significantly reduce the system's thermal performance (over 25% in February). Each day, the pipes and fluid in the remote collectors must be heated before the system can deliver useful heat to the building. At night, this solar heat is dissipated to the atmosphere.

(3) During the monitoring period, the passive solar gains (through heat absorbing glass) were nearly as large as the active solar gains.

(4) The controls of the solar system are behaving as expected and there are no large steady-state heat losses since the pipes and heat exchangers are well insulated.

(5) The performance of this solar system is enhanced due to the maintenance, care and attention of the operating engineer, Ivan Newnham. Solar heating systems, due to their complexity and novelty, require some measure of dedication on the part of the building owner and operator. The owner and operator of the solar system on the Life of Montana Building are dedicated to making it work. Mr. Newnham monitors operation of the system and will often clean the snow from the 316 m^2 of collectors!

(6) During the monitoring period, the resource energy consumed to light the exterior of the building at night was equal to the solar heat collected.

(7) Large amounts of electrical energy are dissipated within this commercial building. Measuring hourly electrical energy facilitates accurate hourly heat balances.

11. ACKNOWLEDGEMENTS

This project was supported by a grant from the Alternative Renewable Energy Sources Program of the Montana Department of Natural Resources and Conservation. This grant program derives operating revenue from a severance tax on coal mined in Montana and is dedicated to promoting "research, development and demonstration of renewable energy resources". The cooperation and support of Rick Itami, Van Jamison and Mike Chapman are acknowledged.

Several members of the staff at Fowlkes Engineering have contributed to this project. Dennis Stillwaggon helped instrument the building and Jody Martinson typed and edited this paper.

12.0 REFERENCES

(1) Fowlkes, Charless W., Montana Solar Data Manual, available from Montana Department of Natural Resources and Conservation, Helena, Montana, 59620, (1979).

Ed. Note: A list of metric-English-metric conversion values appears immediately preceding the Author Index.

Reprint from PROCEEDINGS OF THE 1980 ANNUAL MEETING
Published by American Section of the International Solar Energy Society, Inc.
205B McDowell Hall, University of Delaware, Newark, DE 19711.

PRACTICAL SOLAR PERFORMANCE MONITORING

Charless W. Fowlkes
Fowlkes Engineering
31 Gardner Park Drive
Bozeman, MT 59715

ABSTRACT

This paper summarizes experience gained in developing instrumentation for monitoring the thermal performance of a dozen eolar heated projects in Montana. These projects were typically privately owned, occupied residences. The monitoring period averaged two months and the funds available were in the range of $7K per project including instrumentation. The general areas addreesed in this paper include (a) data requirements, (b) a low-cost data acquisition syetem utilizing the Radio Shack TRS-80 microcomputer, and (c) the practical problems of instrumenting occupied homes.

1. DATA REQUIREMENTS

The fundamental quantities to be measured are temperature, solar radiation, flow and status. Table I liete nominal valuee for the minimum sample rate, accuracy and resolution required. The units of temperature are °C.

TABLE I
NOMINAL SAMPLE RATES AND PRECISION FOR PERFORMANCE MONITORING

Quantity	Samples/hr	Accy.	Resol.
Solar insolation	60	3%	1%
Ambient temp.	4	0.5°C	0.5°C
Room temp.	4	0.5	0.5
Storage temp.:			
Passive system	4	0.5	0.05
Active syetem	10	0.5	0.1
Collector:			
Inlet/outlet	60	0.5	0.05
Δ T	60	0.05	0.05
Flow	60	1%	0.5%
Aux. furnace:			
In/out temp.	300	0.5	0.2
Δ T	300	0.2	0.2
Flow	300	2%	0.5%
Dom. hot water:			
In/out temp.	600	0.5	0.2
Δ T	600	0.05	0.05
Flow	600	1%	0.5%

1.1 Accuracy and Reeolution

Passive storage walls may have a thermal capacity of 30 MJ/°C which meane the wall temperature may only change about 1°C/hour, even during very cold nighte. An hourly heat balance to an accuracy of 10% thus implies knowing the temperature change of the passive wall to an accuracy of $\pm$ 0.05°C. Active collectors may operate with a ΔT of only 3°C which must be measured with an accuracy of 0.05°C to achieve a heat output accurate to 3%. Thus the accuracy requirements for temperature are dictated by the collector ΔT and the resolution requirements by large, passive storage components.

In both cases above, the absolute accuracy of the temperature is not important but the resolution and uniformity of calibration of the probes must be accurate to $\pm$ 0.05°C. These requirements present a non-trivial problem to the inetrumentation engineer, especially if low cost, flexibility and portability muet simultaneously be maintained.

Flow enters as a linear factor in the heat exchange equations and an accuracy of 2% would be desirable. This measurement can be achieved for liquid systeme at reasonable cost. The task of measuring air flow in a real home is complicated by short ducts, inaccessible ducts, irregular flows and leaking dampers. An accuracy better than 10% is often difficult to achieve.

1.2 Sample Rate, Output Rate and Accuracy

The sample rate is dictated by the frequency or rate of change of the quantity to be measured. Environmental and storage temperatures change slowly and can be sampled only a few timee each hour. The auxillary furnace and DHW system can cycle over periods of minutes or less. In order not to miss theee events the sample rate must be at least 600 samplee per hour. As a general rule the sample frequency should be about 10 times the average signal frequency.

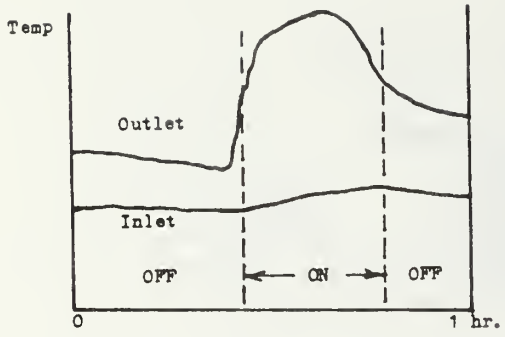

Fig. 1. Schematic of transient heat output

Figure 1 depicts a one hour record of inlet and outlet temperatures of a hypothetical furnace. Before the fan turns on the inlet and outlet temperatures are at equilibrium with their environment and after the fan turns off the temperatures decay toward equilibrium again. Note that the only temperatures that are significant in calculating the heat exchange are the temperatures while the fan is on. If simple hourly average inlet and outlet temperatures were used to calculate the heat exchange this value would have a large, undetermined error. This transient behavior in Figure 2 is characteristic of a solar collector output, thermal storage output, furnace output and DHW output. The "on times" of these devices may be from a few seconds to several minutes.

If a simple data logger is used its output frequency must be scaled to these high signal frequencies. This produces an overwhelming amount of output and is not a satisfactory solution. To reduce the amount of output data and still maintain accuracy on transient heat flows the engineer must either use a smarter data acquisition system or smarter transducers.

One approach is to use heat meters which calculate the transient heat exchange and have an output which can be read periodically by the data logger. Another approach is to implement logic in hardware which will zero inlet and outlet temperatures if there is no flow through the exchanger. If the data logger has averaging capability and a satisfactory scan rate the output frequency can be reduced to around one hour which will be a satisfactory solution.

A typical monitoring project may accumulate a data base of several thousand readings. Economy requires that the data be output in a computer readable format such as memory boards, tape or disk to allow for efficient summary and processing of the data.

2. COMPUTER BASED DATA ACQUISITION SYSTEM

The requirements discussed above point to the advantage of using a computer controlled data-acquisition system. These systems provide a high sample rate, the logic of the test program can be structured in software and the data can be easily output to a mass storage device and printed. A large number of these systems are commercially available but we found that the cost of the systems exceeded our modest budget. At this point we set upon a course to develop our own system. Our approach was to use the low cost TRS-80 microcomputer manufactured by Tandy Corp. and sold in Radio Shack stores. We then developed the interface hardware and software to convert this computer into a smart data logger.

2.1 TRS-80 Data Acquisition System

The system we developed is shown in Figure 2. The TRS-80 is not modified in this application and is used simply to control the system, organize the data, display the data and output the data to cassette tape. The front panel of the interface is shown in Figure 3 and provides inputs for the transducers and a parallel and RS232 serial output port for transmitting data to a printer, modem or another computer.

Each analog input card has eight inputs and up to 6 cards can be accomodated giving a capability of 48 channels. Each card is dedicated to a particular type of transducer and no external signal conditioning is required. The interface contains a 12 bit A/D converter and a real time clock giving month, day, hours, minutes and seconds. A battery backup power supply is normally used so that the system will run for several hours even if the utility power is off. This feature is useful for many of our remote sites in Montana.

The system scans all 48 channels about once each 6 seconds. During the scan, the 12 bit representation of input signals are processed to convert to convenient units and transient heat flows are computed. These quantities are displayed on the video screen every 6 seconds along with the time and date. All quantities are averaged and at write-out time these average quantities are written to cassette tape. The write out period and processing are written in BASIC and can be changed on the site to suit the project.

3. TRANSDUCERS AND TECHNIQUE

Low-cost transducers were selected which approach the accuracies listed in TABLE I. It was important that the output of all transducers be independent of extension lead length. In real monitoring jobs the data system may be from 10 to 100 meters from the transducer or probe. The required extension

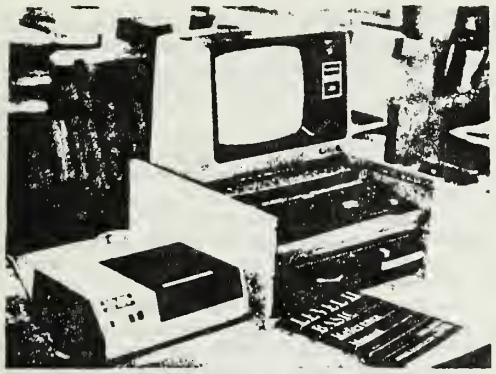

Fig. 2. Front view of system

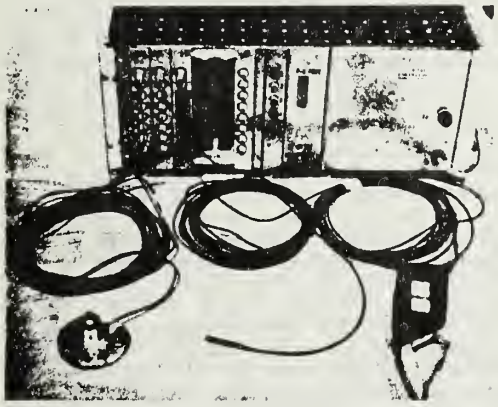

Fig. 3. Rear view showing input cards, transducers and serial/parallel output port

length cannot usually be determined before installing the instrumentation. We normally do a precise calibration in the lab and then use extensions as required at the site. We use RCA-type phono jacks for all transducers. When we instrument a site we take along a large box filled with extensions of various lengths. A probe is mounted at the deeired location and then extensions are ueed to reach to the input panel of the data acquisition system. We have found that running extensions in an occupied house often requires considerable ingeniuity. About one man-week is required to install a system.

We measure temperature with the AD-590 manufactured by Analog Devices. This device has the advantages of low cost, linearity and high output. These probes are individually calibrated using the data acquisition system, appropriate software and reference temperature baths. For the temperature ranges used in solar monitoring the accuracy of the probe depends primarily on the accuracy of the calibration reference temperature which is about $\pm$ 0.1°C. All probes for a given project are calibrated simultaneously to minimize relative error. The resolution of the data system with theee probes is 0.05°C.

Solar insolation is measured with a silicon cell based instrument. For best accuracy we recommend the Li-Cor LI-200 which has the advantage of low cost and is not influenced by tilt. We approximate electric power inputs by measuring current using a clamp-on ammeter. For resistive loads with conetant voltage this device ie accurate to within 4%. On site calibration against the utility kWh meter can increase this accuracy to 1%.

Pumps, fans, dampere and insulating curtaine are normally instrumented with relays, microswitches or mercury switches. The data system senses switch closure and the software generates a 1 or 0 for "on" or "off". These status channels are included as multipliers in the transient heat equations so that the output is only calculated when the device is on. The average status during the hour gives the fractional "on time" and when multiplied by the motor rating will give auxillary energy or pump work. The status channel can be used to calculate true average inlet and outlet temperature "while on". This is done by dividing the zeroed average temperature by the hourly average status.

We adapt a commercial water meter (Hersey MVR-30) for liquid flow measurements. The meter when connected to the data acquisition system can be calibrated to within a few percent. These turbine-type meters seem tolerant of dirt in the line and have the advantage of low cost. The normal flow range is 4 to 100 lpm.

Air flow is our most difficult measurement. Often we are forced to measure flow near elbows and outlets where the velocity is changing with time and the distribution is nonuniform. We probe the cross-section with a hot-wire anemometer to determine the average flow rate for each system configuration and these values are then put into the computer program as constants. We would rather use permanent duct anemometers but have not yet located transducers that are accurate and also low in cost. In all air systems we have monitored we have measured large imbalances in flow around the system due to leaks around dampers as well as leaks into and out of the system.

4. DATA COLLECTION AND PROCESSING

Our monitoring period is normally 2 to 3 months. During this period we record on cassette hourly average data from 15-30 transducers, calculated parameters, such as transient heat flows, collector efficiency, etc., and time. One side of a cassette will hold about 12,000 numbers and muet be changed every 10 to 20 days.

Since many of our monitored sites are several hundred miles from our office we ask the owner to change the data tapes and mail them to our office. We also leave the owner a copy of the program tapes along with instructions on how to load the programs if the system crashes. Often the system will run the full two months without attention but we expect about one crash per project on the average. The home environment of dogs, children, mice, etc. usually leads to a damaged probe at sometime during the test so we plan on one site visit for repairs.

In the office we read the data tapes into another microcomputer and put all raw data on floppy diskette for further processing. The data system itself can be used for processing but the access to cassette data is slow. We typically do a lot of work with the data and the fast, random access of the floppy diskette saves time.

4.1 Heat Balance

A central part of the data processing is setting up a heat balance for the house. In principle the measured data will allow calculation of all the heat inputs to the house; solar, auxillary, electrical and storage. A calculated heat loss factor times the actual temperature difference produces a calculated heat loss value. A computer program is written to scan the data base and output components of the heat balance equation on an hourly and daily basis.

Discrepancies in the heat balance are used to identify bad data and bad assumptions. An informal iterative process is used to improve this heat balance. For example if the calculated heat loss factor can be adjusted by 20% and this improves the heat balance, this is done. The thermal mass of the house is another quantity that is often trimmed to improve the heat balance.

In passive projects it is impractical to get a true sample of the temperature of the storage mass. For example, one underground house we monitored had most of the thermal storage in the concrete structure itself. Hundreds of probes placed at varying depths would have been required to sample the "average" temperature of this mass. By using data from 6 well placed probes and then working with the heat balance equations we were able to achieve a satisfactory heat balance.

If the heat balance seems reasonable then programs are written to determine solar efficiency, solar fraction, storage heat loss, etc. Tables of average interior temperature and swing are output to describe the comfort of the environment. The data is also scanned to note system peculiarities, such as collector fans that turn on at night, or insulating curtains that were open at night or closed during the day, or collectors that are thermosyphoning at night. We usually measure at least one temperature behind the insulating curtain to estimate its effective R value.

4.2 Special Problems

We have monitored two projects which occasionally used a wood stove. There is no simple way to measure the stove output so we placed a temperature probe near the stove to give a crude measure of the status of the fire. We then devised an empirical equation consisting of a constant times the temperature near the stove minus the house temperature at a remote location. This constant was based on the manufacturer's rating of the stove at peak output. We were surprised at how well this equation tended to balance the heat equations during times when the stove was on. The estimate itself was crude but it produces daily energy balances that were about as good as the energy balances on days when the stove wasn't used.

Incidental electrical dissipation from light bulbs and appliances is difficult to determine without massive instrumentation. If the house does not have an electric furnace or some other form of electric heat we simply measure the total power (current) at the input mains. The main interpretation problem is estimating how much of this input power is actually dissipated in the house. The light bulb clearly dissipates nearly 100% of it's power as heat. The heat recovered from electrically heated hot water that goes through the dishwasher or the shower is difficult to estimate. We devise a factor for each house, usually between 0.5 and 0.8, based on the type appliance used. On some projects the incidental electric dissipation will amount to 10 or 15% of the overal heat load so it cannot be ignored.

5. SUMMARY

(1) For solar performance monitoring the data acquisition system must be smart enough to do some processing and averaging on-line to capture transient events while at the same time condensing the output data. A sample rate of 600/hour and an output of once each hour seems about right for many projects. The required temperature resolution and accuracy is at least 0.1°C for collector ΔT and for the ΔT/hour of large, passive storage masses.

(2) The installation of the transducers requires considerable finesse and should be done or supervised by someone having a grasp of the overall project. Judgement is needed because of practical limitations on the number of transducer location. There is normally no backup instrumentation so that if one channel of data is lost the project may be lost. The probes must be carefully installed and the raw data must be inspected as it is produced.

(3) The project is not finished when the raw data is dumped into tables. Considerable interpretation, data processing, cross-checking and common sense must be applied to the data before general conclusions can be drawn. For each month of hourly data we spend nearly a month in processing, interpretation and reporting. We have found that an hourly and daily heat balance is the best way to verify the data. The heat balance can identify errors in the data and in some cases points to ways to correct the data. See Figure 4.

(4) The TRS-80 based data acquisition systems have performed satisfactorily. The flexibility allowed by LEVEL II BASIC and the low cost of the system are its main advantages. We have used three of these systems almost continuously during the past 18 months.

(5) The owners of the houses have cooperated with the monitoring effort and are interested in the data. The owners or designers seldom have an accurate idea of how well the system really works.

6. ACKNOWLEDGEMENTS

The work described in this report was supported by grants from the Alternative Renewable Energy Sources Program of the Montana Department of Natural Resources and Conservation. This grant program derives operating revenue from a severance tax on coal mined in Montana and is dedicated to promoting "research, development and demonstration of renewable energy resources". The cooperation and support of John Orndorff, Bureau Chief, and Jim Iversen, Project Monitor are acknowledged.

Sharon Kleingartner is acknowledged for typing and editing this manuscript and for her contributions in organizing performance data. Carlos Lozano has made significant contributions to the monitoring projects in the areas of instrumentation and data processing. Harley Leach and Kellee Crisafulli have contributed to the design and construction of the data acquisition interface.

DAILY PERFORMANCE SUMMARY FOR BROWN'S GREENHOUSE

MO	DA	HR	SOLAR INSO (MJ)	SOLAR INPUT (MJ)	ROCK STORE (MJ)	ROCK OUTPUT (MJ)	STORED BARREL (MJ)	STORED WALL (MJ)	STORED FLOOR (MJ)	CALC LOSS (MJ)	AMBT TEMP (C)	INSL CURTN (C)	INSIDE TEMP (C)	LOW BED (C)	HIGH BED (C)	ROCK BED (C)	BACK WALL (C)	BARREL TEMP (C)	CURT R VAL
12	30	1	.0	.0	.0	2.4	1.4	2.2	13.0	10.6	-7.2	-.0	17.6	15.8	19.7	11.4	15.7	17.1	4.1
12	30	2	.0	.0	.0	2.3	1.5	2.2	12.5	10.7	-7.7	-.5	17.1	15.6	19.3	10.9	15.5	16.9	4.1
12	30	3	.0	.0	.0	2.2	1.6	2.0	12.0	10.9	-8.7	-1.1	16.7	15.3	18.8	10.4	15.3	16.7	3.9
12	30	4	.0	.0	.0	2.1	1.6	2.3	11.5	11.3	-10.0	-1.6	16.3	15.1	18.4	9.9	15.1	16.5	3.5
12	30	5	.0	.0	.0	2.0	1.6	2.2	10.1	10.7	-9.0	-1.8	15.9	14.9	18.0	9.5	15.0	16.3	4.1
12	30	6	.0	.0	.0	1.9	1.6	2.0	10.1	11.1	-10.2	-2.3	15.6	14.6	17.6	9.1	14.8	16.1	3.7
12	30	7	.0	.0	.0	1.8	1.6	2.0	9.6	10.9	-10.3	-2.5	15.2	14.4	17.2	8.7	14.6	15.9	3.8
12	30	8	1.4	.0	.0	1.6	1.6	2.0	9.6	10.7	-10.1	-2.3	14.9	14.2	16.8	8.3	14.4	15.7	3.7
12	30	9	43.3	19.0	-4.7	.0	.5	1.3	9.1	22.7	-9.7	9.9	16.6	14.1	16.5	9.5	14.3	15.6	.2
12	30	10	96.1	65.0	-13.3	.0	-2.4	-.7	-11.1	26.0	-6.9	19.9	23.3	14.3	17.2	12.5	14.4	15.9	.0
12	30	11	120.5	86.6	-21.9	.0	-4.5	-5.8	-38.5	29.4	-4.9	34.0	29.3	15.1	19.6	14.3	14.9	16.5	.0
12	30	12	109.2	62.3	-20.6	.0	-3.9	-9.4	-48.6	29.8	-4.5	34.8	30.1	16.1	22.0	15.7	15.7	17.0	.0
12	30	13	85.3	65.0	-20.9	.0	-4.4	-12.9	-40.9	29.9	-3.4	36.7	31.3	16.9	23.7	16.9	16.8	17.6	.0
12	30	14	89.3	66.3	-19.7	.0	-3.8	-5.3	-31.3	29.2	-2.5	39.0	31.5	17.6	24.7	17.7	17.3	18.1	.0
12	30	15	44.7	23.0	-12.3	.0	-2.3	1.6	-23.1	27.1	-2.5	30.7	29.1	18.1	25.1	18.3	17.2	18.3	.0
12	30	16	28.4	17.6	.0	1.7	-1.0	2.3	-4.8	26.1	-3.3	25.5	27.1	18.2	24.6	17.9	17.0	18.5	.0
12	30	17	1.4	.0	.0	3.8	1.3	2.4	10.6	12.5	-5.1	7.9	23.9	18.0	23.7	17.1	16.8	18.3	2.1
12	30	18	.0	.0	.0	4.9	1.3	2.6	18.8	12.3	-6.7	3.0	21.9	17.6	22.7	16.0	16.5	18.1	3.3
12	30	19	.0	.0	.0	4.8	1.4	2.4	18.3	12.1	-7.6	1.6	20.5	17.2	21.8	15.0	16.3	18.0	3.4
12	30	20	.0	.0	.0	4.1	1.3	2.3	16.8	11.7	-7.7	.7	19.5	16.8	21.1	14.1	16.1	17.8	3.7
12	30	21	.0	.0	.0	3.5	1.3	2.2	15.4	11.4	-7.8	-.1	18.7	16.5	20.4	13.3	15.9	17.6	4.0
12	30	22	.0	.0	.0	3.1	1.6	2.2	15.4	12.3	-10.6	-.8	18.0	16.2	19.8	12.6	15.7	17.4	3.2
12	30	23	.0	.0	.0	3.0	1.6	2.2	13.9	12.2	-11.0	-1.6	17.4	15.9	19.3	12.0	15.5	17.2	3.4
12	31	0	.0	.0	.0	2.8	1.6	2.0	13.5	12.0	-11.1	-2.3	16.9	15.6	18.8	11.4	15.4	17.0	3.6
12	30		610.5	404.7	-113.4	48.0	1.9	6.1	22.1	403.6	-7.4	9.5	21.0	16.0	20.3	13.0	15.7	17.1	

DAILY HEAT INPUT = 369.51692 CALAULATED LOSS = 403.59303

Fig. 4. Sample output: One day of processed data from a large passive solar greenhouse in eastern Montana. Hourly values of energy balance are shown (MJ) along with various temperatures (°C). Bottom line is daily summary (24 hours).

Progress in Passive Solar Energy Systems Copyright 1983 by
American Solar Energy Society, Inc Printed in U.S A

0731-8626/83$3 00

INSTRUMENTATION AND DATA ANALYSIS FOR BUILDING ENERGY MONITORING

Charless W. Fowlkes, Ph.D., P.E.
Fowlkes Engineering
31 Gardner Park Drive
Bozeman, Montana 59715

ABSTRACT

This paper relates the result of our efforts, spanning several years, toward the goal of making low cost and meaningful thermal measurements on buildings. Experimental pitfalls are illustrated with examples and suggestions for better experimental procedures are given. A data acquisition system using a powerful portable microcomputer in conjunction with compact data acquisition modules is discussed.

This paper also discusses real time data analysis methods that may prove useful for short-term performance monitoring. Results of some data using recursive, digital filtering algorithms are presented. These algorithms when programmed on the computer (which can sense and respond in real-time in the physical world using the data I/O modules) form a system with an order of artificial intelligence. The goal of this intelligent system is to form an Energy Signature for the building. The Energy Signature consists of several equivalent thermal parameters of the building which form an energy signature characterizing the building.

1. INTRODUCTION

To some the notion that we need to instrument buildings to understand and quantify their thermal performance must seem a foolish waste of time. Our magazines and books concerned with solar design are filled with elaborate descriptions of "how it works", complete with colored drawings showing red heat-arrows wiggling through vents in Trombe walls to escape blue cold-arrows, etc.. This powerful combination of artistry and sophistry can leave us with a conviction that there is little left to be learned.

Experience shows the thermal behavior of a building is a composite resulting from the interaction of a large number of subtle and interrelated thermal mechanisms. The intuitive "descriptions" are often just misleading fantasies. The scientific documentation and delineation of the mechanism presents a nontrivial task in measurement and interpretation.

My work in the area of instrumenting buildings for thermal characterization has only spanned a few years. (1-4) During this time I have had the opportunity to make a lot of mistakes in my programs and to observe a lot of mistakes in other programs. Many of these mistakes can be anticipated and avoided if we maintain a balanced view of the experimental process.

Personal interests, preferences and orientation tend to distort the experimental process. The theoretician hopes the experiment will produce data to verify his pet model. The instrumentation hardware specialist may focus on cute ways to measure things. The project manager wants a thick final report to show his boss. All of the people (or functions) are a necessary part of the experimental process. Experimental failures result when one of these separate interests, functions or orientations dominate the experiment.

2. EXAMPLES OF EXPERIMENTAL PITFALLS

(1) Only a few months ago I heard a presentation of results of a building thermal performance monitoring program. The speaker expressed pride in the fact that their print-out of monitoring data was 4 meters high! They were measuring over 100 transducer channels. The presentation of results was a plot of daily auxiliary energy versus degree-days which could have been made by a 12 gauge shotgun at 10m. The minicomputer found a straight line through these points having a correlation coefficient of 0.42 and everyone was apparently pleased with the results.

The instrumentation in this experiment was very powerful and apparently carefully calibrated and maintained. The analysis model was woefully inadequate and this led to results having little information.

(2) Another building research project used a quality data logger to measure 113 transducer channels. Data tapes had been collected (but not analyzed) for 4 months when an intermittent electronic problem was noticed. Internal elec-

trical gains were not being measured and the building was regularly ventilated with a fan that was not instrumented. These two "unknowns" were major features (15 to 35%) of the building energy balance.

The instrumentation hardware was adequate in this case but it was not properly maintained and was not used to measure all the important variables. Better experiment design and equipment maintenance would have enormously increased the significance of this effort.

(3) I observed another monitoring effort conducted by a respected national solar data monitoring group. This experiment was well formulated and the instrumentation hardware and software was excellent. The temperature transducer "measuring ambient air temperature" was mounted near the mouth of a building air vent, on the west side of the building in direct sunlight. A plate was soldered to the transducer making it a better solar collector! Fluid temperature probes were mounted to the surface of the pipes and their readings were erratic. These probes were jiggled around until the readings "seemed reasonable".

The installation of the transducers in this short-term experiment was less than optimum. This produced uncertainties in the results. The "portable" instrumentation system occupied several crates weighing over 200 kg. It was a centralized (rather than distributed) data acquisition system. Two trained technicians spent 4 days installing over 150m of wire to set up the test and one day in removing the instrumentation. Two days of data were collected. A similar effort on another building produced no usable data.

(4) I visited four different projects located around the country where dozens of solar DHW systems had been instrumented with heat meters for performance monitoring. Inspection of the installations coupled with elementary cross-checking of the data showed that at least 80% of the data were worthless. The basic faults were related to equipment failures and improper installation. The participants in the program lacked an appreciation of the art of successful measurement.

(5) Three years ago I was analyzing data on a small building incorporating active air collectors. Specific data on the collectors showed they were leaking badly and were not contributing significant solar heat to the building. The hourly heat balances clearly showed errors when the sun was shining. I had overlooked the fact that the south facing glazed area was nearly equal to the collector area. The analysis model was modified to include direct solar gain through the windows and the hourly heat balances improved dramatically.

These examples are included to illustrate the types of problems that occur during experimental projects. Some of these problems can be avoided.

3. REVIEW OF EXPERIMENTAL PROCESS

The goal of an experimental measurement program is to provide answers to questions that cannot be economically or accurately answered in any other way. A "good" experiment will provide answers having adequate accuracy at a minimum cost. The milestones for the execution of an experiment are INSTRUMENTATION, DATA, MODEL and RESULTS and a report on the elements of an experiment will often be presented in this order. It is important to recognize that milestones during the design phase of the experiment occur in exactly the opposite sequence, Figure 1.

The first step in the Design Phase is to decide what we want to know at the end of the experiment; what RESULTS are needed. We then select or devise a conceptual model representing the system and establish what input data must be measured to produce the output results. This is a difficult and crucial step in the experimental design procedure. If the MODEL and DATA are well defined the INSTRUMENTATION requirements are clearly specified.

The first step in the Execution phase is to calibrate and install the measuring and recording instruments. DATA are collected over a suitable time-period. These are then processed using the analysis MODEL. RESULTS and their expected errors are then summarized.

If the experiment was well designed and executed the errors will be within the allowed range, the new information and results are reported and the job is done. The process seldom runs this smoothly and often we must loop back to some earlier step and re-do the experiment; perhaps returning to the beginning.

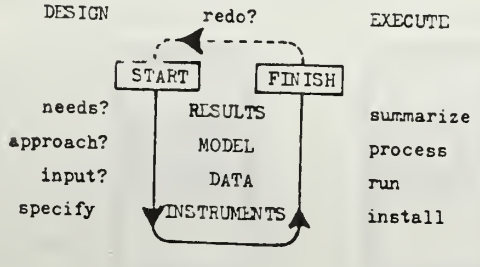

Fig. 1. Experimental Process Model.

4. IMPROVING THE EXPERIMENT

4.1 Experiment Design

It is impossible to over emphasize the importance of the design phase. This begins with a clear definition of the final results desired and the maximum inaccuracy that can be tolerated.

Next is the evolution of a process model and its associated input data. This activity includes questions like; "How simple can the model be?", "What effects can we ignore?", "What is the error in the result for the worst possible combination of input error?" The value of this analysis is to establish whether there is a significant probability of success, before investing time and money in the actual experiment. Errors are discussed further in the following section on Signals and Noise.

4.2 Instrumentation

The steady progress in microelectronics technology has resulted in the availability of cheap and powerful computers and accurate data acquisition equipment. Economic considerations demand the use of these machines for most experiments.

An example of a system suitable for many building monitoring tasks is shown in Figure 2. A portable microcomputer controls the data acquisition, storage, display and processing. A wide range of transducers can be connected directly to the data acquisition modules. The computer communicates with the modules using a digital code carried by a single cable. These modules are located near the transducers to minimize wiring. The system can be expanded by adding more modules as required. One or two modules are adequate for many energy monitoring jobs on small buildings. The whole system costs around $2,000 and can be carried in a brief case. This system is currently being used to control and log data from a side-by-side solar DHW experiment.

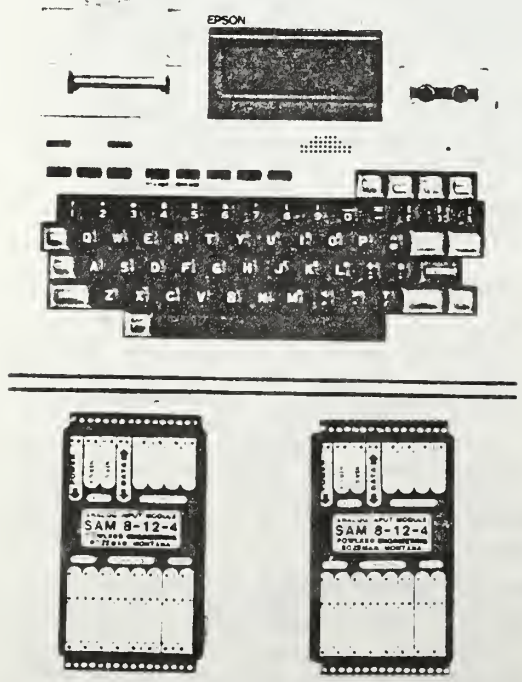

Fig. 2. Portable Data Acquisition System.

Once the data requirements are defined the data acquisition system specifications are easily determined. The crucial considerations in selecting hardware are accuracy, reliability, cost and ease of use. The installation and calibration of the transducers are of utmost importance. The examples of pitfalls given earlier in this paper are not unique. The success of the experiment can be ruined if you are not really measuring what you think you are measuring.

4.3 Data Processing and Results

If the experiment has been properly planned you already know what to do with the data as it comes in. It is a good idea to start processing the data as soon as possible. There are two motivations for doing this; (a) it is fun to see if the experiment is working and to find out the initial results. (b) if the experiment is not working you will want to revise it before generating a pile of useless data.

5. SIGNALS AND NOISE

Thermal monitoring experiments are usually aimed at measuring some component of energy gain or loss. It is often impossible to specifically measure the component of interest in a real building. The building thermal response is a composite reflecting the interactions of many thermal inputs, outputs and storage effects. Table 1 lists nominal values for 14 identifiable (at least in concept) heat exchange components for a "hypothetical" residence. This data explains why simple energy analyses using limited data such as fuel bills and a simple conductive model often yield results so noisy that general conclusion are impossible.

Assume we have a simple experiment consisting of an electric heater in a small test cell with constant inside and outside temperature. We plot energy input versus ΔT for a range of values and get a nice straight line. The results show little scatter because we have good control over the important variables.

Now assume that a lab assistant enters the test room several times a day, uses the heater to boil water for coffee, sits and reads his newspaper and opens the window if he feels too hot.

TABLE 1.

NOMINAL DAILY HEAT EXCHANGES, MJ

Heat into Space is Positive

Description	Winter	Spring/Fall
Envelope Conductive	-450	-150
Infiltration, stack	-100	-40
*Infiltration, stack	-10	-2
Infiltration, wind	-45	-15
*Infiltration, wind	-5	-3
Furnace heat	400	35
*Humidifier	15	5
Electrical dissipation	120	100
*Bathing, Cooking	20	20
Solar gain, windows	80	80
Sol-air effects	±30	±30
Stored heat	±50	±40
Mechanical venting	-20	-20
*Mechanical venting	-5	-10
Occupant effects, unknowns	±30	±30

*Latent heat exchanges

We now innocently plot our data and the points are scattered all over the page.

The point of this simple example is to illustrate the inevitable noise that enters any experiment. The noise in the hypothetical experiment is a real physical event that we can't control or maybe do not conceive. It is due to a mismatch or a poor fit between our model of the process and whatever is going on out there.

A second type of noise is related to faulty instruments. In principal we can deal with these problems more effectively. Our concepts of properties are better defined and the instruments are simpler systems complete with calibration standards, trouble shooting hints and repair procedures.

6. DATA PROCESSING TECHNIQUES

6.1 Batch Processing

Many experiments are analyzed using a procedure that may be described as batch processing. The data logger, over some interval of time, produces a "batch" of data. This batch of data is transferred to a computer and statistical algorithms such as linear regression are used to find the "best" values which fit an a priori process model.

This approach is depicted graphically in Figure 3. The model of the parameter represented by the data has a value that is constant with time. The data is scattered due to random noise in the measurements and random noise due to approximations inherent in the simplified process model. The true signal having a value of 100 was corrupted by adding a random value (noise) having a range of ±50.) The best fit to the model is a line passing through 100.

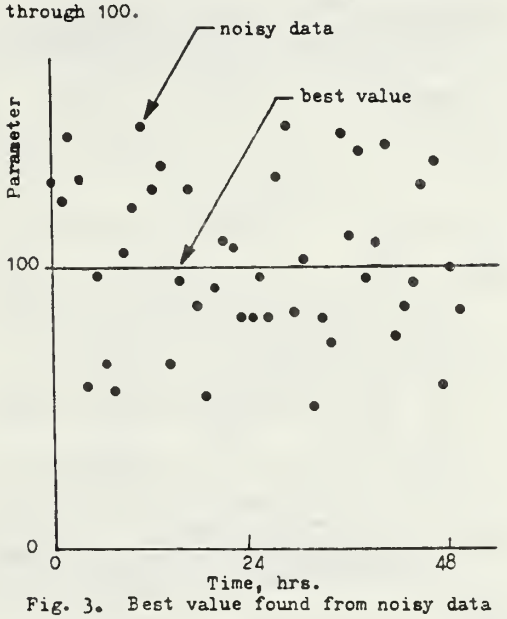

Fig. 3. Best value found from noisy data after test.

6.2 Real Time Processing

We have been experimenting with real-time processing of building data. Since a computer is already part of the system it is possible to write programs to keep a running summary of the data, in real time, as it comes in from the sensors.

There are numerous algorithms for processing real-time data. These methods referred to as "digital filters, stochasistic algorithms, recursive filters, observers," etc. Basic to all algorithms is the notion of a current estimate of the true value and rules for improving this estimate in response to new data coming in.

We usually input a starting value, our best estimates before the first data point. We also input information about how noisy we think the data will be. This basically adjusts the gain or sensitivity of the estimator to new data.

To illustrate the general idea we take the example data set and imagine the response of an estimator that reacts to the new data one point at a time. We give it a starting value of zero out of playfulness. We could formulate a "fickle estimator" that assumes each new data point is the true value. The graph of the history of the fickle estimator's estimate is shown in Figure 4. It is clear that the fickle estimator doesn't learn from experience and does not help us filter out the noise.

For contrast we could formulate a hypothetical

"conservative estimator" and give him a starting value. As the data comes in the conservative estimator slowly and sluggishly responds to the data, Figure 4. Given a sufficient time the conservative estimator may converge on the true value.

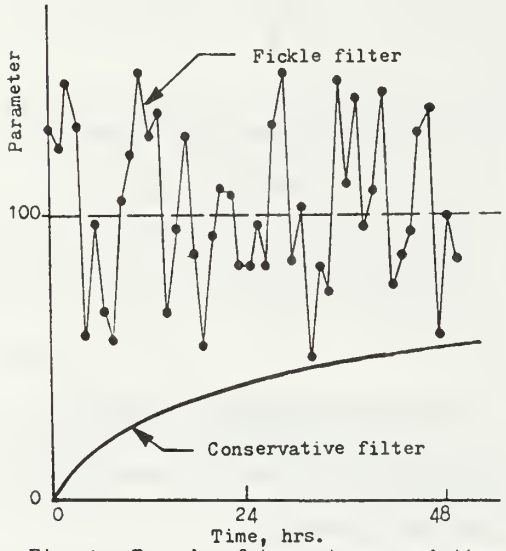

Fig. 4. Example of two extreme real-time estimators or filters.

Neither of these estimators or filters appears very helpful for finding a best value in a short time. Fortunately much mathematical work has been done to develop smarter and more optimal estimators or filters. (5) A good example of an optimal filter is the Kalman filter developed in the 1960s (6).

6.3 Smarter Filters

The Kalman filter "catches on" to the trend of the data and can find the best value rather quickly. At each new data point it reevaluates it's current gain or sensitivity and thus, in a sense, learns from experience to make better estimates. As it approaches the best value it becomes insensitive or conservative and starts to ignore the noisy data. (We have "warned" the filter about the noise in our formulation of the problem.) Another property of the Kalman filter is that it eventually finds the same best value that we would find by processing a batch of data using standard regression methods.

A computer simulation of the response of a Kalman filter to our noisy test data set is shown graphically in Figure 5. Note that after only 15 data points it is within 5% of the true value. After 20 points it is locked in on the true value and never varies more than ± 1%.

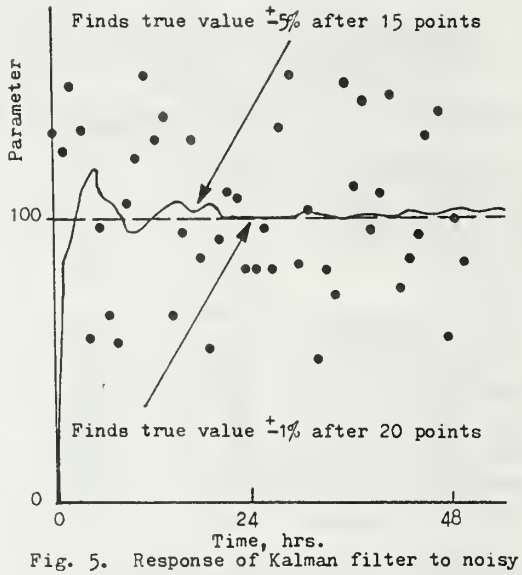

Fig. 5. Response of Kalman filter to noisy data.

7. APPLYING REAL-TIME PROCESSING

We have applied the method of real-time filtering or estimation to processing building thermal response data. An energy balance equation for the building is formulated in terms of unknown coefficients and measured driving forces. The coefficients are terms like overall envelope conduction factor, equivalent solar aperature, equivalent thermal mass, etc. This set of coefficients forms an Energy Signature for the building. (7,8) The measured driven forces are temperatures, solar radiation, electricity entering the building, etc.

Each coefficient is given a "reasonable" starting value. At each stage of the process, the new data is fed into the energy balance equation and the error or imbalance is determined. The error is partitioned and each coefficient is adjusted in the direction of smaller error according to a filter algorithm.

Table 2 shows the behavior of a Kalman filter using hourly raw data from a building we monitored three years ago. A simple 5 element model was used to represent the building and the filter parameters were fairly crude. The first part of the table shows the results after 24 and 48 hours when the filter was given "good" starting values. The second part shows the estimates resulting from "poor" starting values. For comparison we have shown the values we derived after analyzing 10 weeks of hourly data.

The remarkable fact is how quickly these crude filters approach the long term values. These data suggest that if the proper filters were

included within the data acquisition program results could be made available, in real-time at the site. The computing power required is easily within the capability of the system shown in Figure 2. Further work is needed to test the adequacy of the thermal model and to study the response of different filters.

TABLE 2.

FILTER RESPONSE TO REAL DATA

TIME	BUILDING U	FURNACE OUTPUT	ELECTRIC RECOVERY	SOLAR RECOVERY
hrs.	MJ/°C-hr	MJ/hr	MJ/MJ	MJ/MJ/m^2
0	.67	18	.9	2.4
24	.66	20	.8	2.2
48	.61	23	.9	2.2
0	.46	28	1.0	2.8
24	.61	21	.7	2.7
48	.62	22	.7	2.7
Reference	.67	22	.8	2.4

8. CONCLUSIONS

In this paper I have reviewed some of the problems and pitfalls surrounding the topic of thermal performance measurements of buildings. The effectiveness of this type of work can be improved by careful experimental design and appropriate selection of instrumentation. The combination of cheap, portable, computing power and advanced real-time analysis methods point to a possible avenue for greatly improving our ability to diagnose the thermal behavior of buildings.

9. ACKNOWLEDGEMENTS

The observations reported in this paper are based on experience gained while instrumenting buildings for the Department of Energy and the Montana Department of Natural Resources. The instruments and real-time analysis application were developed by Fowlkes Engineering. Sharon Kleingartner is acknowledged for typing and editing this manuscript.

10. REFERENCES

(1) Fowlkes, Charless W., "Measured Thermal Performance of a Passive Solar Residence in Bozeman, Montana," Proceedings of the Fourth National Passive Solar Conference, Kansas City, MO, 1979.

(2) Fowlkes, Charless W., "Experimental Problems in Measuring the Thermal Perform ce of Passive Solar Systems," Proceedings of the Fifth National Solar Conference, Amherst, MA, 1980.

(3) Fowlkes, Charless W., "Passive Cooling Monitoring at the Class B Level," Proceedings of the ASME Solar Energy Division Fourth Annual Conference, Albuquerq[illegible], NM, 1982.

(4) Fowlkes, Charless W., "Thermal Performance of a Commercial Building at the Class B Level," Proceedings of the 1982 Annual Meeting, A.S.E.S., Houston, TX, 1982.

(5) Gelb, Arthur, "Applied Optimal Estimation," MIT Press, 1974.

(6) Kalman, R. E., "A New Approach to Linear Filtering and Prediction Problems," A.S.M.E. Journal of Basic Engineering, March, 1960.

(7) Hammarsten, S., et al., "Energy Signatures of Varying Complexity," presented at ACEEE meeting, Santa Cruz, CA., 1982.

(8) Sonderegger, R. C., "Modeling Residential Heat Load from Experimental Data: The Equivalent Thermal Parameters of a House," pp. 183-194 in Proceedings of the International Conference on Energy Use Management, Vol. II, R. A. Fazzolare and C. B. Smith, Eds., Pergamon, Oxford, 1977.

APPENDIX 1: KALMAN FILTER

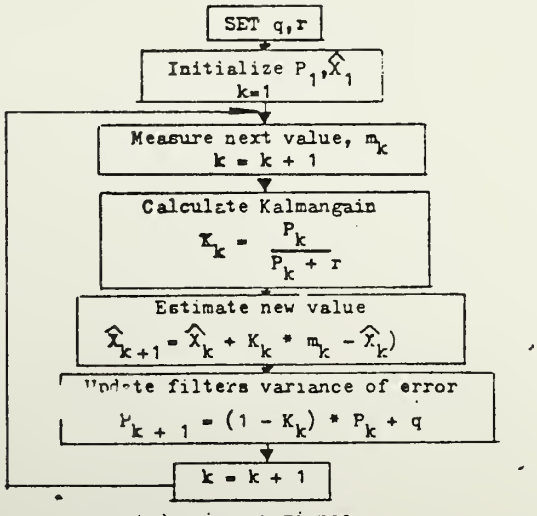
SET q,r
Initialize $P_1, \hat{X}_1$
k=1
Measure next value, m_k
k = k + 1
Calculate Kalmangain
$K_k = \frac{P_k}{P_k + r}$
Estimate new value
$\hat{X}_{k+1} = \hat{X}_k + K_k * m_k - \hat{X}_k)$
Update filters variance of error
$P_{k+1} = (1 - K_k) * P_k + q$
k = k + 1

q,r - expected noise, variance
P - error covariance
X - estimate of parameter

Fig. A-1. Flow chart showing Kalman algorithm for estimating parameter based on real-time data. See References (5,6) for complete discussion and derivation.

16 copies of this public document were published at an estimated cost of $7.00 per copy, for a total cost of $112.00, which includes $112.00 for printing and $.00 for distribution.